In presenting the dissertation as a partial fulfillment of the requirements for an advanced degree from the Georgia Institute of Technology, I agree that the Library of the Institute shall make it available for inspection and circulation in accordance with its regulations governing materials of this type. I agree that permission to copy from, or to publish from, this dissertation may be granted by the professor under whose direction it was written, or, in his absence, by the Dean of the Graduate Division when such copying or publication is solely for scholarly purposes and does not involve potential financial gain. It is understood that any copying from, or publication of, this dissertation which involves potential financial gain will not be allowed without written permission.

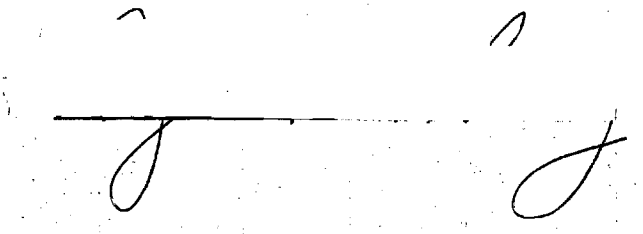

7/25/68

INTERACTION OF THE INERT GASES WITH HEXAGONAL BORON NITRIDE

A THESIS

Presented to

The Faculty of the Graduate Division

by

Reginald Norris Ramsey

In Partial Fulfillment

of the Requirements for the Degree

Doctor of Philosophy

in the School of Chemistry

Georgia Institute of Technology

January, 1970

INTERACTION OF THE INERT GASES WITH HEXAGONAL BORON NITRIDE

Approved

Chairman

Date approved by Chairman: 5 May 1970

ACKNOWLEDGMENTS

The author wishes to express his sincere appreciation to all those who assisted in making this investigation possible.

Thanks are due the author's thesis advisor, Dr. Robert A. Pierotti, for his encouragement and assistance throughout the investigation. It was through Dr. Pierotti's efforts that this project was begun and necessary financial aid was made available. Messrs. Malcom Rucker, Donald Lillie, and Gerald O'Brien should also be recognized for their advice and efforts in constructing the experimental equipment.

Funds provided by the National Aeronautics and Space Administration, Petroleum Research Foundation, and Department of Defense (Project Themis) to carry out this work are appreciated.

TABLE OF CONTENTS

TABLE OF CONTENTS (Concluded)

LIST OF TABLES

LIST OF TABLES (Concluded)

LIST OF ILLUSTRATIONS

LIST OF ILLUSTRATIONS (Concluded)

LIST OF SYMBOLS AND ABBREVIATIONS

A = 1. constant
2. area

Å = Angstrom

A1 = nickel weld at bottom of sample cell

A2 = solder seal between inlet tube and sample cell top

AN = steel angle sides of rack

AT = air trap

AW = Apiezon W wax seal

B = 1. constant
2. canvas reinforced phenolic board

B_{2S} = second gas-solid virial coefficient for expansion in (f/kT)

B_2 = second gas virial coefficient at temperature T_i

B_{iS} = i^{th} gas-solid virial coefficient for expansion in (f/kT)

BA = base of rack in BB

BB = pipet box

BC1 = brass cylinder at top of cryostat

BC2 = brass cylinder at top of cryostat

BHV = helium valve

BLV = Teflon stem leak valve

BM = pipet manometer

BN = boron nitride

BS = one mm bore stopcock above the pipets

BT = brass tube to cryostat

LIST OF SYMBOLS AND ABBREVIATIONS (Continued)

BTE = brass tee above cryostat

BTM = Beckmann thermometer in manometer housing

BVC = brass vacuum can

BVV = valve

cm = centimeter

cm^3 = cubic centimeter

C = 1. constant
2. correction

°C = degrees Centigrade

C1 = Teflon cap for resistance thermometer

C_{2S} = second gas-solid virial coefficient for expansions in (P/kT)

$C_{i+1,S}$ = $i+1^{th}$ gas-solid virial coefficient for expansions in (P/kT)

CA = cathetometer (telescope and micrometer slide)

CAC = screw clamped collar for micrometer slide of cathetometer

CB = copper block

CBB = copper block bottom

CBT = copper block top

CC = Cajon coupling

CI = constant level illuminator

CL = constant mercury level manometer arm

CM = capacitance manometer

CS = steel cathetometer support rod

CSP = cryostat support plate

CW = slot in PG1

LIST OF SYMBOLS AND ABBREVIATIONS (Continued)

d	= density
d_1	= density of mercury at 0°C
d_g	= density of gas
$d_g(z)$	= density of gas at a vertical distance z from the surface
d_{He}	= density of the helium in CL
dc	= direct current
D	= constant
D1	= Dewar
DSC	= Dewar support cannister
emf	= electromotive force
E1	= eyelet holder for supporting copper block
E2	= eyelet holder for supporting copper block
EPS	= epoxy seal in pipet box
FC	= focal cylinder of cathetometer
FD1	= fritted disk filter
FD2	= fritted disk filter
FM1 FM2 FM3	= fiducial marks
g	= 1. acceleration of gravity 2. gram
g_1	= standard value of g
G	= gas
G1	= Dewar cannister guides
GT	= gold mercury trap
GV	= metal bellows valve

LIST OF SYMBOLS AND ABBREVIATIONS (Continued)

h = true height of the mercury column

h_1 = height of mercury column at 0°C

h_a = apparent difference in height of the mercury columns in VL and CL

h_c = corrected pressure

h_{gas} = vertical length of the gas column from the sample cell to CM

h_{He} = vertical length of the helium column from mercury level in CL to middle of CM

h_o = height of column where $g = 980.665$ cm/sec^2

h_{O_2} = vertical length of the oxygen column from the sample cell to CM

H = 3/16 inch hole in BC1

H1 = tube heater

HC_P = hydrostatic correction for pressure in the pipets

HC_{13} = hydrostatic correction for pressure in the sample cell

HE = brass heat exchanger

Hg,hg = mercury

HPC = high purity coarse

HPF = high purity fine

i = integer

i.d. = inner diameter

I = function in equation 105

I1 = gas inlet tube above SC

I2 = gas inlet tube

LIST OF SYMBOLS AND ABBREVIATIONS (Continued)

I3	= auxillary inlet tube
IO	= drill hole in sample cell top
j	= integer
J	= hole in BC2
J1, J2	= copper block heaters
J3	= lower inlet tube heater
k	= Boltzmann's constant
kg	= kilogram
°K	= degrees Kelvin
KS	= Kovar seal
LC	= mercury level setting device
L and N	= Leeds and Northrup
m	= 1. mass of mercury 2. number of determinations of the amount of gas in the system 3. integer
mm	= millimeter
mv	= millivolts
M	= mass
M_w	= 1. molecular weight 2. atomic weight of adsorbate
M_{wgas}	= molecular weight of gas
MB	= standard meter bar
MBS	= meter bar brass support cylinder
MC	= constant level arm microscope (bifilar)
MH	= manometer housing

LIST OF SYMBOLS AND ABBREVIATIONS (Continued)

MHV = valve

MI = L and N galvanometer lamp for MB illumination

MLV = Teflon stem leak valve

MM = microscope mount

MR = mercury reservoir

MRV = valve above mercury reservoir

MS1
MS2
MS3 = metal-glass seal

MT = mercury trap

MT1 = cold trap

MVV = valve

n = integer

N_a = number of moles of gas adsorbed

N_m = number of moles of gas in a monomolecular layer

N_p = number of moles of gas in pipets

N_i = number of moles of gas in the i^{th} volume

N_T = total number of moles of gas in system

$\bar{N}_T$ = average value of the total number of moles of gas in the system

N_{T_i} = total number of moles of gas in the system determined from the i^{th} measurement

$\tilde{N}$ = Avogadro's number

NBS = National Bureau of Standards

NM = dc null meter

LIST OF SYMBOLS AND ABBREVIATIONS (Continued)

o.d. = outer diameter

O_2 = oxygen

O1 = o-ring seal at top of DSC

OC1 = Swagelok o-ring fitting at bottom of MR

OC2 = Swagelok o-ring fitting at top of MR

ORC = o-ring connector on cryostat

P = pressure

P1 = phenolic resin cap

P2 = aluminum plate

PG = Philips gauge

PG1
PG2
PG3 = Plexiglas windows in manometer housing

PL = steel base plate for manometer

PS = phase separator

q_{st} = isosteric heat of adsorption

r_e = internuclear separation at the potential minimum

r_o = internuclear separation when the potential energy is zero

R = gas constant

R_N = resistance measurement made with commutator in the N position

R_o = resistance of the resistance thermometer at 0°C

R_R = resistance measurement made with commutator in the R position

R_t = thermometer resistance at temperature t

R1 = retainer for copper block bottom

RC = steel rudder cable

LIST OF SYMBOLS AND ABBREVIATIONS (Continued)

RN_m = gas constant R times the number of moles of gas in a monolayer

RO = 3/4 inch rods in BB

RT = platinum resistance thermometer

S1 = monel Swagelok union

S2-S8 = Swagelok fittings

SB = silver brazed joint in the pipet box

SC = sample cell

SC1, SC2 = stopcocks

SCB = sample cell bottom

SCS = one mm bore stopcock above the sample cell

SCT = sample cell top

SI = sides of pipet box

SL = Swagelok fitting

SL1, SL2 = Swagelok "L" fittings

SP = copper block supporting plate

SST = stainless steel tee near valve GV

ST = Wood's metal solder trough in BVC

ST1-ST4 = Swagelok tees

SV1-SV3 = stainless steel valves in manometer mercury line

t = temperature in °C

t_{mb} = temperature of MB in °C

T = thermodynamic temperature

$\bar{T}$ = average temperature along the gas inlet tube

LIST OF SYMBOLS AND ABBREVIATIONS (Continued)

T_{13} = sample cell temperature

T_{gas} = temperature of gas

T_i = temperature in °K of the i^{th} volume

T_{NBS} = temperature measured by the platinum resistance thermometer

T_p = pipet temperature

T2 = air and impurity trap

TB = turnbuckles

TC1-TC16 = thermocouples

TCS = thermocouple selector switch

TJ = Pyrex female tapered joint

TJ1, TJ2 = metal to glass seal

TO = top of rack

TR = threaded rod (3/4 inch) for adjusting VI height

TS = inlet tubing junction

V = volume of mercury at temperature t

V_1 = tubing inside the manometer housing

V_2 = volume of tubing from FM1 to SCS and housing wall

V_3 = volume of tubing above BC1 through stopcock SCS

V_4 = volume of monel tubing soldered inside the brass cylinder, BC1

V_5-V_{12} = volumes located along the sample cell inlet tube between H and the sample cell

V_{13} = volume of the sample cell

V_{BN} = volume of boron nitride sample

LIST OF SYMBOLS AND ABBREVIATIONS (Continued)

V_i = i^{th} volume (in cc)

V_o = volume of mercury at 0°C

V_p = pipet volume

V_{SC} = total sample cell volume

V3, V4 = solenoid valves

VI = illumination for manometer arm VL

VL = variable mercury level manometer arm

VW = windows in PG2

W1 = thermometer well

W2 = Pyrex wool well in sample cell top

WW = water well

z = 1. vertical distance of an adsorbate molecule from a surface
2. activity

z_o = distance from the center of an adsorbate molecule to the plane which passes through the center of the atoms in the surface layer of the solid when the interaction energy is zero

Z_N = configuration integral

Greek symbols:

α = coefficient of linear expansion

β = coefficient of cubic expansion

$\Gamma(\ )$ = the gamma function

ϵ^* = depth of the single gas molecule-solid potential well

ϵ^*_{3D} = depth of the molecular pair potential well

θ = fraction of surface sites covered by adsorbate

LIST OF SYMBOLS AND ABBREVIATIONS (Concluded)

σ = the collision diameter

μ = micron

Ξ = grand canonical partition function

SUMMARY

An adsorption virial equation of state is used in the investigation of the argon-boron nitride (hexagonal modification of boron nitride) system. The n^{th} coefficient of an adsorption virial equation, derived by statistical mechanical techniques, is related to the simultaneous interaction of n-1 gas molecules with the adsorbent and with each other. The statistical relation for the second gas-solid virial coefficient, with a Lennard-Jones (3-9) potential energy function for one gas molecule-surface interaction is used to determine the depth of the potential well and the approximate boron nitride surface area from experimental data.

A precision adsorption apparatus for making measurements on low surface area solids suitable for the virial treatment is described. The sample temperature can be controlled to ± 0.001°K over the temperature range from below the normal boiling point of nitrogen to above room temperature and the gas pressure is measured with a mercury manometer from 1-76 cm hg with a precision of ± 0.01 torr. The surface area of the boron nitride sample used is calculated to be 4.98 square meters per gram from BET treatment of a 90°K isotherm and other apparatus calibration procedures are described in detail.

Other adsorption isotherms are measured in the seldom used region above the adsorbate critical temperature. For the argon-boron nitride system several isotherms are measured in the interval from 141°K to 273.15°K and for the xenon-boron nitride, neon-boron nitride, and

krypton-boron nitride systems measurements are made at 273.15°K. These isotherms are interpreted to show that at least two different types of energy surface are present in the system. One surface (lower energy) is assumed to be the basal plane and the other surface (higher energy) is probably crystal edges. Due to the surprisingly large effect of the high energy surface, the isotherms were measured at too high pressures and a Henry's law region is not observed which complicated graphical determination of the virial coefficients. For this reason the isotherm data are treated by a computer technique to determine the gas-solid virial coefficients for each isotherm. The experimental second gas-solid virial coefficients for the argon-boron nitride system with several assumptions are used to calculate the depth of the potential well for each surface. The results of this treatment are given in the table below.

Depth of Potential Wells for the Inert Gas-Hexagonal Boron Nitride Systems

Gas	High Energy Surface (°K)	Low Energy Surface (°K)
Ne	565	346
Ar	1680	981[a]
Kr	2080	1321[b]
Xe	2700	1651

[a] R. A. Pierotti, J. Phys. Chem., 66, 1810 (1962).

[b] Alvin C. Levy, Master's Thesis, Georgia Institute of Technology, 1966.

CHAPTER I

INTRODUCTION

Imperfect Gases

The objective of the physical chemist is to apply the techniques of chemistry and physics in the measurement of properties of chemical systems. After experimental studies have been made, existing chemical and physical laws are used to formulate new theories which will adequately explain the experimental findings. The theory is usually expressed in the form of a mathematical model. This model is then tested on other systems and if necessary modified with more complete experimental information so that the behavior of unstudied systems can be predicted without making measurements. A model may become widely accepted even though it does not describe a system accurately or is only useful over short ranges. In these cases empirical equations are generally formulated which give good agreement with experimental findings but yield no information on fundamental molecular interactions.

The development of an equation of equilibrium state for real gases has been approached in this manner. In 1662 Robert Boyle found that for a given amount of gas at constant temperature, the volume decreased as the pressure was increased and it could be expressed mathematically as

$$V = \text{constant}/P \qquad (1)$$

where V = the volume of the gas

P = the pressure exerted by the gas in volume V.

Almost one and a half centuries elapsed before Gay-Lussac in 1802 discovered that the volume of a constant quantity of gas at constant pressure increased as the temperature increased

$$V = \text{constant} \times T \tag{2}$$

where T = the absolute temperature.

The findings of Boyle and Gay-Lussac along with Avogadro's prediction (equal volumes of gas at the same temperature and pressure contain the same number of molecules) are incorporated into a single ideal gas equation

$$PV/NT = \text{constant} \tag{3}$$

where N = the number of moles of gas.

This equation represents gas phase properties very well at low pressures (below one atmosphere). Van der Waals attempted to improve this equation with his famous two constant equation

$$(P + a/V^2)(V - b) = RT. \tag{4}$$

This model recognizes that molecules have forces acting between them which attract at large distances and repel at small separation distances. Since neither of the above equations described the gas phase over the entire temperature-pressure range, empirical equations were sought which would more accurately describe the experimental results. Clausius[1] and Berthelot[2] modified van der Waals' equation, Dieterici[3] introduced an

equation with an exponential factor, and Beattie and Bridgeman[4] developed a five constant equation.

In 1901 Kamerlingh Onnes[5] fit experimental compressibility data using the virial equation of state

$$P\bar{V} = A + \frac{B}{\bar{V}} + \frac{C}{\bar{V}^2} + \ldots . \qquad (5)$$

where A = first gas virial coefficient

B = second gas virial coefficient

C = third gas virial coefficient

P = pressure

$\bar{V}$ = molar volume.

The coefficients of the virial equation have been related to intermolecular potential functions by means of statistical mechanics. This allows for quantitative interpretation of deviations from ideality to be described in terms of molecular interactions. A statistical mechanical derivation (see Appendix A) yields B, in integral form, in terms of a molecular pair interaction energy $\epsilon(r)$ and a distance r. This distance r is chosen to be the distance between atomic centers of interacting atoms.

The exact nature of $\epsilon(r)$ is not known but generally a Lennard-Jones 6-12 form can be used when the gas is monatomic or spherically symmetric. Then $\epsilon(r)$ can be expressed in terms of two parameters, ϵ^*_{3D} and r_o (Figure 1), where r_o is the distance between molecular centers when the interaction energy is zero and r_e is the internuclear separation at the potential minimum, ϵ^*_{3D}. The integral for B can be solved

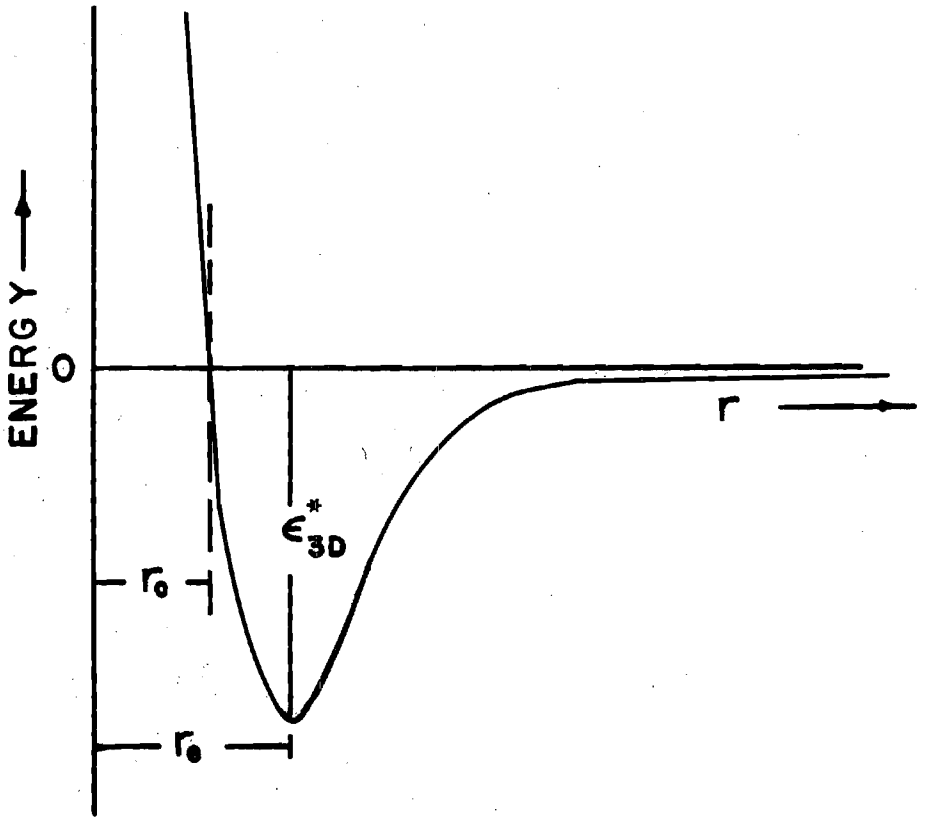

Figure 1. Lennard-Jones (6-12) Potential for Two Molecules

analytically in terms of r_o and ϵ^*_{3D}/kT. Experimental data at various temperatures can be used to extract the parameters ϵ^*_{3D} and r_o. Evaluation of the equation for B at various temperatures shows that there is a temperature where B is zero. This temperature is designated the Boyle temperature, and the gas behaves ideally over the lower pressure range. When treating molecules with rotational degrees of freedom, more complex potential energy functions are required. Attempts have been made to calculate the interaction between atoms using properties such as polarizability, ionization potential, etc. Some of these attempts (such as those of Kirkwood-Muller, Slater-Kirkwood, and London) have been quite successful.

Adsorption

General Discussion

The introduction of concentration gradients in a fluid (adsorbate) by a liquid or solid surface (adsorbent) is called adsorption. (Only gaseous adsorbates and solid adsorbents will be considered here.) This process occurs at all temperatures and pressures and the average density near the surface may be greater than or less than the bulk gas phase density. The magnitude of the effect of a second phase on the gas density is a function of temperature, gas pressure, surface structure, the interaction energy between individual gas molecules and the atoms of the solid, and the lateral interactions energy between adsorbed gas molecules.

Adsorption can be subdivided into two types: chemical adsorption (chemisorption) and physical adsorption (physisorption). Chemisorption only occurs in certain systems where electron exchange or orbital overlap

are possible and it may involve an activation energy. Generally the heat of chemisorption will be at least one or two orders of magnitude larger than the heat of vaporization of the adsorbate. Once a monolayer* has been formed, chemisorption is complete and physisorption may occur on the newly formed surface. An example of a chemically adsorbed system is oxygen on charcoal. The temperature required for removal of the oxygen is sufficiently high to cause evolution of carbon monoxide and carbon dioxide.

Physical adsorption does not involve an activation energy and will occur with any gas-solid system. This is an exothermic process with heats of the same order of magnitude as the adsorbate heat of vaporization. At temperatures near the adsorbate normal boiling point, it is convenient to picture adsorption as condensation of the adsorbate on the adsorbent surface. As the gas pressure is increased condensation continues, first forming a monolayer** which can be treated as a two-dimensional gas, solid, or liquid. If the gas pressure is increased after monolayer formation occurs, then a second layer starts forming and in this fashion multilayers of adsorbate can be condensed on the adsorbent surface by adjusting the pressure. Conventionally, physical adsorption measurements are made near the boiling point of the adsorbate. The amount of gas in the system after exposure to the adsorbent is calculated from pressure, volume, and temperature (PVT) measurements and sub-

---

*A monolayer is a film of adsorbate, deposited on the adsorbent surface, with an effective thickness of one molecular diameter.

**Actually, formation of the second molecular layer begins before the first layer is complete.

tracted from the amount of gas introduced into the system. The difference divided by the number of grams of adsorbent is reported to be the gas adsorbed at the pressure and temperature of the sample container. Other measurements are made at the same sample container temperature and the amount of gas adsorbed versus pressure is plotted for each point. (A series of points taken in this fashion at a constant temperature is called an adsorption isotherm.) For any adsorbent-adsorbate system, a series of isotherms are measured and these are used to extract thermodynamic information about the system. The most commonly reported data taken from a family of isotherms are the isosteric heats, $q_{st}(N_a)$ (Figure 2), at various adsorbate surface concentrations. This heat, $q_{st}(N_a)$, is the amount of heat absorbed when one mole of gas at constant temperature, T, and pressure, P, is desorbed from an infinitely large surface without changing the surface concentration of the adsorbate. Direct application of the Clausius-Clapeyron equation gives

$$(d\ln P/d(1/RT))_{N_a} = -q_{st} \qquad (6)$$

where N_a = the number of moles of gas adsorbed

P = pressure

T = absolute temperature.

A plot of lnP versus 1/RT at constant N_a for the isotherms measured yields a nearly straight line. The slope of this line is the isosteric heat. Plots of the isosteric heats (Figure 3) versus the amount of gas adsorbed[6] yield qualitative information about the surface used and

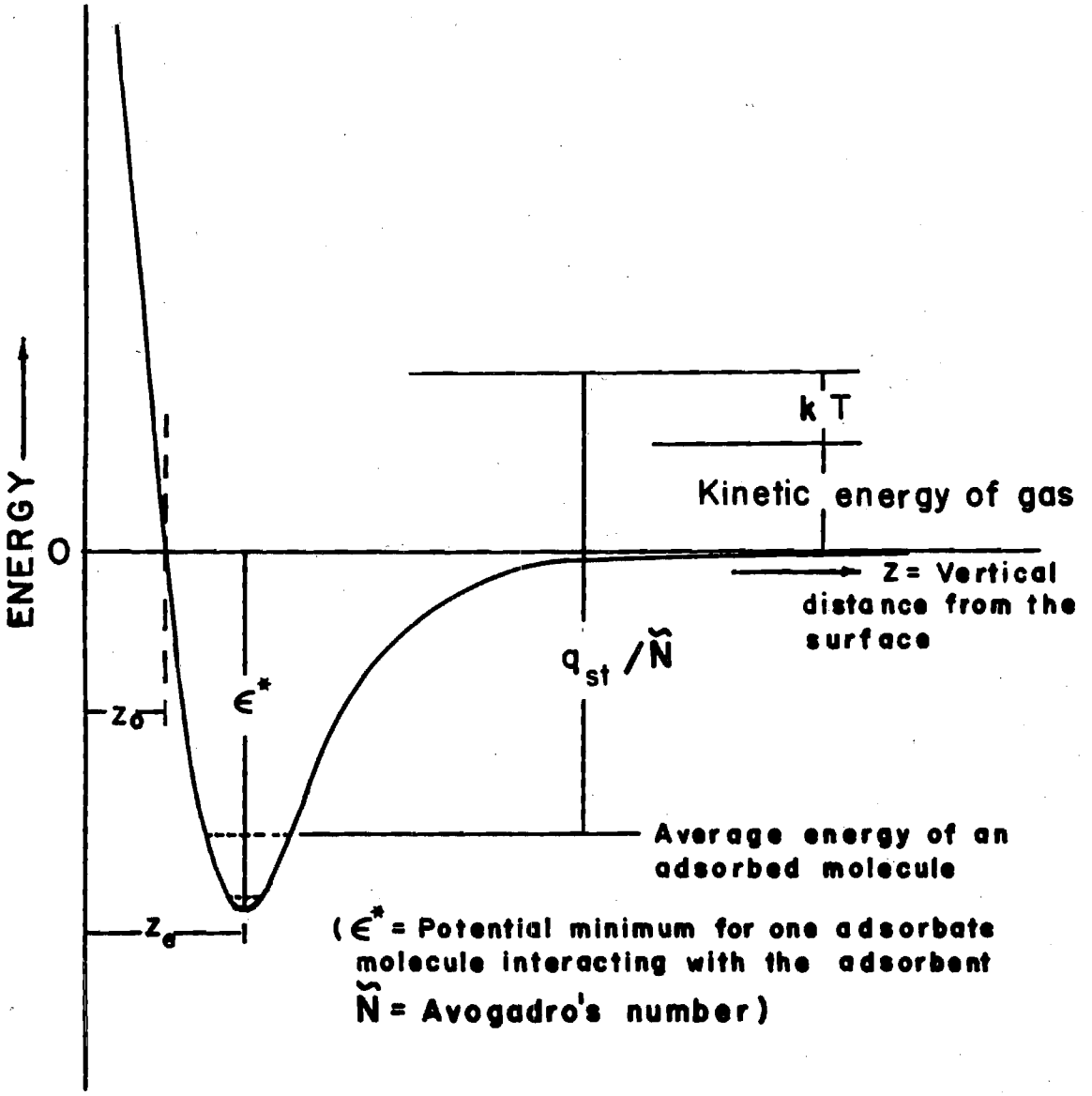

Figure 2. Isosteric Heat-Energy Relationships for a Single Adsorbate Molecule Interacting with an Adsorbent

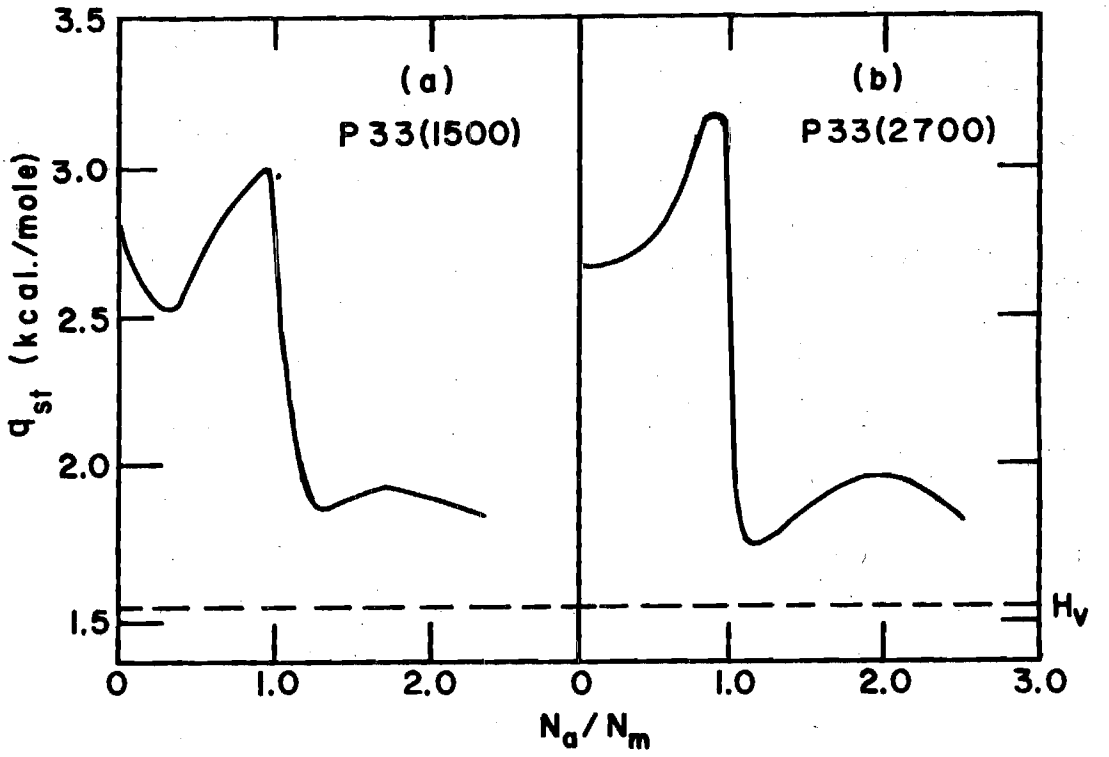

Figure 3. Isosteric Heats of Adsorption versus Coverage at 78°K for Argon on Two Graphitized Carbon Blacks (H_v is the heat of vaporization for bulk argon. N_m is the number of moles of gas required to form a monomolecular layer on the surface being discussed.)

the lateral interaction between admolecules.*

Figure 3 shows a graph of q_{st} versus N_a/N_m for the argon-P33(2700) and argon-P33(1500)(graphitized carbon black system). Several conclusions can be drawn from the figures.

1. The isosteric heat decreased initially as the high energy locations were covered on the P33(1500) but there are not a significant number of high energy areas on the P33(2700) surface to exhibit this effect.

2. There is an attractive energy of lateral interaction between adsorbed molecules because the isoteric heat increases as coverage increases to about one monolayer. This interaction seems to be less for P33(1500) but this discrepancy was possibly caused by a second layer formation on the high energy areas.

3. The isosteric heat decreases rapidly with the number of layers filled and one expects this to approach the heat of vaporization for argon at high coverages.

These surfaces (P33(2700) and P33(1500)) illustrate the difference between a homogeneous surface, P33(2700), and a heterogeneous surface, P33(1500). A surface (lying in the Cartesian x,y plane with a two dimensional unit cell (a,b,γ) is said to be homogeneous if the potential, $\mu(x,y,z)$, of an admolecule at (x,y,z) is equal to $\mu(x + ma + nb \sin\gamma, y + nb \cos\gamma, z)$ for all positive and negative integral values of m and n. A heterogeneous surface is one for which $u(x,y,z) \neq u(x + ma + nb \sin\gamma, y + nb \cos\gamma, z)$

---

*adsorbed molecules

for all positive and negative integral values of m and n. Surface imperfections such as cracks, edges, polycrystalline surfaces, surface dislocations, and imperfections inside the solid are the major causes for heterogeneity. The above definition in principle eliminates all surfaces from being homogeneous but surfaces are called homogeneous if the percent of non-uniform energy areas is small (about 0.1 percent of the total surface area). Theoretical treatments of surfaces generally are developed using the concepts of homogeneous surfaces but generally the experimental data for comparison are measured using heterogeneous surfaces.

Three distinctly different approaches to treating adsorbed layers are used. Two of the techniques treat the first adsorbed layer as a two-dimensional phase. The first method treats admolecules as if they are localized at sites* on the surface with vibrational but no translational degrees of freedom. The second treatment employs the concept of mobile adsorption where the admolecules can translate freely parallel to the surface and the vertical translational degree of freedom is replaced by a vibration. The two-dimensional parameters, spreading pressure (π) and area (A'), are more easily visualized using the spreading pressure experiments performed using films of fatty acids on water with a moving barrier film balance. The behavior of these films at low concentrations is equivalent to the ideal gas law in two dimensions

$$\pi A' = RT \tag{7}$$

where π = the spreading pressure

*A site is a surface position capable of accommodating only one molecule.

A' = the average area available to a mole of molecules in the surface film

R = Boltzmann's constant multiplied by Avogadro's number

T = thermodynamic temperature.

The spreading pressure in adsorption is not a directly observable parameter (and has no physical significance when assuming localized adsorption) but it can be related to the bulk gas pressure by the Gibbs' absorption equation

$$d\pi = (RT/A')\ d\ln f \tag{8}$$

where f = the fugacity of the bulk gas phase (the bulk gas phase will be assumed ideal and P will be used for further discussion).

If one assumes that a gas adsorbed on a solid will obey the same type ideal two-dimensional equation found with low concentrations of fatty acids on water, then substituting into the Gibbs' equation after taking the partial derivative of π at constant T and integrating yields $P = K'/A'$. This equation can be adjusted to yield

$$P = K\theta \tag{9}$$

where K = constant

θ = the average area available to a mole of adsorbate molecules at monolayer coverage divided by A', so that θ is a fractional surface coverage,

which is the adsorption equivalent of the Henry's law equation when dealing with dilute solution. The linear low coverage portion of an isotherm is generally referred to as the Henry's law region and K is called the

Henry's law constant.

In 1918 Langmuir, using a kinetic approach to adsorption as a dynamic equilibrium between gas and adsorbed molecules, derived the equation known as the Langmuir isotherm equation

$$\theta = bP/(1 + bP) \tag{10}$$

where b = a constant* which is equal to $1/P_{(\theta=\frac{1}{2})}$

θ = fraction of the surface sites covered by adsorbate.

Langmuir used the localized model for the adsorbed phase and assumed that interactions between adsorbed molecules were negligible. At high pressures it is evident that the denominator of this model approaches bP so that the maximum coverage predicted is $\theta = 1$ (a monolayer). This limits the use of the equation to the submonolayer region. At very low pressures it is seen that the isotherm will predict Henry's law behavior as the term bP becomes negligible compared with one in the denominator. Other localized models have been developed which consider the lateral interactions between adsorbed molecules. Steele[6] states that the most frequently used localized monolayer model is the Bragg-Williams or Fowler-Guggenhein isotherm.

$$KP = (\theta/(1-\theta)) \exp(-cw\theta/kT) \tag{11}$$

where K = constant

w = energy of interaction of a pair of molecules on nearest neighbor sites

---

*Fowler[7] derived an explicit expression for b using statistical mechanics.

c = number of nearest neighbor sites per site on the surface.

In 1938 Brunauer, Emmett, and Teller generalized the localized monolayer treatment to include formation of multimolecular layers to infinite thickness at the saturation vapor pressure. The resulting equation is known as the BET equation and can be written

$$\theta = \frac{CP}{(P_o - P)(1 + (C-1)P/P_o)} \tag{12}$$

or

$$\frac{P}{N_a(P_o - P)} = \frac{1}{N_m C} + \frac{(C-1)P}{N_m C P_o} \tag{13}$$

where C = constant

N_a = number of moles of gas adsorbed

P = pressure

N_m = number of moles of gas in a monolayer

P_o = saturated vapor pressure of liquid adsorbate at the isotherm temperature.

Assumptions made in developing this model are:

1. Localized adsorption.

2. All surface sites are equivalent.

3. A molecule adsorbed on a site becomes a site for another molecule so that different numbers of molecules may be stacked above different sites.

4. The heats of vaporization of the second and higher layers are assumed to be the same as the heat of vaporization of the bulk liquid.

5. Lateral interaction between adsorbed molecules is negligible..

Equation 13 shows that the constants, C and N_m (the number of moles in a monolayer), can be determined from the slope and intercept of a plot $P/(N_a(P_o-P))$ versus P/P_o. Once the number of moles of gas in a monolayer has been determined, the surface area of the adsorbent can be calculated from a product of the cross sectional area of a molecule, Avogadro's number, and the number of moles in a monolayer. The cross sectional area[8,9] to be used for the adsorbate is determined from the density of the adsorbate bulk phase corresponding to the isotherm temperature. The constant C has been related to the difference in heat of vaporization for pure adsorbate and heat of vaporization from a monolayer by Hill[10] and Cassie.[11] Many attempts have been made to modify the BET equation to account for lateral interactions of the adsorbed molecules and other models have been developed such as the Frenkel-Halsey-Hill isotherm modified by Singleton and Halsey[12] for lateral interactions. The modified Frankel-Halsey-Hill equation is

$$\ln(P/P_o)_n = - E_1/(n^3RT) + (W/RT)(1-g) \qquad (14)$$

where n = layer number

E_1 = net interaction energy for the first layer

g = surface packing factor

W = molar lateral interaction energy.

Mobile Absorption

Models employing mobile adsorption are developed from the two-dimensional form of a gas equation of state or by modifying a liquid

theory. The Volmer* [13] and the Hill-de Boer[14] equations were derived by assuming that the adsorbed film behaved as a two-dimensional gas obeying the equation

$$\pi = kT[\theta/(1-\theta) - ((\alpha\theta^2)/(kT\beta))]/\beta \qquad (15)$$

where β = constant

α = constant in Hill-de Boer equation

α = zero in Volmer equation

θ = fraction of the adsorbent surface covered by adsorbate.

The two-dimensional models are converted into the isotherm equations

$$P = K(\theta/(1-\theta)) \exp [\theta/(1-\theta) - (2\alpha\theta/kT\beta)] \qquad (16)$$

where K = constant

α = zero in the Volmer equation

α = constant in the Hill-de Boer equation

using the Gibbs' relation. Other equations for mobile monolayer adsorption with lateral interactions on a homogeneous surface have been developed from existing liquid theories; Devonshire[15] applied the Lennard-Jones Devonshire cell theory of liquids,[15] Steele[16] adapted the scaled particle theory, and Pierotti and McAlpin[17] modified the significant structures theory of liquids.[18] These treatments have been developed from statistical mechanical treatments with parameters directly associ-

---

*Discussed recently by J. P. Stebbins and G. D. Halsey, Jr., Journal of Physical Chemistry, 68, 3863 (1965).

ated with molecular interactions.

Several different authors[19] (Appendix B) have used the techniques of statistical mechanics to extend the virial treatment of imperfect gases to adsorption. The gas adsorbed by a solid is expressed

$$N_a = \sum_{i \geq 1}^{\infty} B_{i+1,S}(f/RT)^i \qquad (17)$$

where B_{iS} = i^{th} gas-solid virial coefficient*

f = fugacity of the adsorbate in the bulk gas phase

N_a = the number of moles of gas adsorbed.

The virial coefficients, B_{iS}, are functions of temperature and are related to the interaction between individual gas molecules and the surface, and the interaction among adsorbed gas molecules. Thus one can gain definite information about the adsorptive process by relating the virial coefficients to interaction parameters.

Virial Approach to Adsorption

Halsey and his co-workers[21-27] were first to demonstrate the applicability of the virial equation to experimental adsorption. Steele and Halsey[21] measured adsorption isotherms on several high surface area heterogeneous adsorbents in the little used range above the bulk adsorbate critical temperature where capillary condensation, multilayer formation, and lateral interactions can be ignored. Isotherm points were measured in the low coverage region that obeys the Henry's law adsorption equation. In this region the only effective interaction is between

---

*Notation for B is that used by Pierotti.[20]

individual gas molecules and the surface. (The surface was defined as the plane passing through the centers of the atoms that make up the surface and was assumed to be energetically uniform.) A Maxwell distribution was assumed for the gas density so that the apparent volume of the sample cell was given by the equation

$$V_{app} = \int_{V_{geo}} e^{-\epsilon/kT}\, dV \tag{18}$$

where V_{app} = apparent volume of sample cell

V = volume

V_{geo} = geometric volume of the sample cell

ϵ = interaction energy between a gas molecule and the adsorbent

and

$$V_{ex} = \int_{V_{geo}} (e^{-\epsilon/kT} - 1)\, dV \tag{19}$$

where $V_{ex} = V_{app} - V_{geo}$ = excess volume.

An interaction potential of the Sutherland[28] type was chosen to represent the interaction of an adsorbate atom with an atom of the adsorbent. It was further assumed that the summation over each atom of the solid could be replaced by an integration to yield

$$\epsilon = 0 \qquad z \leq z_0 \tag{20}$$

$$\epsilon = (-\epsilon^* z_0^3)/z^3 \qquad z > z_0$$

where ϵ^* = potential minimum for interaction between an adsorbate molecule and the adsorbent

z = vertical distance from the surface

z_o = distance of closest approach.

When this potential function was substituted into the equation for excess volume, the resulting expression could be integrated to yield

$$V_{ex} = Az_o \sum_{j=0}^{\infty} (j!(3j-1))^{-1} (\epsilon^*/kT)^j. \qquad (21)$$

Since V_{ex} was determined experimentally, Az_o and ϵ^*/k could be adjusted until a best fit of the experimental data was found. The ϵ^* was used with the Kirkwood-Muller equation to evaluate z_o which in turn allowed A to be calculated from Az_o. This approach allowed the surface area to be evaluated without estimating the adsorbate molecule cross sectional area.

Freeman and Halsey[23] extended the theoretical treatment to cover simultaneous interaction between adsorbate molecule pairs and the surface. The experimental work done by Steele and Halsey and Freeman and Halsey was on poorly defined surfaces so that more clear results could be obtained on a well characterized surface. Constabaris[24] developed a precision adsorption apparatus for use with the low surface area, homogeneous graphitized carbon black P33(2700). The apparatus was calibrated and preliminary measurements were made with several P33(2700) inert gas systems.

Sams, Constabaris, and Halsey[22,24,25] did extensive experimental work on P33(2700) with the inert gases, methane, deuteromethane, hydrogen,

and deuterium using the apparatus described by Constabaris. The apparent sample cell volume was determined at several different pressures for each isotherm. Extrapolation of a plot of apparent volume versus pressure (to zero pressure) gave the apparent volume at zero pressure. This apparent volume was equal to a sum of the geometric volume of the sample cell plus the second gas-solid virial coefficient, B_{2S}. B_{2S} was defined by the equation

$$B_{2S} = \int_{V_{geo}} (e^{-\epsilon/kT}-1)\, dV. \qquad (22)$$

Four different potential models used to analyze the data were:

1. The Sutherland potential integrated over a semi-infinite solid.

2. A Lennard-Jones 6-12 potential integrated over a semi-infinite solid to yield a 3-9 potential.

3. A Lennard-Jones 6-12 potential integrated over a semi-infinite solid for the attractive part to yield a 3-12 potential.

4. A Lennard-Jones 6-12 potential integrated over an infinite plane to yield a 4-10 potential.

The first model has been discussed with the Steele and Halsey treatment, and others can be expressed in terms of the potential minimum ϵ^* and a position z_o where the interaction energy is zero (Figure 4). (When the surface is assumed to be energetically uniform as has been done with this treatment, then z_o is the vertical distance from the surface.) Figure 4a shows how the potential energy of a single atom varies as a function of its vertical distance from the surface if the system is dilute enough so that interaction with other molecules in the gas phase

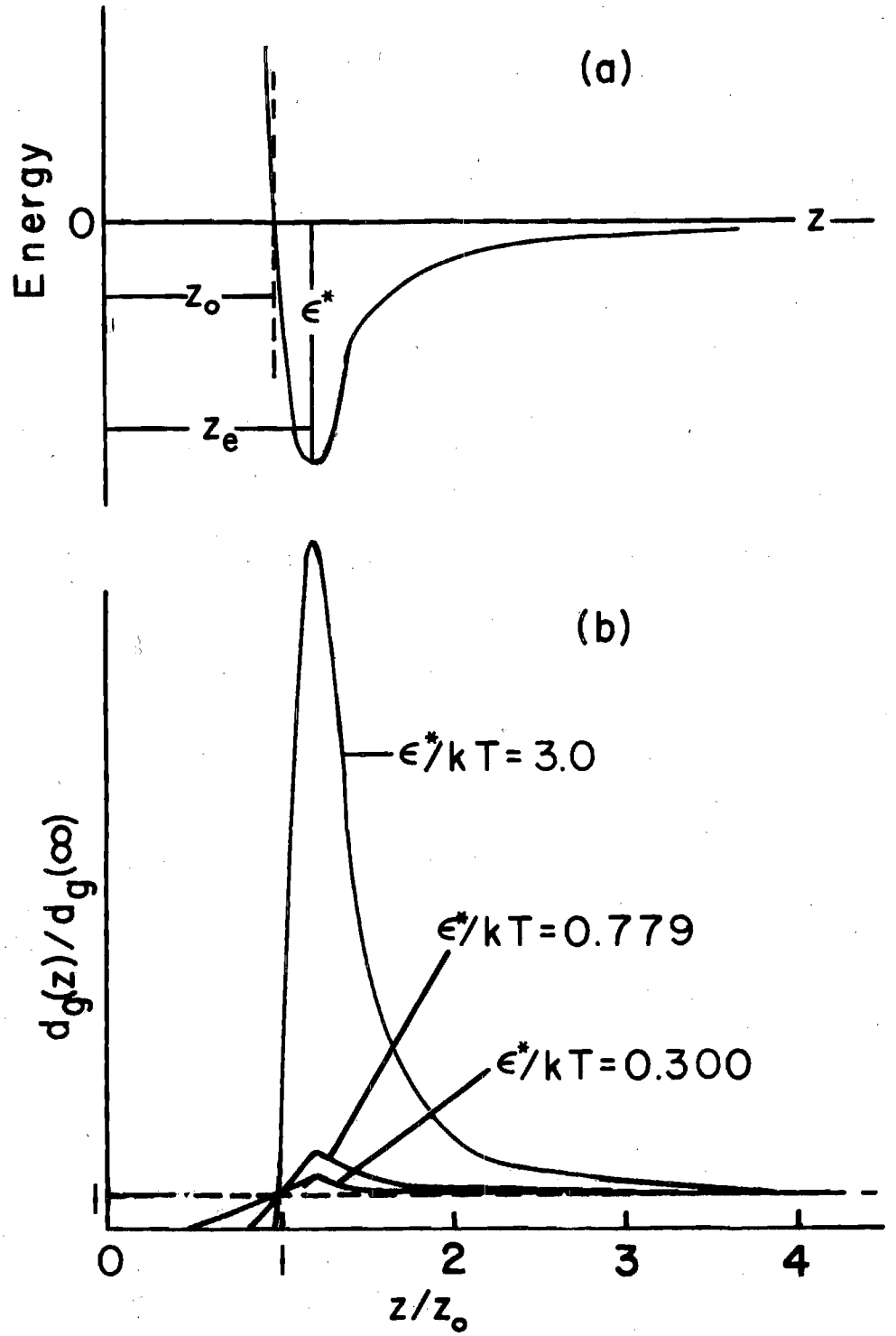

Figure 4. a. Potential Energy of an Admolecule as a Function of Distance from the Adsorbent Surface

b. Reduced Density versus Reduced Distance from the Surface for the Adsorbent-Adsorbate System in 4a at Different Values of ϵ^*/kT (Admolecules were assumed not to interact in this figure.)

can be neglected. Curves for the three reduced temperatures, kT/ϵ^*, in Figure 4b show how the reduced density, $d_g(z)/d_g(\infty)$, for the dilute gas described above varies in the potential field shown in Figure 4a ($d_g(z)$ is the gas density at a vertical distance z from the surface, $d_g(\infty)$ is the density of the gas when it is not in the potential field of the surface). Pierotti[29] used the three curves in Figure 4b to illustrate positive and negative adsorption in the Henry's law region. If the area under the reduced density curve is greater than the area under the dotted line, then there will be positive adsorption and if the reverse is true then there will be negative amounts of gas adsorbed. If the area under the reduced density curve is exactly equal to the area under the dotted line, then B_{2S} is zero and this temperature corresponds to the gas-solid analogue of the Boyle temperature. A plot of $[d_g(z) - d_g(\infty)]/[dg(z_e) - d_g(\infty)]$ versus the vertical distance of admolecules from the surface (Figure 5) demonstrates that for low ϵ^*/kT larger percentages of the total amount of gas adsorbed are from long range concentration gradients than for high ϵ^*/kT. ($d_g(z_e)$ is the maximum gas density which occurs at a distance z_e from the surface.)

The equation for B_{2S} has been solved analytically (Appendix C) when Lennard-Jones potential functions were substituted for ϵ and the integration over V_{geo} was replaced by integration over all space to give equations of the form

$$B_{2S} = Az_o\, f(\epsilon^*/kT). \tag{23}$$

Replacing V_{geo} by infinity is a reasonable assumption since these potential functions represent short range interactions.

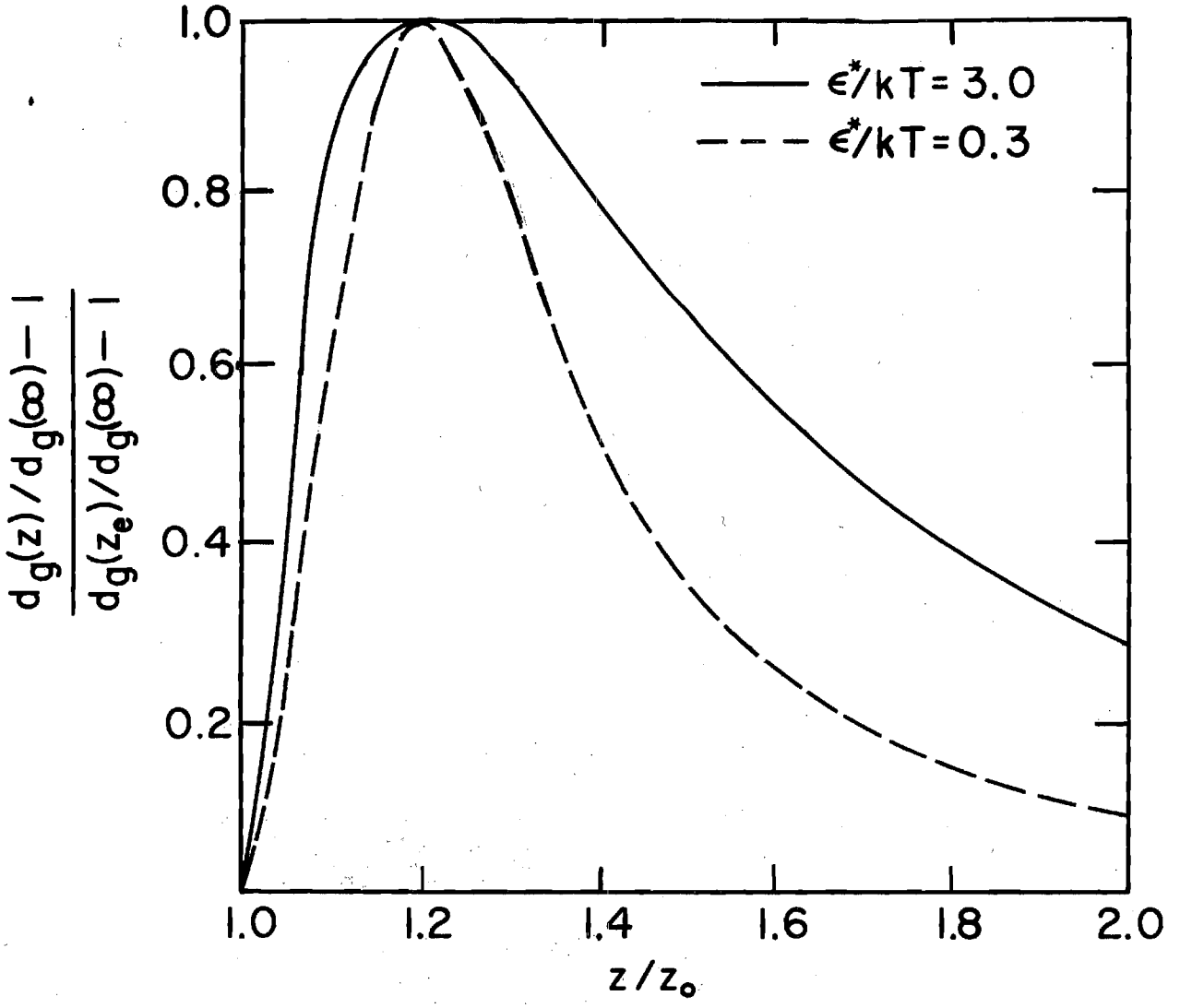

Figure 5. A Function of Density versus Reduced Distance

Equation 23 was rearranged to

$$B_{2S}/f(\epsilon^*/kT) = Az_o \qquad (24)$$

and was used to obtain a locus of values of Az_o and ϵ^*/k for each B_{2S}. A plot of Az_o versus ϵ^*/k was made for each B_{2S} and a representative curve was drawn through the points (see Figure 35). When this was done for each B_{2S}, the lines intersected at a point which represented the best fit value of ϵ^*/k and Az_o. (This fitting technique is usually done using a computer.) A poor fit was found when using the Sutherland model but the ϵ^*/k values for the three potential functions derived from the Lennard-Jones 6-12 models were close and a best model could not be chosen. Various attractive potential models such as the Slater-Kirkwood, Kirkwood-Muller, and London were used to calculate surface areas from the attractive potential of the interaction models used. The Kirkwood-Muller model gave more consistent results than the other two but the areas were about 40 percent smaller than the BET values. Experimental values for the third gas solid virial coefficient, B_{3S}, were determined. The second and third gas-solid virial coefficients were related to the second virial coefficient[26] of an imperfect two-dimensional gas on the absorbent surface. This virial coefficient was then used to obtain the interaction parameter ϵ^*_{2D} for two adsorbed molecules and the area of the adsorbent, A. This was a new method for determining the surface area without assuming an attractive potential form such as the Kirkwood-Muller equation. The ϵ^*_{2D} value was nearly that predicted by Sinanoglu and Pitzer's[30] equation for interacting molecules in a potential field. Barker and

Everett[31,32] have modified the two-dimensional gas treatment to correct for non-planarity of adsorbed molecules.

The efforts of Halsey and his co-workers have stimulated much theoretical activity toward treating adsorption as an imperfect gas in a potential field. However, little new experimental data (other than Halsey's) is reported. This is probably because of the precision equipment and time required to make such measurements.

Statement of the Problem

The purpose of this work was to initiate an investigation of the interactions of the inert gases with a homogeneous surface (other than graphitized carbon blacks) using the virial approach described above.

Choice of adsorbents was limited but the hexagonal modification of boron nitride has been reported to be homogeneous.[33] Boron nitride, BN, is a fine white powder of thin platelets whose surface is assumed to be the planar surface. BN is isoelectronic with graphite and has a graphite like structure. This material has not been as well characterized as the graphitized carbon blacks but several authors[34-36] have calculated the potential minimum, ϵ^*, for the BN inert gas systems.

The method of attacking the problem was:

1. To design and build an apparatus with capabilities similar to those of Constabaris'.[24]

2. To characterize the apparatus.

3. To measure adsorption isotherms for neon, argon, krypton, and xenon at the ice point and make measurements with argon at other temperatures.

4. To reduce the raw experimental data to useful form and determine the values of ϵ^* and Az_o for the argon-solid system and compare ϵ^* with the calculated values.

5. To treat the data to get ϵ^*_{2D} for two interacting admolecules and to compare it with the value predicted by Sinanoglu and Pitzer's equation.[30]

CHAPTER II

APPARATUS

Introduction

An apparatus is described for making adsorption measurements of sufficient accuracy for the determination of the second (B_{2S}) and third (B_{3S}) gas-solid virial coefficients. The requirements of such an apparatus have been discussed in detail by Constabaris.[24]

To obtain B_{2S} and B_{3S} from equation 17, the parameters P, T, and N_a must be known. Pressure was measured with a manometer, temperature was measured with a resistance thermometer, and N_a was determined indirectly from gas measurements by computing the apparent amount of gas in the system before and after exposure to the adsorbent. The difference gave the amount of gas adsorbed. This technique required accurate values for all of the system temperatures and volumes. Thus the apparatus is discussed in three major sections: the sample temperature measurement and control system, the pressure measuring system, and the dosing system. These are presented under the titles: The Cryostat, The Manometer, and The Gas Transfer System.

The Cryostat (Figure 6)

Two types of cryostat were considered for this system: the adiabatic calorimeter described by Constabaris, Singleton, and Halsey,[24] and the massive metal block thermostat of Morrison and Young.[37] Both were suitable for this work since they were capable of temperature control to

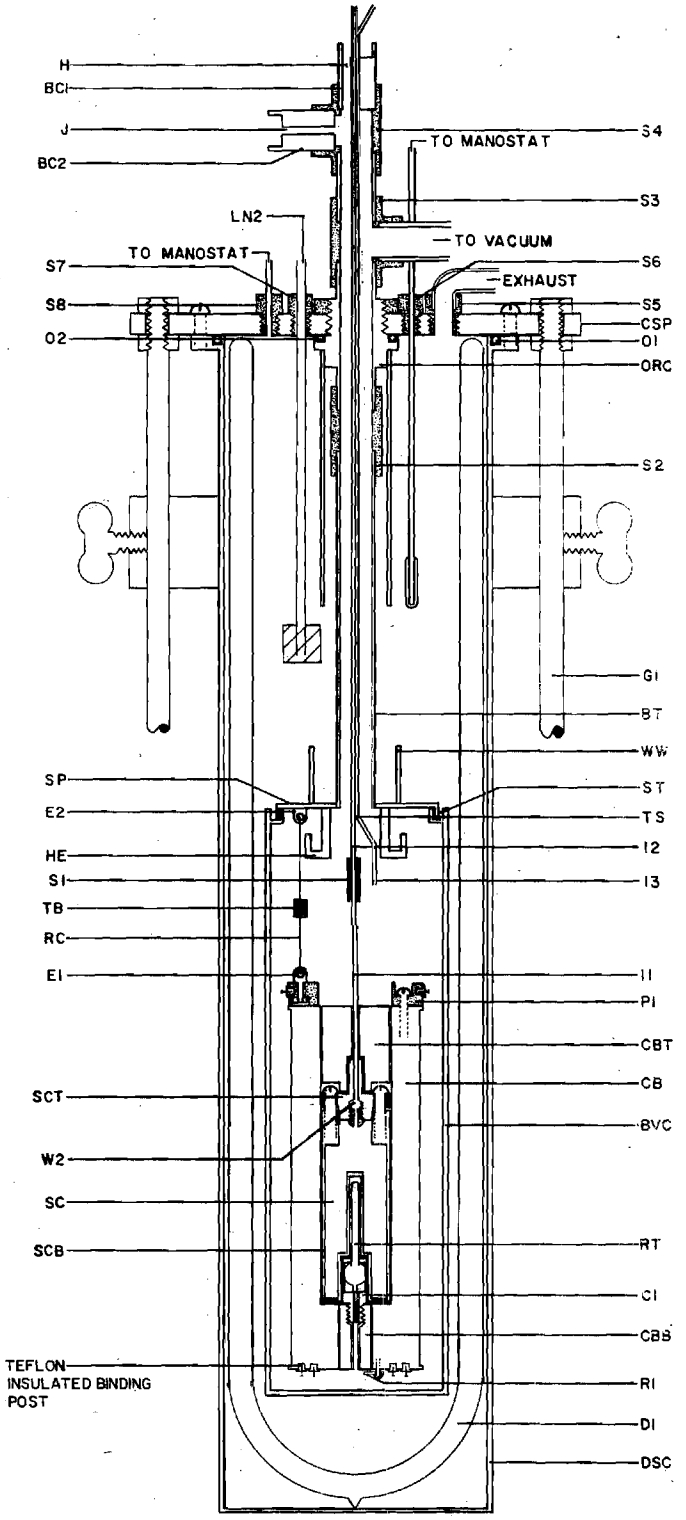

Figure 6. Cryostat

.001°C for extended periods and could be used over long temperature ranges (i.e. from below 78°K to above 273°K). Since the two systems offered the same temperature range and control, selection was made on the apparent ease of operation and construction. The apparatus of Morrison and Young required that only the resistance thermometer be monitored and one heater controlled. Constabaris' system required continuous monitoring of three thermopiles and control of three heaters. For this reason it was decided that the metal block thermostat (Morrison and Young) would be used although the thermometer would be located in the middle of the sample cell as in Constabaris' design.

The adsorbent was contained in the sample cell, SC (Figure 7), which had an internal volume of about 80 cm^3. This large volume was necessary for the amount of adsorbent required to give a reasonable surface area for this work. SC was all nickel construction with a thermometer well, El, welded* into the bottom at Al for the platinum resistance thermometer, RT. The top of SC, SCT, had a 1/16 inch axial hole, IO, extending from the threaded recess, W2, to the outside of the sample cell. IO was drilled with a 51 drill and Nioro solder** was used to solder a 1/16 inch piece of monel tubing into it. The monel tubing seemed to dissolve in this solder. A 52 drill was used to reopen the plugged hole, leaving a thin film of gold-nickel solder on the surface. Gas inlet

---

*Welded by Potter and Rayfield, Inc., 1570 Northside Drive, Atlanta, Georgia.

**Eighty-two percent gold - 18 percent nickel, trademark Nioro, purchased from Western Gold and Platinum Company, 525 Harbor, Boulevard, Belmont, California.

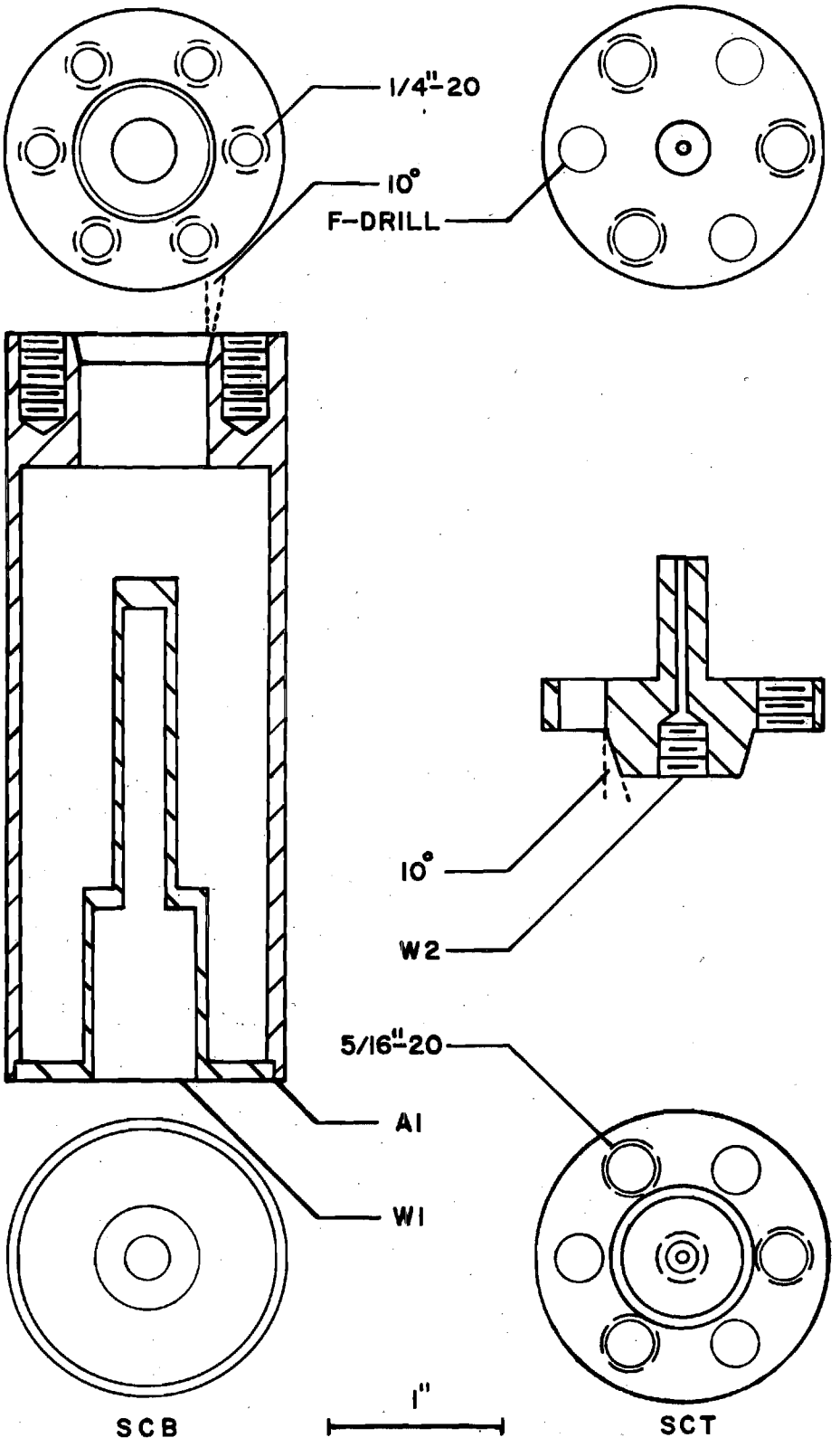

Figure 7. Sample Cell, SC

tube I1* was pushed through I0 to W2, and silver soldered** at A2. Use of a graded solder seal was necessary because the silver-copper solder did not "wet" nickel. A 1/4 - 20 stainless steel screw with a drill size 52 hole through its center was used to hold a piece of loosely packed Pyrex wool in W2. This Pyrex wool was used to prevent the adsorbent from being blown from SC when the pressure above it was reduced. SCT was connected to the sample cell bottom, SCB, by placing a previously prepared and well annealed copper gasket*** between their tapered surfaces,[38] then evenly tightening the six equally spaced 1/4 - 20 stainless steel bolts which had been previously coated with "silver goop"**** to prevent galling. After assembling the sample cell, it was evacuated and heated to 400°C; on cooling the bolts were retightened. This design was very effective; no leakage was observed after several cyclings between the liquid nitrogen temperature and about 550°C.

The head of the resistance thermometer, RT, was encapsulated in a Teflon container, C1. C1 had a threaded top with four holes that allowed passage of the resistance thermometer leads to RT. The top of C1 served as a radiation shield and was threaded into a copper cylinder, CBB, thus allowing all of the resistance thermometer, RT, to be mounted in the

---

*One-sixteenth inch monel tubing with ten thousandths wall thickness purchased from Superior Tube Company, Wapakoneta, Ohio.

**Aircosil M. Brazing Alloy, purchased from Air Reduction Company, Atlanta, Georgia.

***The gasket was made from a sheet of 0.010 inch thick electrolytic grade copper.

****"Silver goop" purchased from Crawford Fitting Company, 884 East 140th Street, Cleveland, Ohio.

thermometer well, W1, in the sample cell bottom. Thermal contact between the walls of W1 and RT was provided by a thin film of vaseline.* The top of the copper block, CBT, was a "split" copper cylinder with a diameter 0.005 inch smaller than that of SC. It had six equally spaced holes that fit over the sample cell top retainer bolts. CBT also had a center hole that allowed passage of inlet tube I1, and a 1/4 inch diameter counter set hole that fit the top of SCT. The assembly CBT and SC fit snuggly inside the large copper block, CB, with CBB, the copper block bottom, fitting in a hole in the bottom. CBB was held in place by a retainer, R1. Copper block CB was the main thermostating block with a mass of about six kg and walls of 5/8 inch thickness. A canvas reinforced phenolic resin cap, P1, was attached by three equally spaced screws threaded into the copper block, CB. P1 had three equally spaced eyelet holders, E1 (one is shown in Figure 5), which provided support for CB. E1 was connected to E2, an eyelet soldered to the main supporting plate, SP, by a piece of 1/16 inch steel rudder cable, RC. CB was leveled by adjusting the three turnbuckles, TB, which were located near the midpoint of RC. SP was silver soldered to a 3/4 inch outer diameter brass tube, BT. Also, silver brazed to the support plate, SP, was a brass heat exchanger, HE, and a water well, WW. WW was filled with water to prevent damaging wires that entered the cryostat when the brass vacuum cannister, BVC, was attached to AP by filling the solder trough, ST, with Woods metal. The brass tube, BT, was joined to a specially machined bulkhead

---

*Vaseline, White Petroleum Jelly, Chesebrough-Ponds, Inc., New York, New York.

type o-ring connector, ORC, by a 3/4 inch brass Swagelok* union, S2. ORC provided a rigid connection to the 3/8 inch thick brass plate, CSP, which supports the cryostat assembly. CSP was attached to the top of an I-beam which extended from the floor and was further supported in front by Dewar cannister guides, G1. Access to the inside of BVC was provided above the cryostat support plate, CSP, by joining two 3/4 inch Swagelok tees, S3 and S4 (using Teflon front and brass back ferrules) to the external port of the special o-ring connector, ORC. S3 was connected to a high capacity diffusion and roughing pump station through 3/4 inch copper tubing and associated valves. A brass cylinder, BC1, with two 1/16 inch monel tubes (I2 and I3) brazed in adjacent longitudinal holes, was mounted in the port of S4 that was parallel to the brass tube, BT. I2 was the gas inlet tube for the sample cell, SC. It was connected to I1 by a 1/16 inch monel Swagelok union, S1 (monel front and rear ferrules). Sample cell inlet tube I1 has been connected to and removed from I2 at S1 several times with no apparent leakage after the connection was remade. I3 was an auxiliary gas inlet tube to be used if I2 became clogged or broken. A 3/16 inch hole, H, extends from the top of brass cylinder, BC1, parallel to I2, to the inside of S4. A second brass cylinder, BC2, with a 1/4 inch diameter axial hole, J, extending from the recessed area at the top through the length of BC2, was fitted into the remaining opening in S4.

The cryostat support plate, CSP, was faced on its underside so that a vacuum tight fit could be made with the Dewar support cannister,

---

*Swagelok--registered trademark of the Crawford Fitting Company, 29500 Solon Road, Solon, Ohio 44139.

DSC, at the o-ring seal, O1, on the top of DSC. DSC was attached to CSP by tightening eight screws through CSP into tapped holes in the flange of DSC, outside of O1. A closely fitting Dewar,* D1, mounted inside the Dewar support cannister, DSC, was supported at its bottom by a formed cork support and at its sides by one thickness of 1/16 inch rubber sheet. When the Dewar support cannister, DSC, and the cryostat support plate, CSP, were attached, entrance into D1 for environment control was through a series of Swagelok tube to pipe fittings S5-S8. A 1/2 inch copper tube leads away from S5 to a tee. One arm of the tee exhausted the system through a normally open solenoid valve, V3, directly to the atmosphere. The other arm of the tee was directed through a normally closed solenoid valve, V4 (not shown), to a vacuum pump. The valve, V4, was operated by an oxygen vapor pressure thermometer (not shown). The probe for the manometer was admitted to the system through S4, a 1/8 inch brass fitting. The other solenoid valve was operated by another vapor pressure thermometer. This manometer used the inside of the Dewar D1 as the probe and the bath as its controlling liquid. The connecting tubing for this manometer entered through S8. The last entry into the Dewar was S7, a 1/4 inch brass fitting that admitted the refrigerant filling tube. This tube had a phase separator, PS, on its end.

Two bundles of wires entered the cryostat: one through hole H, in brass cylinder, BC1, and the other through hole J, in brass cylinder, BC2 (Figures 8 and 9). The bundle that entered through hole H was the inlet tube wiring consisting of one heater, H1, and eight thermocouples,

*Purchased from H. S. Martin and Son, Evanston, Illinois, catalog number M203100-S, cylindrical 120 mm i.d., 150 mm o.d., 700 mm deep.

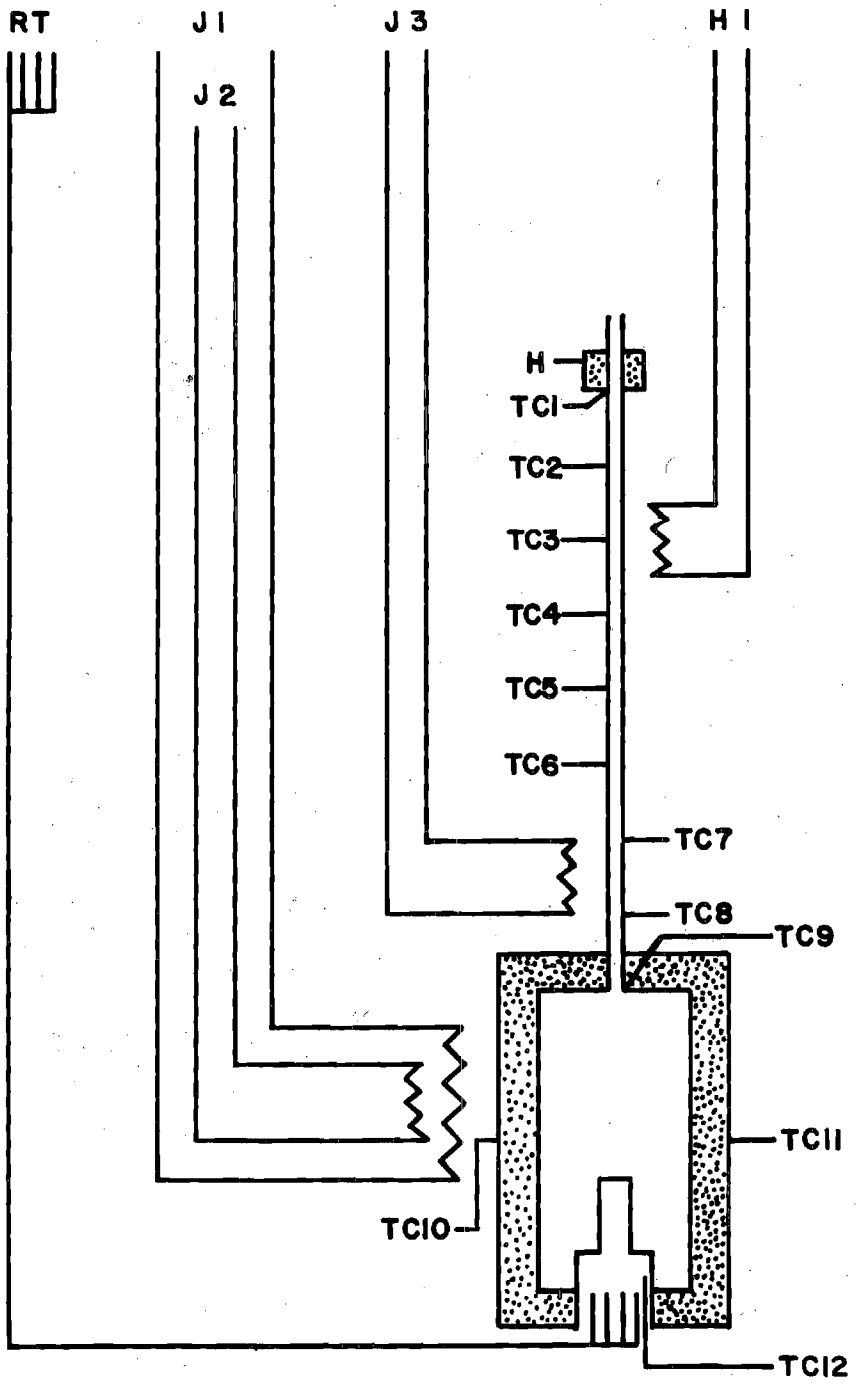

Figure 8. Internal Cryostat Wiring

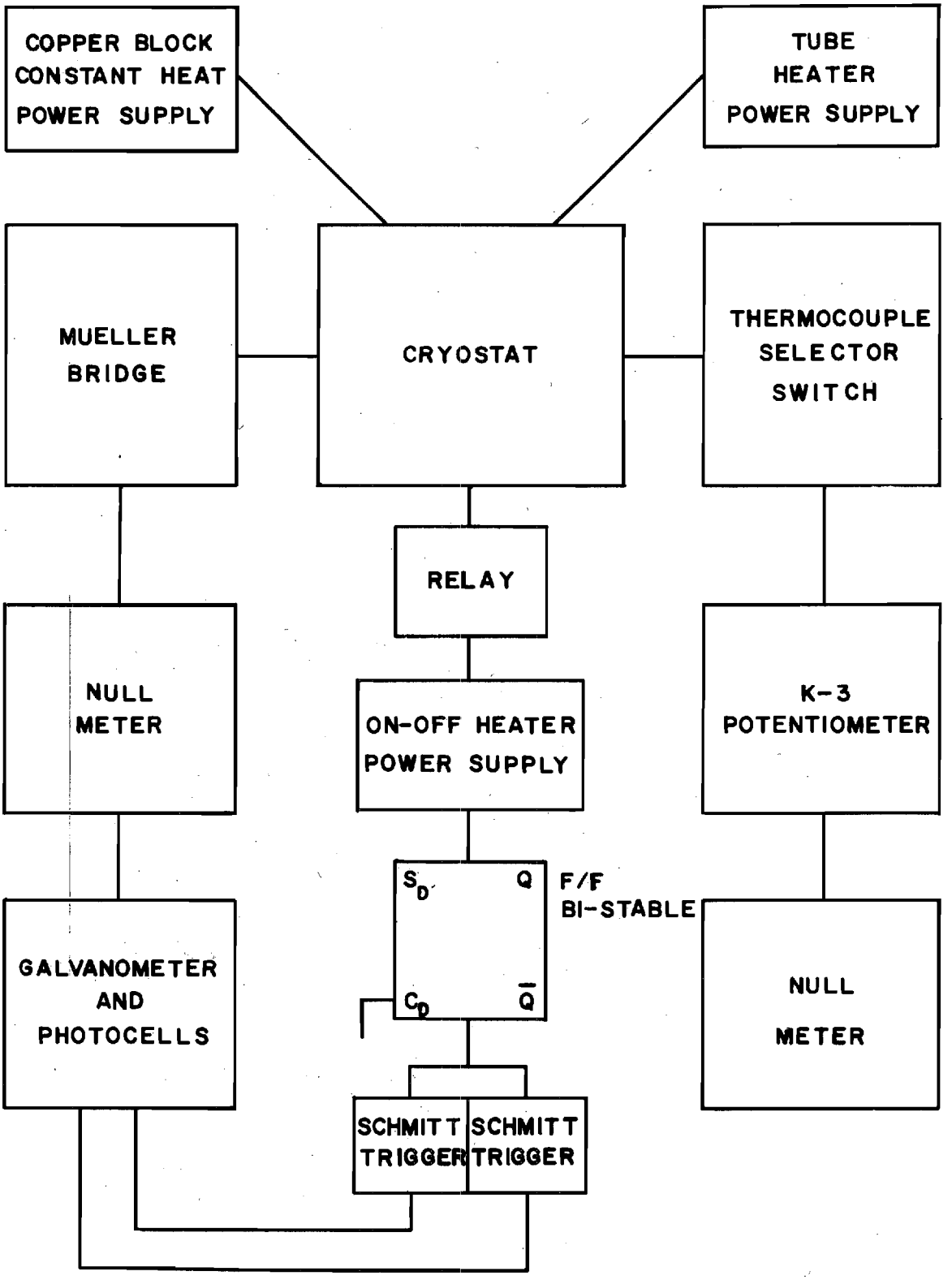

Figure 9. Block Diagram of Circuits

TC1 to TC8. This method of preparation made the tubing and its wiring separate from the remainder of the cryostat wiring so that it could be removed if necessary for repairs or replacement without disturbing the remainder of the cryostat and its wiring. The tubes I2 and I3 were soldered together along their length and seven equally spaced (7.67 cm) nichrome clips were soldered between the tubes from below the brass cylinder BC1 to where they separate at TS, above the Swagelok fitting S1 (Figure 6). The tubes were then coated with Glyptal* and baked with infrared lamps for eight hours. Eight copper-constantan** thermocouples, which had been previously prepared by carbon arc welding in a helium atmosphere, were positioned along the tubes with one junction held in position by each nichrome clip and the eighth one hanging about eight centimeters below the tubing junction, TS. The junction of each thermocouple was insulated by pressing it between two pieces of "Stripteeze"*** before positioning them under the nichrome clips. When all thermocouple junctions were in position, the lead wires were taped in the groove between the tubes so that later they could be pulled through hole H in brass cylinder BC1. The tubes were then wound with Leeds and Northrup 24 gauge cotton and enamel insulated constantan wire from TS to the bottom of brass cylinder BC1. This winding was designated tube heater H1. The heater and thermocouple lead wires were bunched together and wrapped with two thicknesses of Teflon tape to prevent scraping or breaking the insu-

---

*General Electric type 1202 clear varnish.

**Leeds and Northrup cotton and varnish insulated 32 SWG wires.

***Stripteeze--one half inch wide Teflon pipe thread tape distributed by the Crawford Fitting Company, Solon 39, Ohio.

lation when the wires were pulled through hole H. The wiring on inlet tubes I2 and I3 from TS to BC1 was painted with Glyptal and baked. The cup on top of brass cylinder, BC1, was heated and Apiezon W wax was melted into the cup until it ran freely around the wires through hole H and appeared to "wet" the brass cup. Just above BC1, all the constantan wires were soldered to the constantan lead of a copper constantan thermocouple that was used in an ice bath as a reference. The copper leads, including the reference, were connected to a Leeds and Northrup type 8248-16 thermocouple selector switch, TCS. The tube heater H1 was powered by a Hewlett Packard model 6125A dc power supply (0-60 volts, 0-250 ma).

The second bundle of wires entered the cryostat through hole J in brass cylinder BC2. This bundle contained leads for the resistance thermometer, four thermocouples, three heaters, and several extra wires. A seven foot length of the wire bundle was pulled through hole J and waxed in with Apiezon W wax as were the tube wires. The seven foot length of wires was wrapped with 1/4 inch polyethylene heli-wrap. When BC2 was to be fixed into position in Swagelok tee, S4, the ends of the wires were pulled through S4 and down brass tube BT, then wrapped three times around heat exchanger well, HE, and taped into position. The lower loose end was cut so that about 16 inches extended below the heat exchanger, HE, and the heli-wrap was cut where the wires left HE. About one half of the length of the wires near HE were wrapped in a figure eight shape one inch long and tied. The ends of the thermometer and thermocouple wires were tinned and each wire was marked with a number so that it could be identified easily and attached to the proper binding

post. Banana plugs were put on the ends of the heater leads and they were marked J1, J2, and J3.

The outside of the copper block, CB, was painted with Glyptal and baked. Then two thermocouples, TC10 and TC11, were placed at opposite sides of CB and centered with respect to the top and bottom. The couples were insulated by pressing each junction between two small pieces of Teflon tape. These were held in position by tape while other work was being done. Four pieces of 24 gauge cotton and enamel insulated copper wire and one copper constantan thermocouple, TC12, were run the length of copper block, CB, with about four inches extending past the ends, and taped in position. The block was then tightly wound its entire length with 24 gauge constantan wire to form heater J1 (about 136 ohms); winding was started at the bottom so that both ends of the wire extended from the top of CB. The new wire on CB was painted with Glyptal and baked with an infrared heater about 20 hours. A second layer of constantan wire, heater J2 (about 140 ohms), was wound on CB in a similar manner, Glyptaled, and baked with an infrared heater as before. The 24 gauge copper wires were connectors for resistance thermometer, RT. They were attached to Teflon insulated terminals on the phenolic cap, P1, (top of the copper block), and to the same type of terminal at the bottom of CB. The wires from RT could be quickly joined to the Teflon insulated terminals on the bottom of CB and the wires from the Mueller Bridge entering through hole J were soldered to the Teflon insulated terminals at P1. The heater wires from the block were soldered to banana jacks on top of P1. The block heaters J1 and J2 were powered by a twin dc power supply (Power Design type TW5005). During operation one heater, J1, was furnished

power at a constant rate which very nearly balanced the heat lost to the bath by radiation and conduction, and the other heater, J2, was an on-off heater controlled from the resistance thermometer so that the temperature was maintained nearly constant. The fourth copper-constantan thermocouple, TC9, was arranged so that it could be placed on top of the sample cell, SC, by running it between the copper block top, CBT, and the sample cell inlet tube, I1. The constantan leads of the thermocouples TC9-TC12 were soldered to one of the Teflon insulated terminals. The copper leads were attached to the same type terminals but only one copper wire was soldered to each binding post. The constantan terminal served as a common junction for joining the couples inside the cryostat to an ice bath reference junction. A constantan wire was provided in the bundle entering through hole J for this purpose. Copper wires were furnished for leads from the thermocouple terminals on the phenolic cap, P1, to the thermocouple selection switch, TCS. Two additional wires were necessary in this bundle. These wires furnished power for the tube heater, J3. This heater warmed the gas inlet tubing from where tubes I2 and I3 split at TS to the top of the copper block, CB. If this had not been done, the adsorbate may have condensed in the sample cell inlet tube, I1. Heater J3 was a section of 24 gauge constantan wire which had been folded on the adhesive surface of fiber glass backed tape. This heater could easily be removed and replaced. TC8 was taped into position on I1 halfway (6.1 cm) between TS and the top of the copper block, CBT, before putting the heater tube J3 on the sample cell inlet tube, I1.

The resistance of RT was measured with a temperature controlled Mueller Bridge (L and N #8069B, Ser# 1551895) powered by a L and N type

099034 constant current power supply. Bridge balance was indicated by a guarded dc null meter, NM (L and N type 9834), which also served as part of the control for operating copper block on-off heater J2 (Figure 9). NM had a recorder output terminal that was used to control an on-off relay for heater J2. The recorder signal from NM was fed through a 200 K-ohm resistor into a galvanometer (L and N type 2284). The light from a lamp was reflected from the galvanometer onto a panel with two photo cells which were positioned to be operated by the reflected light when the temperature at RT changed by about five ten thousandths of a degree. One photo cell activated a relay completing a circuit between the TW 5005 power supply and copper block on-off heater, J2; the other photo cell deactivated the relay so that no current passed through J2.

A L and N K-3 potentiometer was connected to the thermocouple selector switch, TCS, for measuring the thermocouple emf's. This potentiometer required a working voltage supply, a standard cell, and a null indicator for operation. The reference cell used was an Epply Laboratory Company 100 ohm internal resistance standard cell (Ser# B7176), and the reference voltage was supplied by a L and N constant voltage supply type 099034. Potentiometer balance was indicated by a L and N 2430-A galvanometer (Ser# 1066423).

The Manometer

The mercury manometer (Figures 10 and 11) was a U tube design with one inch inner diameter precision bore tubes* VL and CL. VL was the variable mercury level arm of the manometer with the space above the

*Precision bore tubes purchased from Fischer-Porter Company, 674 North Highland Ave., N.E., Atlanta, Georgia (tolerance 15/10,000).

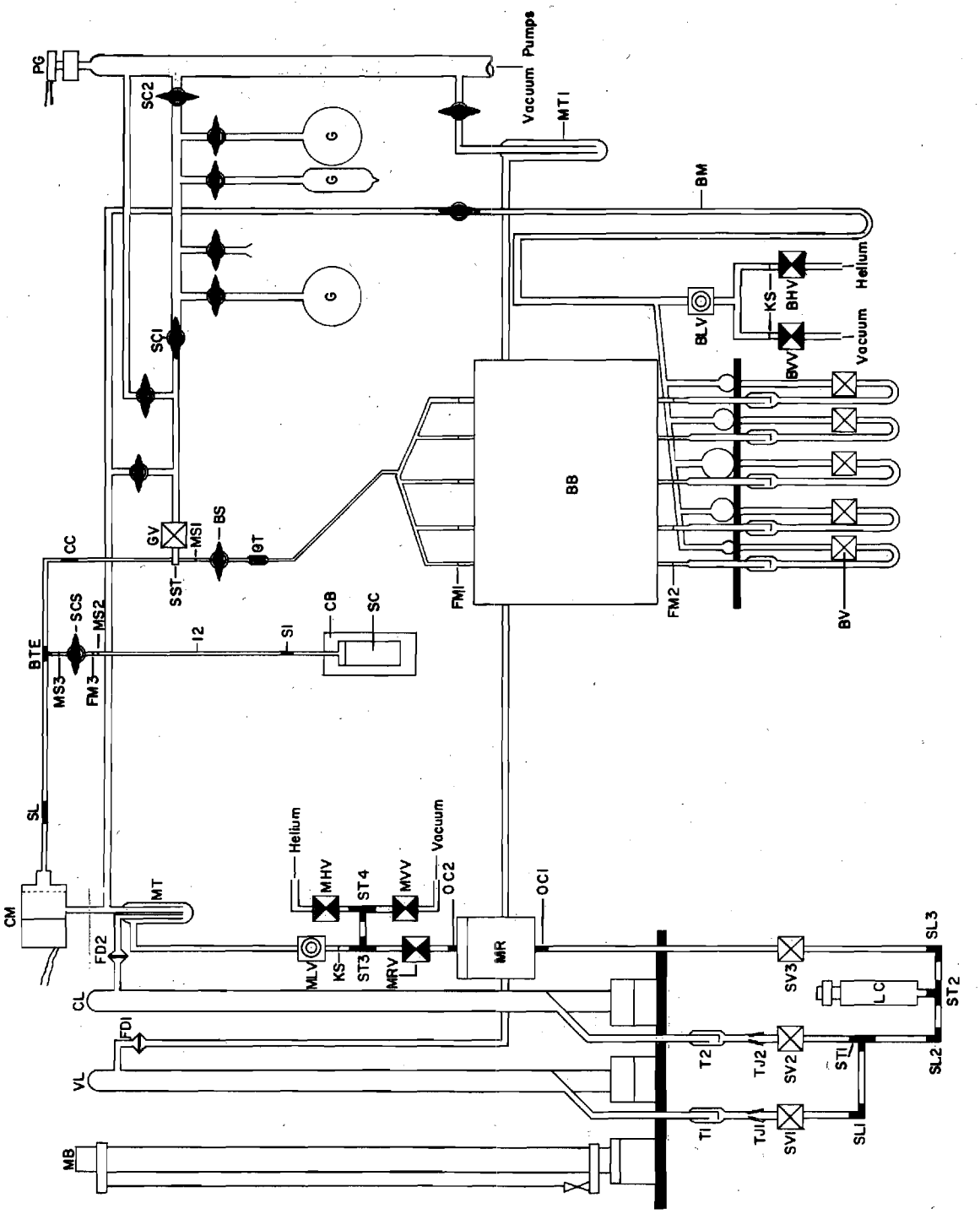

Figure 10. Manometers and Gas Transfer Systems

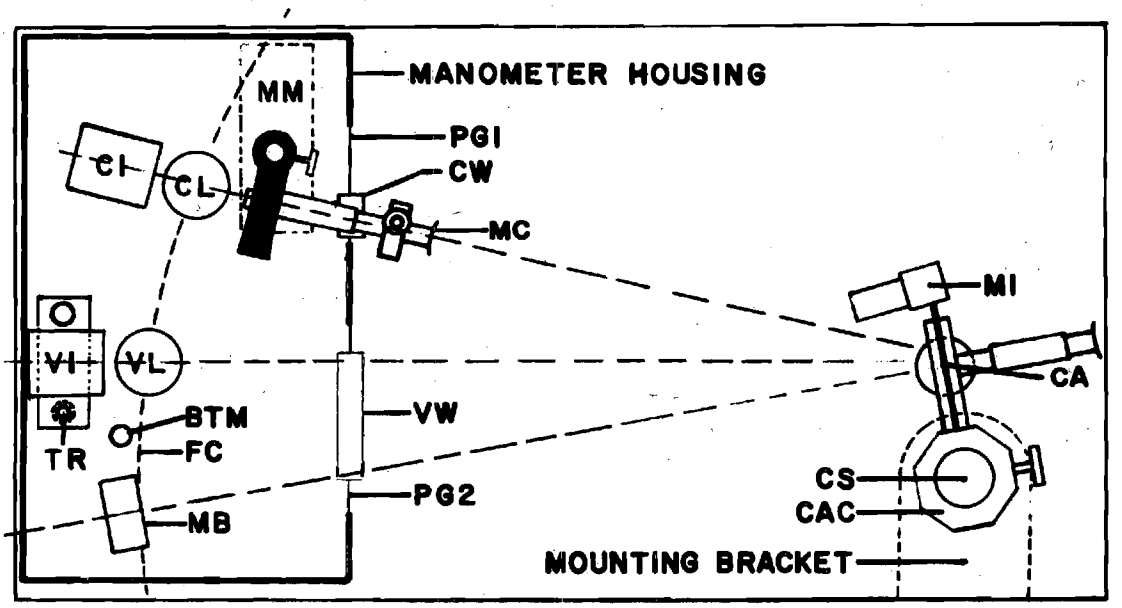

Figure 11. Manometer and Cathetometer Arrangement

liquid evacuated to less than 10^{-5} torr during measurements and CL was the variable pressure, constant mercury level side. The pressure above the mercury in CL was the pressure to be measured. VL, CL, and a standard meter bar,* MB, were mounted in the focal cylinder, FC, of cathetometer,** CA (Figure 11). CL and VL were mounted so that the focal cylinder of CA passed through their centers. The meter bar, MB, was positioned with its calibrated face tangent to FC and perpendicular to the focal path of CA when it was observed. MB was lighted by a L and N galvanometer lamp, MI, through a slot in window VW. The mercury in CL was illuminated by a lamp, CI, from the back side so that a sharp meniscus was seen when viewed through the bifilar microscope, MC. MC could be rotated so that CL could be seen by the cathetometer telescope, CA, through slot CW in the sliding Plexiglas panel, PG1. Lamp VI was used to light the mercury meniscus in variable level arm VL. The entire manometer system was mounted in thermostated manometer housing, MH, except the meter bar illuminator, MI, and the cathetometer, CA.

The micrometer slide and cathetometer telescope were attached to a six foot length of two inch diameter ground finished steel rod, CS, by a screw clamped collar, CAC. CS was supported with ball bearings in upper and lower mounting brackets. CS was adjusted to vertical by positioning the upper ball bearing support with respect to the lower ball support using a plumb bob.

---

*Gaertner M1010 type 416 stainless steel meter bar, Ser# 150 Au with calibration certificate.

**Gaertner M-300-P micrometer slide with a modified M-508 telescope (20X eyepiece, 160 cm focal length objective) on a specially constructed mounting.

A firm platform was built for the manometer from cement filled concrete blocks covered by a 3/8 inch steel plate, PL. PL was firmly secured to the pedestal by bolts that were anchored in the cement. Three quarter inch plywood panels were attached to the sides of the block platform. Fixed to the top of PL were two 2-1/2 inch deep brass cups for mounting the constant level tube, CL, and the variable level tube, VL. The manometer arms were mounted vertically in the cups by using a plumb bob and held in the vertical position by clamps. Apiezon W wax was melted into the cup until about half the brass cup was filled; after cooling, the remaining space in the cup was filled with plaster of Paris. Also attached to steel plate PL was a brass cylinder, MBS, with an adjustable holder for the meter bar, MB. Threaded vertically into this cylinder was a three quarter inch steel rod that was parallel to and behind MB. This rod was supported at its top by a collar that had been fixed to the manometer housing frame. An adjustable length collar for the meter bar, MB, extended through the three quarter inch steel rod, thus anchoring the top of MB. MB was made vertical by the adjustments on MBS and was indicated by a plumb bob suspended from a clamp attached near the top of MB and hanging over a second indicator clamp at the bottom of MB. The two clamps were made nearly identical by machining them together as if they were one piece. This insured that the plumb bob string hole was directly over the indicator when MB was vertical.

CI was modeled after the lamps of Collins and Blaisdell.[39] This lighting required that a cylindrical lens with an illuminated slit at its principal focus be used to project a beam of parallel light over the mercury meniscus. CI was positioned behind CL, opposite the cathetometer

telescope CA and was aimed so that there was a 0° angle between the light and the telescope axis. With this arrangement the apparent position of the meniscus was less sensitive to the lamp's slit width and vertical position. CI was adjusted by three screws as follows. CA was focused on the middle of the exit slit in CI, and then the light from CI was projected on a card in front of CA. When the light was projected on the middle of CA's telescope and the cross hairs were focused on CI's exit slit, adjustment was assumed correct, and CI was tightened into position.

The constant level arm microscope, MC, was attached by means of a screw clamped collar to a three quarter inch piece of stainless steel rod. This rod was mounted on ball bearing supports in the frame of the microscope mount, MM. MC was positioned by first placing a mark on the front center surface of the constant level tubing, CL, then MC was adjusted so that the mark on CL could be seen through MC and the center of the eyepiece of MC could be seen through CA (which had been previously aimed at the mark on CL and refocused to the eyepiece of MC). At this point a stop at the bottom of the three quarter inch steel rod on which MC was mounted was tightened in position with set screws and the steel rod was removed from MM. The bearing positions were adjusted to vertical by use of a plumb bob. Then MM was fixed into position and the rod rechecked to see that it was still properly aligned.

Lamp VI was constructed similar to CI but it was supported on an adjustable level platform. This platform was driven up and down behind the variable level arm, VL, by a three quarter inch threaded rod, TR. TR was powered by a reversible, variable speed motor* which could be

*Chemical Rubber Company, Model 37-315C reversible motor with 37-318 speed control for reversible motor.

operated by a switch near the cathetometer CA. The other end of the platform moved on a 3/4 inch stainless steel rod attached to the platform through a ball bearing sleeve. The threaded rod, TR, and support rod were held at the top and bottom by identically made 1/2 inch brass plates. The rod was pressed into the holes in these plates machined for it. The threaded rod rested in a ball bearing mount at the bottom and extended through a press fit bearing at the top. The top of TR was connected to the drive motor by a universal joint. TR was not perfectly straight and VI had some lateral movement when being raised or lowered but the apparent meniscus remained constant when changing the position of this light up or down over short distances of about 1/2 mm. The threaded rod's drive motor was mounted on a 5/16 inch thick piece of aluminum plate, P2, situated about 3-1/2 feet above steel plate PL. P2 was attached to the metal frame of MH, the enclosure around the manometer. The sides of MH were 3/8 inch plywood with three Plexiglas windows, PG1, PG2, and PG3. One window, PG3, allowed access to the items located in the top of MH, and the other two, PG1 and PG2, were located side by side about three feet from the floor and were the length of the manometer arm, VL. Plexiglas window PG1 on the right side of MH had a 1-1/2 inch by 2-1/2 inch slot that permitted the eyepiece and micrometer of MC to be rotated and positioned through the window for observing the mercury level in the constant mercury level arm of the manometer, CL. This same slot permitted CL to be observed through CA. The other window, PG2, could be adjusted up and down by a counterbalanced pully system located near the cathetometer, CA. The maximum vertical movement of PG2 was about 13 inches. This window had three 1/2 inch wide and four

inches long slots cut through it and spaced so that the mercury level in VL and MB could be seen through one of the slots using CA without looking through Plexiglas. The temperature inside the manometer housing, MH, was controlled by a Sargent thermonitor (Model S, Catalog #S82050) and was measured with an ISI .01°C Beckmann thermometer (Ser#645017), BTM, located between the manometer arms 50 cm above the slit in the constant level illuminator, CI. The thermonitor controlled the temperature of the box so that there were long time (8-10 hours) temperature changes of ± 0.025 °C and short time (1-2 hours) changes of ± 0.01 °C. The heater controlled by the thermonitor was two parallel wired 100 watt light bulbs in a closed container inside and near the top of MH. Air forced from the room by a 1/20 hp fan through a length of vacuum cleaner hose into the bulb box was carried to the bottom of the manometer housing by a two inch glass tube to be circulated by convection and another fan through MH.

The manometer arms, VL and CL, were connected to mercury reservoir MR through a series of glass and stainless steel tubes and valves (see the left side of Figure 10). An eight millimeter Pyrex tube with an air and impurity trap, T2, was positioned between the bottom of the constant level arm, CL, and a 10/30 Pyrex female tapered joint, TJ.

A piece of 304 stainless steel was machined with a 1/8 inch axial hole through it, a 10/30 male taper on one end, and a 1/4 inch diameter tube on the other. The 1/4 inch diameter tube end was fitted into a stainless steel valve,* SV2, using Teflon and stainless steel ferrules. This valve controlled the flow of mercury to and from the constant level

*Valves SV1, SV2, SV3, BV, and GV are 316 stainless steel Nupro type 4BK with Kel-F seat and 1/4 inch Swagelok fittings on the ports.

arm of the manometer. The steel male and glass female tapers were joined using "Torr Seal,"* a low vapor pressure epoxy resin, being careful to use a thin ring of the resin near the top so that it would not make contact with mercury. Valves SV1, SV2, and SV3 were mounted on a 1/4 inch aluminum plate attached to the 3/4 inch plywood on the front of the concrete block mount. VL was connected to its mercury flow control valve, SV1, in the same way that CL was connected to SV2. Leading from SV2 to a 1/4 inch Swagelok tee, ST1, was a length of 1/4 inch diameter metal tube. (All metal tubing used in this part of the apparatus was 1/4 inch o.d. 304 stainless steel purchased from J. M. Tull Metals Company, Atlanta, Georgia, and all fittings were 1/4 inch type 316 stainless steel Swagelok fittings with Teflon front and stainless steel rear ferrules.) One port of ST1 was directed through an "L" fitting, SL1, into SV1, and the other port was joined through another "L" fitting, SL2, to a tee fitting, ST2. One port of ST2 admitted a mercury level setting device, LC, and the other arm of ST2 was joined to valve SV3 as shown (Figure 10). SV3 was the main shut off valve to the mercury reservoir, MR. This valve was attached to MR by metal tubing and a Swagelok 400-1-OR-316 o-ring fitting, OC1, threaded into the bottom of MR.

The mercury reservoir was constructed** from 304 stainless steel. The pressure inside MR was controlled through a valve system which allowed MR to be filled with helium or evacuated to vacuum. The arrangement

---

*Torr Seal (low vapor pressure epoxy resin), Varian Associates, Palo Alto, California.

**Metal work and welding done by the Engineering Experiment Station, Georgia Institute of Technology, Atlanta, Georgia.

of valves MRV, MLV, MHV, and tees MVV, ST3, and ST4 is shown in Figure 10. MHV* controlled helium pressure in the tubing connecting these valves and MVV* was used to evacuate the tubing between the valves with a "best" vacuum of about 20 microns. MRV was used in series with MHV and MVV to adjust the pressure inside the mercury reservoir. A Teflon stem leak valve, MVV,** was attached to ST3 by kovar seal, KS1, and was used with MHV and MVV to adjust the pressure in manometer arm CL. ST3 and ST4 were Swagelok 1/4 inch stainless steel tees which were used to connect the valves and their associated tubing.

The mercury level control, LC (Figure 12), was a 304 stainless steel piston and cylinder volume changing device used for fine adjustments of the mercury position in the constant level arm, CL. The threaded bottom of the cylinder was wrapped with one thickness of Teflon tape and screwed into the 304 stainless steel cap with a 1/4 inch tube end. The 1/4 inch tube end was fitted to Swagelok tee, ST2. With the cap tightened into position, Apiezon W wax was melted around the outside joint between the cylinder and cap to make a vacuum seal. The piston moved against three Teflon o-rings that were counter set in the cylinder near the top. These rings made a vacuum seal between the piston and cylinder and they also provided guides for the piston to move back and forth without hitting the cylinder walls. The piston was adjusted up and down by the threaded rod assembly shown in Figure 12.

---

*Nupro B4H brass bellows valve with Swagelok fittings with Teflon front and brass rear ferrules.

**Teflon stem leak valve, Fischer and Porter Catalog #795-500-114.

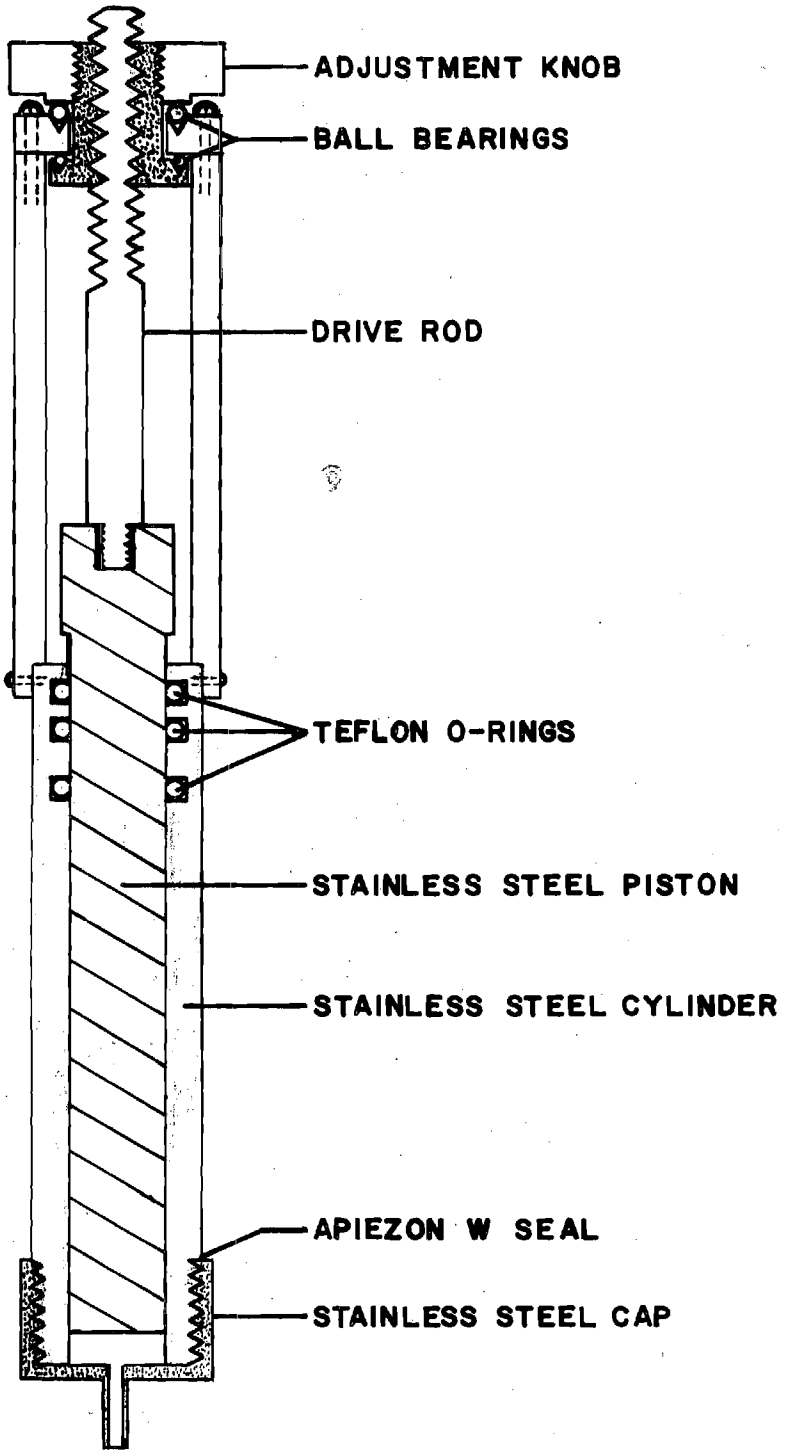

Figure 12. Final Mercury Level Control

The manometer arm, VL, was evacuated by a Consolidated Vacuum Corporation GF 20 oil diffusion pump and Welch Duo Seal 1405B mechanical pump. Located in the line between VL and the pumps were a four mm vacuum stopcock,* a cold trap, MT1, and a fritted disk filter, FD1. The stopcock isolated VL from the pumps when necessary. MT1 trapped impurities, such as grease, before they reached the mercury in VL and also prevented mercury vapor from reaching the Philips gauge,** PG, and from being evacuated into the room. FD1 prevented particles such as glass chips that may have been left in other parts of the system during construction, from blowing back into VL.

CL was joined to the Teflon stem leak valve, MLV, the pipet manometer, BM, and port B of the capacitance manometer,*** CM (Figure 13), through a fritted disk and cold trap. CM had a sensing head with two chambers, A and B, separated by a thin metal diaphragm. Entrance to the chambers was through port A and port B. The diaphragm was used in conjunction with a probe to form a sensitive differential pressure measuring capacitor which was one arm of a capacitance bridge. Pressure differentials across the diaphragm cause displacement which changed the probe-diaphragm capacitance. This change produced an imbalance in the bridge circuit which was indicated by a meter. Diaphragm deflections of a few millionths of an inch were detectable and correspond to pressure differ-

---

*All stopcocks used in this system were lubricated with Apiezon N grease.

**Consolidated Vacuum Corporation, Model PHG010A cold cathode discharge gauge (0.5 torr to 10^{-7} torr).

***Series 212 Model B, Granville-Philips Company, 5676 East Arapahoe Avenue, Boulder, Colorado.

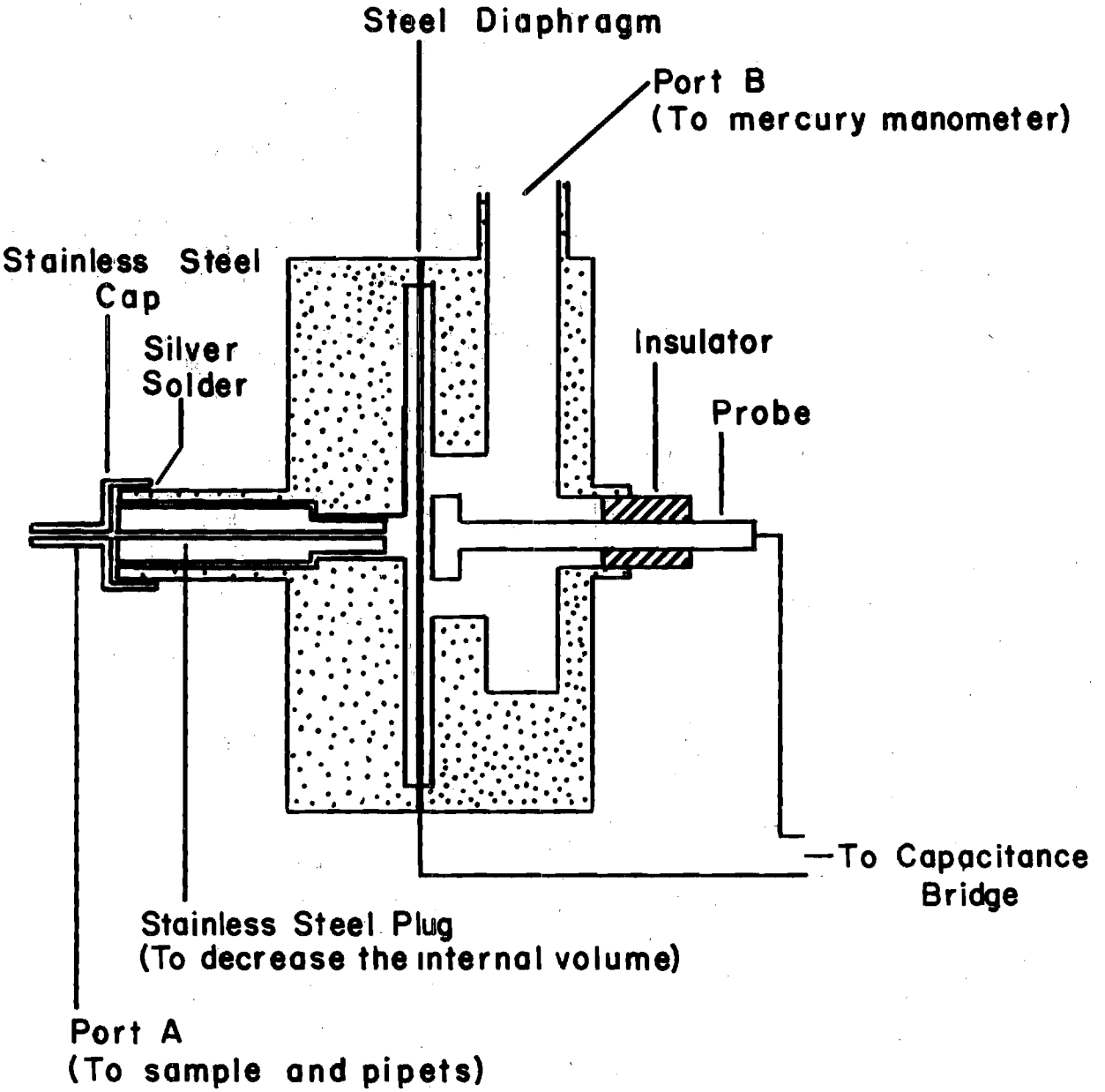

Figure 13. The Capacitance Manometer

entials of less than 5×10^{-3} torr. CM consist of three parts: a bakeable sensing head, the balance unit, and the indicator. The balance unit was attached to the sensing head and had to be removed before high temperature (100°C-450°C) outgassing of the head. The indicator was attached to the balance unit by shielded cables and could be placed in a conveniently accessible position within about 20 feet of the sensing head. When CM was purchased it had a metal bellows and kovar seal on port A. These were removed and a stainless steel cylinder with a 1/16 inch axial hole through it was machined to fit snuggly inside of and to be flush with the end of port A (Figure 13). A cap, with 1/16 inch tubing brazed into it, was fitted over port A and silver soldered into position. This modification was part of the effort to keep the volume of the tubing and associated parts of the system small. CM was incorporated into this system to provide a partition between the short arm of the manometer and the sample cell. This eliminated the problem of constructing manometer arm CL so that it had a small and known volume, which would have been the case if it were attached directly to the sample system. CM also prevented mercury vapors from diffusing into the sample cell and made it possible to include in the system a pipet manometer, BM, which will be discussed later.

Following the advice of Constabaris,[24] great care was taken to insure that the manometer was clean before introducing mercury. The piston and cylinder of LC, the mercury reservoir, and the steel tubing were washed with nitric acid and distilled water before assembling them. The valves SV1, SV2, and SV3 were disassembled and washed with water, then dried in an oven at 100°C. When cooled, the Kel-F press fit seats were

found to be loose in the valve stems. The valve stems were drilled through with a size 60 drill so that the drill passed through the Kel-F stem. When all valves had been drilled, the drill end opposite the fluted edges was cut into three pieces to be used as retainer pins for the seats. The valve parts (without Kel-F seats) were washed with benzene two times to remove any oil on them and then they were dried. The valve bodies were soaked in distilled water several days and dried at 120°C for about five hours. The Kel-F stems were wiped clean and washed with carbon tetrachloride and dried in the oven. The stems were rinsed in distilled water and dried in the oven at 120°C. When the valves had been reassembled, the metal tubing, valves, and mercury reservoir were assembled as described earlier and distilled water passed through the opening in the mercury reservoir, MR, the variable level arm valve, SV1, and the constant level arm valve, SV2. This water was collected at ST2, which had been turned so that almost all the water ran out the port where LC was to be connected. A vacuum pump with a cold trap was attached at ST2 to remove any water remaining in MR, SV1, SV2, SV3, and associated tubing. Valves MRV, SV1, and SV2 were closed and the pump was started. The external ports were covered with aluminum dust caps after vacuum drying the system. The piston, cylinder, and stainless steel cap of LC were washed with nitric acid and soaked in distilled water. These pieces were dried in an oven at 120°C for several hours and assembled. The vacuum pump was removed from ST2 and LC was positioned.

Before being installed, the manometer arms VL and CL were filled with ethanol-KOH solution for one day. Then they were rinsed with distilled water and filled with a strong nitric acid solution. When the

nitric acid was removed, the arms were flushed with about 10 liters of distilled water and the entrances to the tubes were covered with aluminum dust cap covers. After being fitted into their brass cups, the manometer arms were steamed for several hours. The bottom entrances of VL and CL were attached to SV1 and SV2. VL was connected to the high vacuum pumping system through a cold trap. Water remaining in the system was evacuated by a roughing pump and cold trap attached at the top of CL. The roughing pump was replaced by a modified Hickman still. This still had been cleaned by the same methods used to clean the manometer arms but it was dried in an oven. All entrances were sealed and the high vacuum pumps were used to evacuate the system. The manometer arms were wrapped with heating tape and heated to 150°C. The metal tubing, connecting glass tubing, and steel reservoir were heated with a hand heat gun periodically. Pumping was continued for two days until the pressure measured by Philips gauge, PG, was about 10^{-6} torr and not affected significantly by warming the tubing with a heat gun. When heating was discontinued, the pressure dropped to about 10^{-7} torr. The still was opened and about 800 cm^3 of triply distilled mercury* was poured in. The system was evacuated by high vacuum pumping for another day and then distillation was started. Mercury was distilled into CL at 50-70 cm^3 per hour. At the end of the distillation the system was raised to one atmosphere using nitrogen gas, the still was removed, and the final connections to the manometer system were made.

---

*Bethlehem Apparatus Company, Inc., Heller Town, Pennsylvania, Lot #B-203, impurity less than 25 parts per billion.

The Gas Transfer System

The dosing system (right side of Figure 10) design was similar to the one used by Constabarís.[24] Five pipets (10, 20, 40, 80, and 160 cm^3) were built into the system to provide dosing volumes from 10 to 310 cm^3. These pipets were mounted in an insulated box that could be thermostated with an ice bath. The ice bath obstructed direct mercury sighting in the thermostated box so that another method was needed to determine the mercury level while filling the pipets to prevent blowing mercury through the system. This indication was provided by a manometer between the pipet mercury reservoir and the constant level arm of the main manometer, CL. The pipets were connected to the capacitance manometer CM and the sample cell by glass tubing, metal tubing, and several stopcocks. The pipets were filled with gas samples from Pyrex flasks through a metal bellows valve, GV.*

The gas inlet tube to the sample cell, I2, was attached to a one millimeter bore stopcock,** SCS. This connection was made by sanding I2 until it could be snuggly inserted into the stopcock capillary tubing to fiducial mark FM3 that had been burned onto one stem of SCS. I2 was then cleaned and inserted into the capillary tube until its end was directly under the fiducial mark on SCS. A ring of "Torr Seal" was placed around the metal-glass intersection, MS2, and worked into the space between the tubes until it reached a point near the end of I2. More "Torr Seal" was added at the glass-metal intersection and allowed to harden.

---

*Nupro 4BK 316 stainless steel bellows valve, stainless steel rear and Teflon front ferrules.

**Number 7559, Corning Glass Works, Corning, New York.

The other side of SCS was attached to monel tubing* at MS3 in a manner similar to that used at MS2. This tube was silver soldered into a machined brass tee, BTE. One side of BTE was connected to the capacitance manometer CM with monel tubing and a 1/16 inch monel Swagelok union (Teflon front and monel rear ferrules). The monel tube from the other exit of brass tee BTE was silver soldered into a specially machined 304 stainless steel tee, SST. (A 1/16 inch stainless steel Cajon coupling, CC, was silver soldered into the line between brass tee BTE and SST.) The steel tee was machined so that one port could be inserted into the 1/4 inch Swagelok fitting (Teflon front and stainless steel rear ferrules) of valve GV. A short length of monel tubing was silver soldered into the final hole in SST. This tube was connected to pipet stopcock** BS by a "Torr Seal" joint, MS1, made in the same manner as MS2 and MS3. Valve GV provided the only entrance into the sample cell, capacitance manometer, and gas pipets from other parts of the system.

A mercury trap, GT, was attached to BS. GT consist of about two grams of two to three millimeter diameter gold spheres*** in a one inch long and five millimeter outer diameter glass tube. This trap was used instead of a cold trap to eliminate the necessity for monitoring the cold trap temperature and calibrating it as a separate volume.

The line from GT to the pipets was constructed from three mm outer

---

*All monel tubing used in this apparatus is 1/16 inch o.d. with 0.010 inch walls.

**One mm stopcock

***Twenty-four carat gold purchased from Nixon and Holcombe Dental Company, 303 Courtland Street, N.E., Atlanta, Georgia. Formed into balls by melting and quenching in water.

diameter and 0.75 mm inner diameter Pyrex tubing. This tubing was shaped to form a manifold with five inlets. Each inlet was Pyrex welded to one of the five gas pipets just above the fiducial marks, FM1.

The gas pipet system was built into pipet box BB (Figure 14) which was mounted on a piece of aluminum channel bolted to the laboratory bench vertical supports. BB's back, sides, and bottom were made from canvas reinforced phenolic board. Four 3/4 inch rods, RO (threaded with 1/2 to 20 threads on both ends and faced at the shoulder so that a flat surface was formed at the ends of the threads), were used to hold the stainless steel rack in BB. The rack was made with steel angle sides, AN, silver brazed at SB to base BA. A top, TO, for the rack was held in place by four bolts brazed to the top ends of AN.

The pipets were positioned in box BB before placing the top TO. (They were arranged so that approximately the same weight would be on each side of the box when all pipets were filled with mercury.) The pipets were seated in holes in BA and Apiezon W wax, AW, was melted around the metal-glass intersections to hold them in position. A ring of epoxy was placed around the tubes where they passed through the phenolic bottom of BB to prevent leaks when the box was filled with ice. The top, TO, and B were then positioned and a 1/4 inch Plexiglas window was epoxied into the front of BB.

Connection between the pipets and mercury reservoirs was made with 1/4 inch o.d. glass tubing. This tubing was glass welded to air traps, AT, located just below the lower fiducial marks, FM2. The length of tubing that connected a pipet with its reservoir was U shaped to prevent any air, glass chips, etc. from reaching the pipet side. Flow control

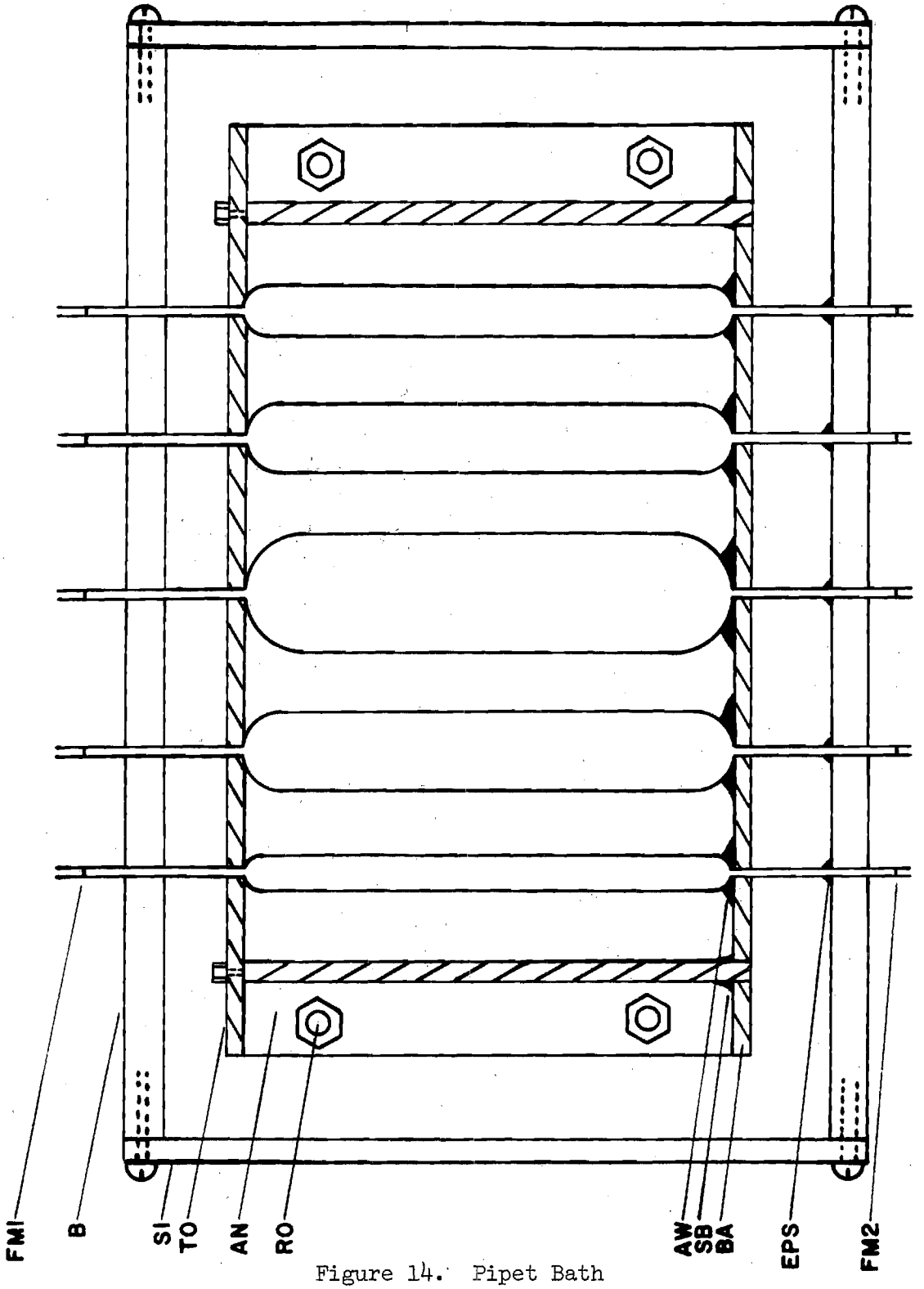

Figure 14. Pipet Bath

between a pipet and its reservoir was by bellows valve BV. The 1/4 inch glass tubing was fitted directly into the Swagelok fittings of BV using Teflon front ferrules and zytel rear ferrules. Prior to fastening the glass tubing into these fittings, the tube ends were beveled. A straight piece of 1/4 inch o.d. Pyrex tubing was used to connect the reservoir with BV. These reservoirs were mounted on a length of three inch aluminum angle that was bolted through a 1/8 inch aluminum sheet to a piece of aluminum channel. The aluminum sheet provided a back for a Plexiglas box to be built about the reservoirs. This box was built so that the reservoirs and associated plumbing could be kept in an ice bath to shorten the mercury temperature equilibration time in the pipets. The reservoir ice bath was never used because equilibration times were allowed for the gas-sample system which were longer than the time required for mercury temperature in the pipets to equilibrate.

All five pipet reservoirs were attached to a manifold that led to a tee. One side of this tee was attached to a Teflon stem leak valve,* BLV, and the other side led to a U tube mercury manometer, BM. BM was used to indicate the difference in pressure between the constant level arm of the manometer, CL (the pressure above the mercury in the pipets was approximately equal to the pressure in manometer arm CL), and the mercury in the reservoir. An outside indication of the mercury level was required when the pipet box, BB, was filled with ice. Otherwise the pipets may have been filled too quickly and mercury would have been blown through the system. The gas pressure above the reservoirs was controlled

---

*Fischer-Porter #795-500-0014, 1-1/4 mm needle valve.

by BLV. This valve was connected through a tee and 1/4 inch kovar seals to two valves,* BVV and BHV. BVV was attached to a Welch 1400 duo-seal pump and BHV was joined to a helium cylinder by appropriate tubing and a two-stage regulator.

The pipet system was evacuated through valve GV and two stopcocks, SC1 and SC2, by a CVC GF20 oil diffusion pump and Welch 1405B duo-seal roughing pump. Pressure during pumping was measured by Philips gauge, PG, attached to the top of the main pumping manifold. When gas was to be admitted into the pipets, SC2 and GV were closed but SC1 was left open. The stopcock leading to the gas, G, to be used was opened for a short time, then closed. GV was opened slowly until gas started to enter at a slow rate as indicated by the capacitance manometer. This leak rate was balanced by leaking helium into manometer arm CL through Teflon stem leak valve MLV. When the desired pressure was attained, the two valves, MLV and GV, were closed in steps so that the capacitance manometer, CM, would remain near balance.

Materials

The inert gases used in this experiment were research grade purchased in Pyrex glass flasks from Air Reduction Sales Company. They each had a manufacturer's mass spectrometer analysis. Xenon had the greatest amount of impurities with 81 parts per million. Seventy parts per million were krypton and 11 parts per million were nitrogen with no other detectable impurities. Krypton had seven parts per million impurity, five were

---

*Nupro B4H brass bellows valves (Teflon front, brass rear ferrules).

xenon and the remaining two parts per million were nitrogen. There were 12 parts per million helium in the neon. No detectable impurities were reported in the manufacturer's assay for the two remaining gases used, argon and helium. All gases were used without further analysis or purification.

The adsorbent used was boron nitride. The hexagonal modification of boron nitride is a soft, white, greasy feeling powder whose physical properties are reviewed by Giardini[40] and Muetterties.[41] The structure (Figure 15) and cell constants of BN and graphite are almost equal. The cell constants are:

	BN[42]	Graphite[40]
a	2.504 Å	2.456 Å
b	6.662 Å	6.696 Å
bond length	1.446 Å	1.42 Å

The coefficients of expansion for BN are different for inter-planar expansion and expansion along the plane. The coefficient for inter-planar expansion[40] is 41.15×10^{-6} °C and the coefficient along a plane is -2.9×10^{-6} °C and will be assumed to be zero for this work. The density of BN determined by X-ray diffraction is 2.27 g/cm^3.[42]

Two different BN samples were obtained from The Carborundom Company, Refractories and Electronics Division, Latrobe, Pennsylvania. These samples were designated HPF (high purity fine) and HPC (high purity coarse). The manufacturer's assay stated that both samples were better than 99.5 percent BN. The particle size distribution* for HPC (Figure 16) was

*Particle size distribution for HPC was done by Dr. Clyde Orr, Jr. Chemical Engineering Department, Georgia Institute of Technology, Atlanta, Georgia.

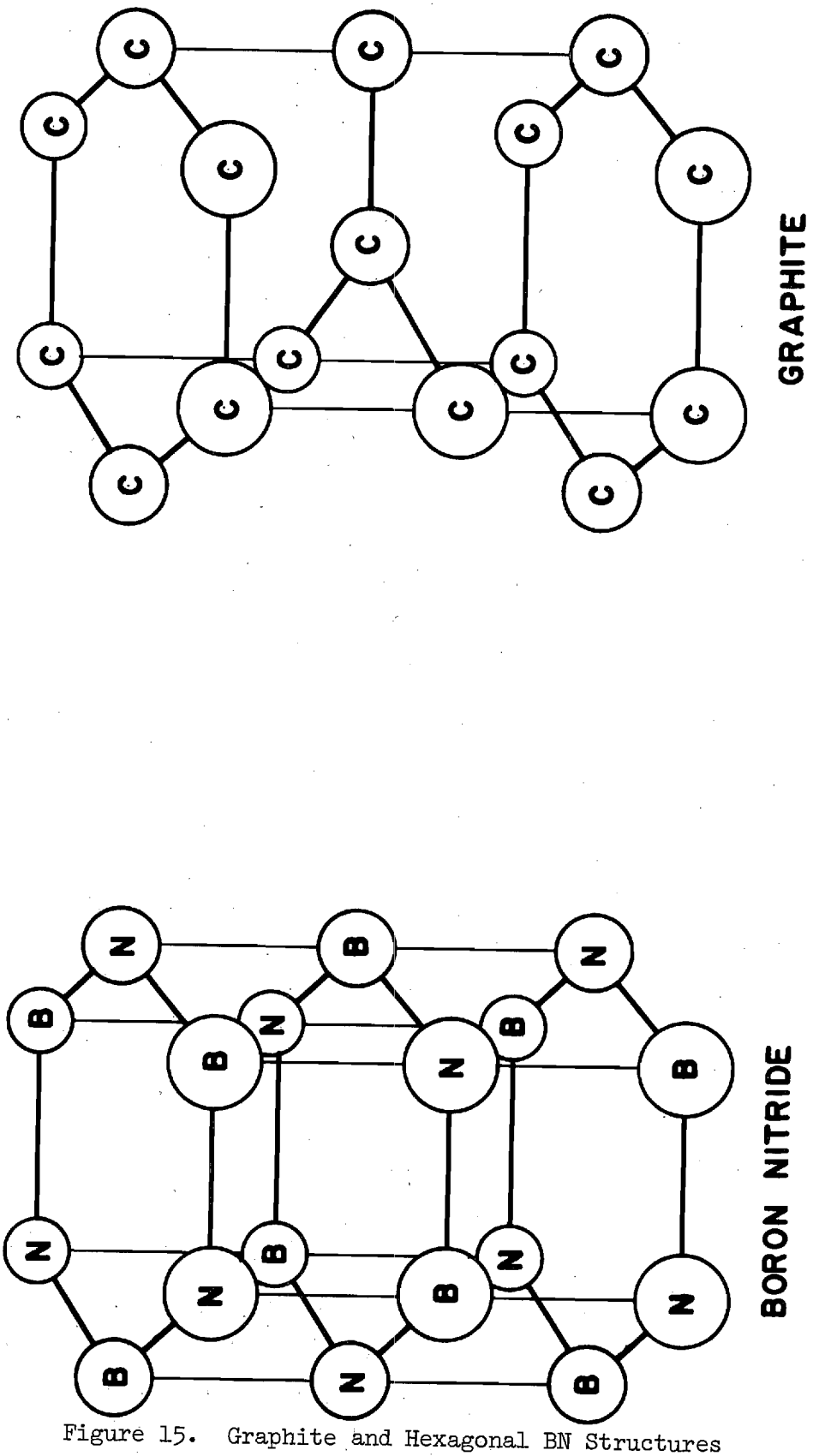

Figure 15. Graphite and Hexagonal BN Structures

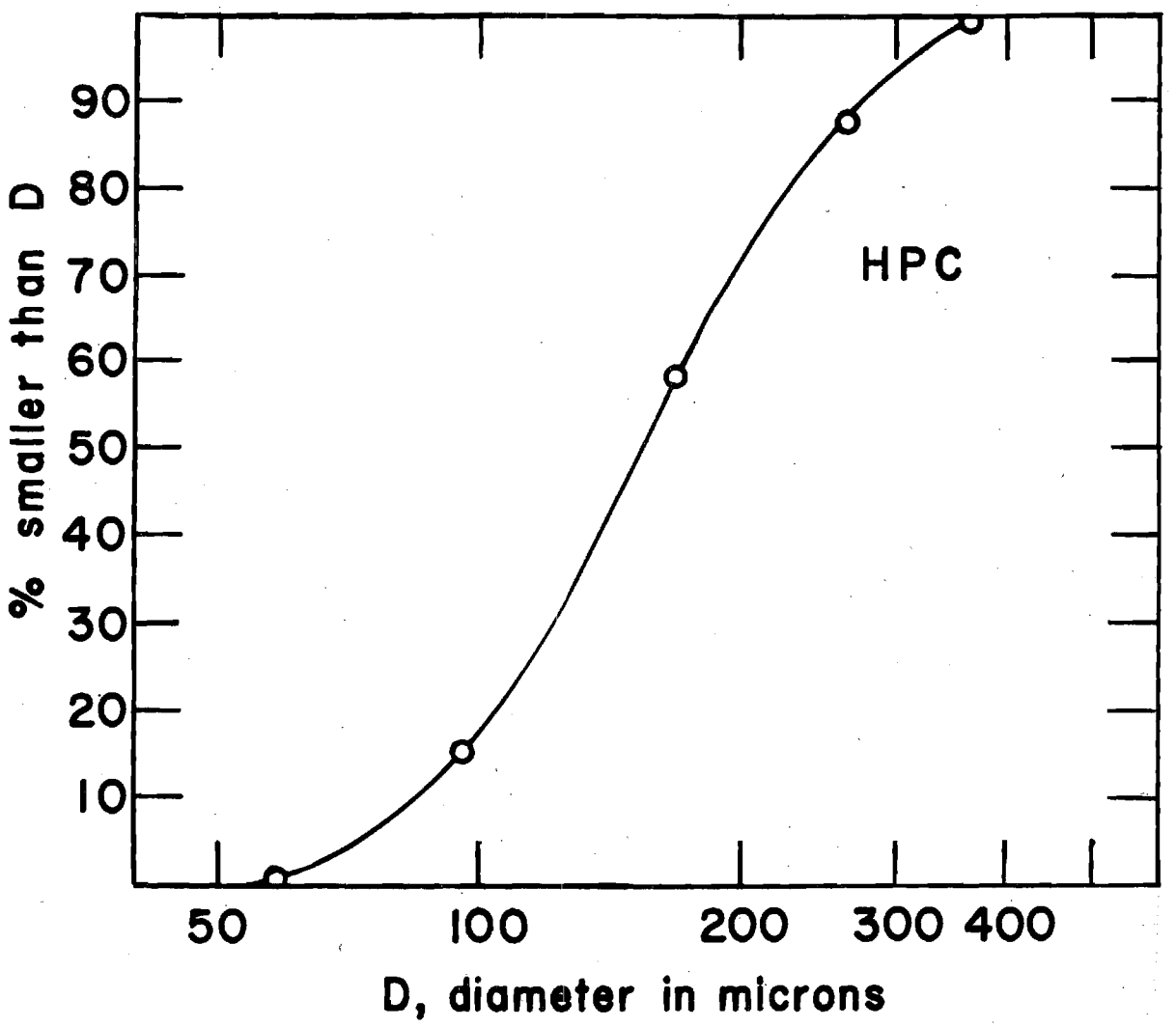

Figure 16. Particle Size Distribution for HPC BN

determined using various sized sieves, and particle sizing for HPF* (Figure 17) was done with a Coulter counter. The average size of a HPC particle was estimated to be 150-190 microns and the average HPF particle size was two to four microns. Electron micrographs** (Figures 18-29) indicated that the HPC particles were conglomerates of the HPF type particles. The HPF and the small particles that made up the HPC conglomerates seemed to be flat crystals with thin edges. The edges were estimated for several particles from the figures to contribute about five to ten percnet of the total surface area. Thus a significant amount of the surface was contributed by the crystal edges. (The larger flat face was assumed to be the BN basal plane.)

A BET type area determination (Figure 30 and Table 22) using argon was run on the HPC at 90°K (the only sample on which adsorption isotherms were run). The area obtained from this isotherm (using the cross sectional area of argon[8] to be 14.1 Å^2 and the saturated vapor pressure of argon at 90°K to be 109.42 cm[43] mercury) indicated that the total surface area for the sample used (83.470 grams) was 415.6 m^2 or 4.98 m^2/gram. When a 10.352 gram sample taken from the shipping container was heated to 550°C for 24 hours in vacuum (10^{-5} - 10^{-7} torr) its weight decreased by 0.0125 gram. This weight loss was assumed to be a monolayer of water. Using this weight loss per gram (1.21×10^{-3} gm loss/g BN) the area of the sample was estimated to be 5.06 m^2/g (cross sectional area of a water molecule was taken to be 12.5 Å^2[8]).

---

*Particle size distribution for HPF was done by Dr. Paul Boland, Engineering Experiment Station, Georgia Institute of Technology, Atlanta, Georgia.

**James Hubbard, Georgia Institute of Technology, Engineering Experiment Station, using Cambridge Instrument Company scanning electron microscope.

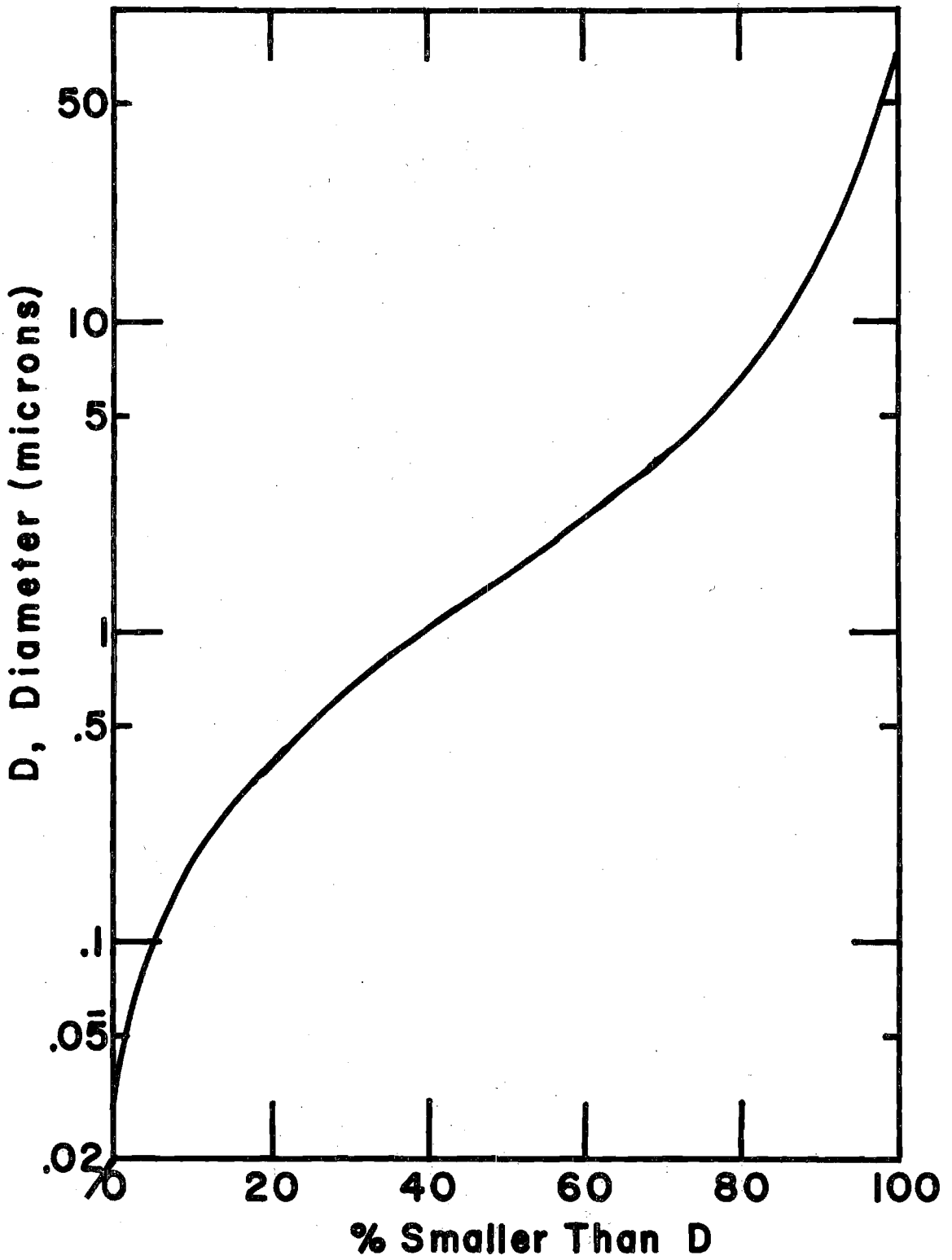

Figure 17. Particle Size Distribution for HPF BN

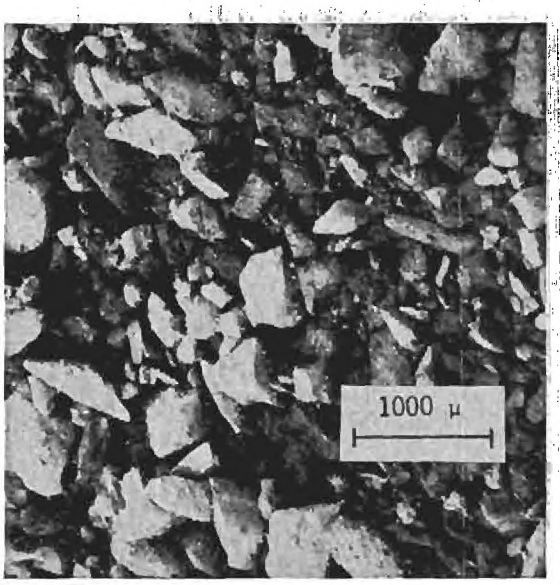

Figure 18. HPC Boron Nitride.

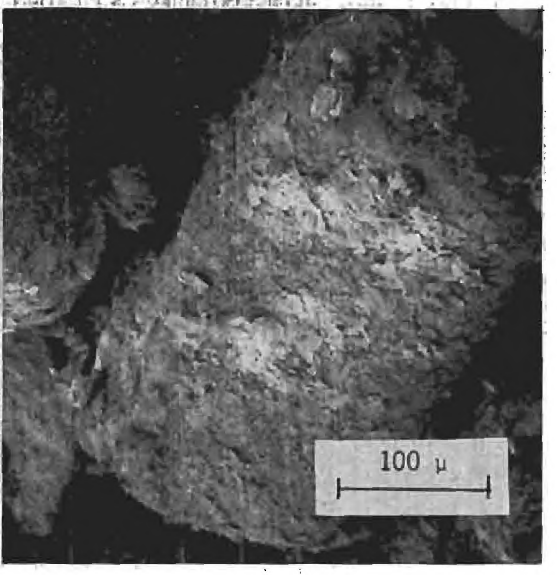

Figure 19. HPC Boron Nitride.

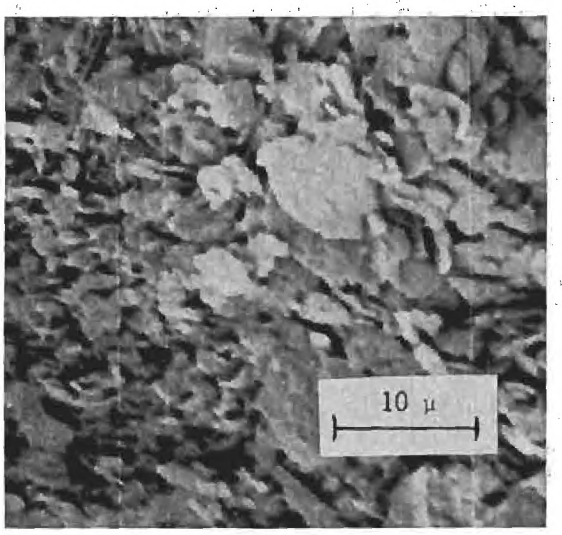

Figure 20. HPC Boron Nitride.

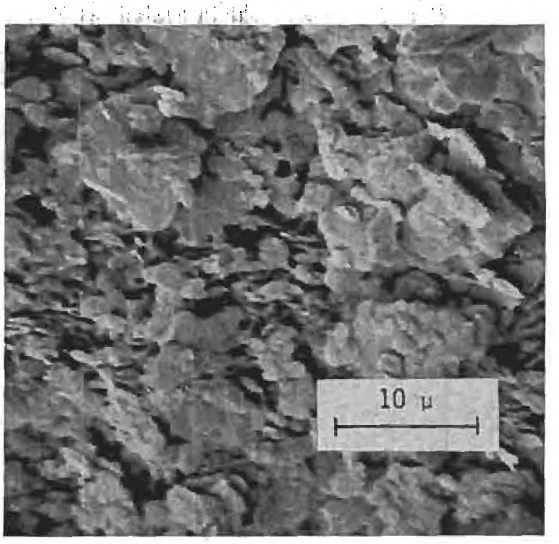

Figure 21. HPC Boron Nitride.

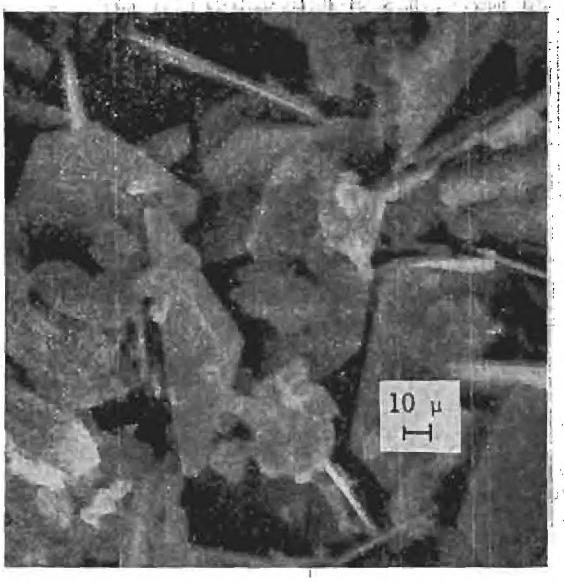

Figure 22. HPC Boron Nitride.

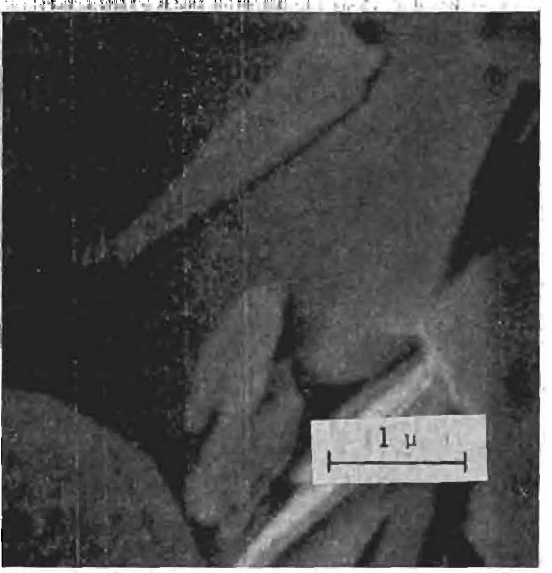

Figure 23. HPC Boron Nitride.

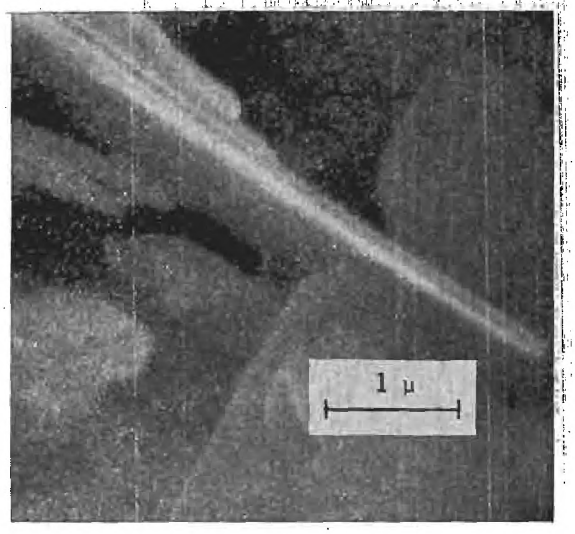

Figure 24. HPC Boron Nitride.

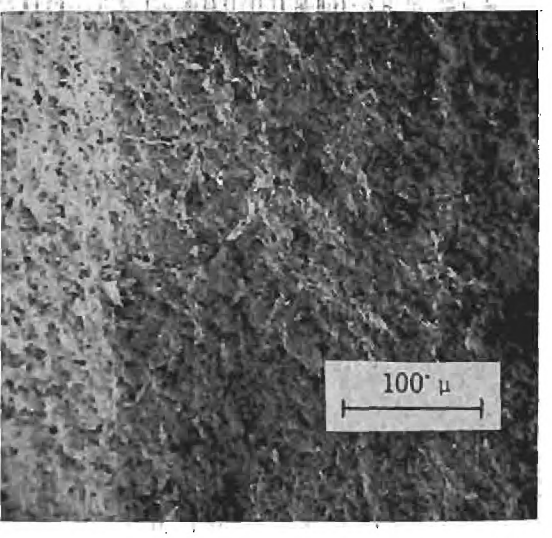

Figure 25. HPF Boron Nitride.

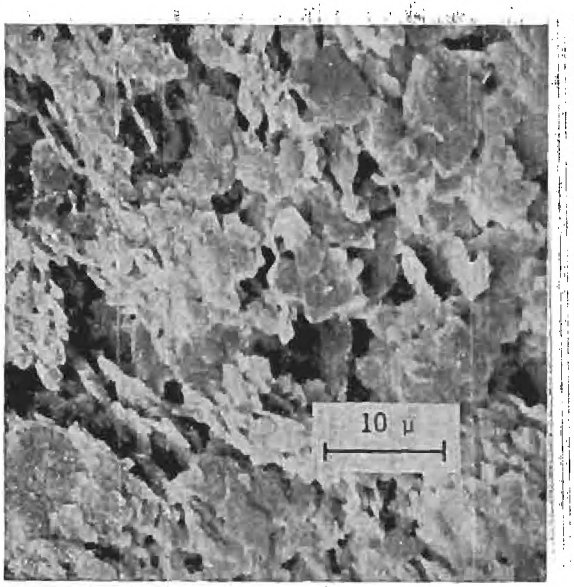

Figure 26. HPF Boron Nitride.

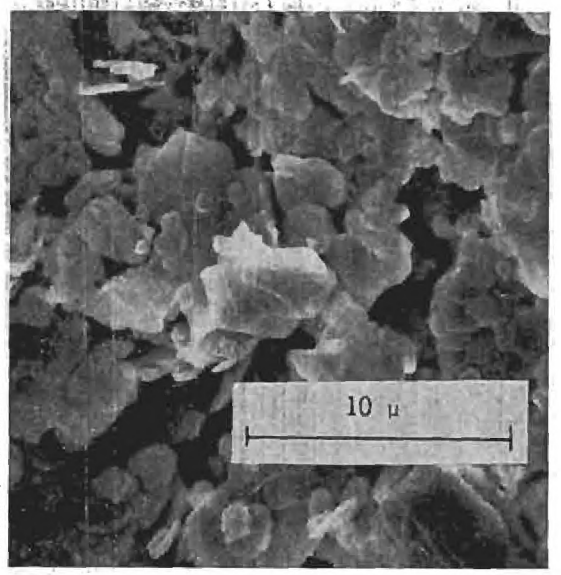

Figure 27. HPF Boron Nitride.

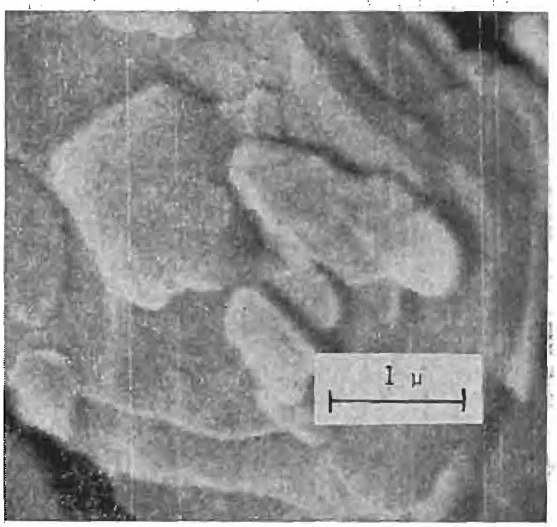

Figure 28. HPF Boron Nitride.

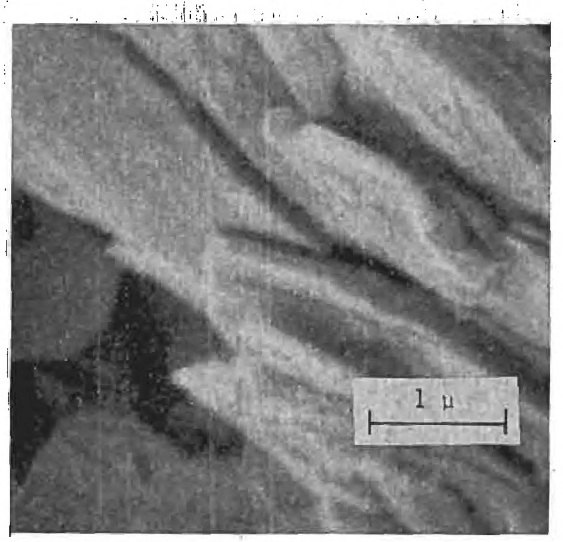

Figure 29. HPF Boron Nitride.

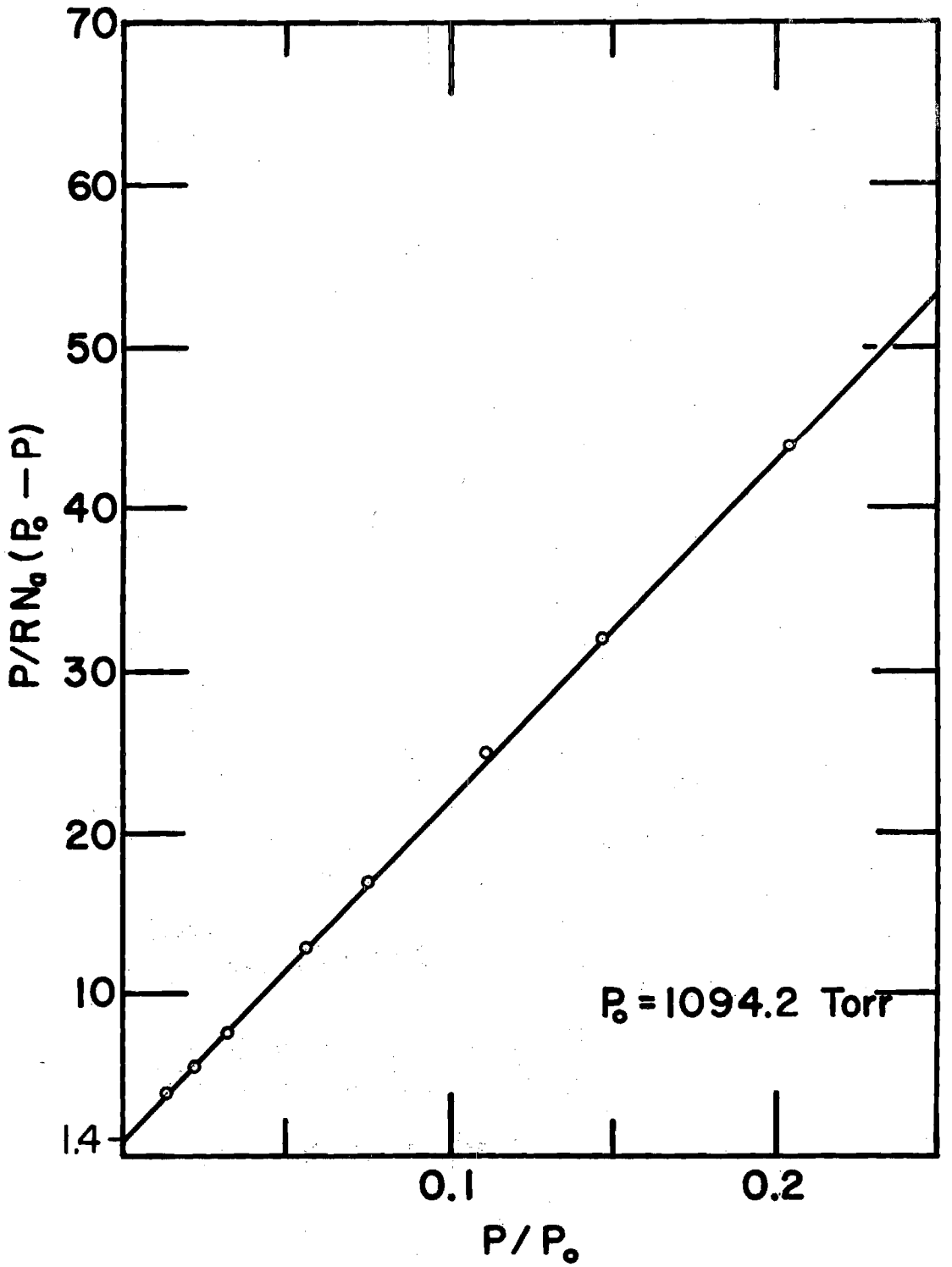

Figure 30. BET Plot of 90°K Ar-BN Data

CHAPTER III

VAPOR PRESSURE OF OXYGEN

At this point it may be worthwhile describing an experiment that was done for familiarization with the operation of the cryostat and manometer. The vapor pressure of oxygen was measured between 67°K and 90°K. The values determined were compared with other data.[47]

The sample cell, SC, and capacitance manometer head, CM, were heated to 450°C and 200°C, respectively, while the system was being outgassed. When Philips gauge, PG, indicated the pressure had been reduced to about 10^{-6} torr, heating was discontinued. The capacitance manometer electrical connections were replaced when the sensing head had cooled sufficiently. (The part of the head with electrical wiring must be removed when outgassing at temperatures above 50°C.) The manometer housing, MH, was closed and allowed to equilibrate to a pre-set temperature. After sample cell SC cooled to room temperature, it was smeared with grease and thermometer well W1 was filled with vaseline. The resistance thermometer assembly (RT, C1, and CBB) was installed and copper block, CB, was then lifted so that SC entered about two inches. The resistance thermometer's lead wires were directed through the hole at the bottom of CB and CB was lifted until sample cell SC was nearly seated. Thermocouple TC12 was pushed through a longitudinal groove in the side of copper block bottom CBB until it touched sample cell SC. The copper block CB was lifted until sample cell SC was seated and the suspension wires were

joined at the turnbuckles. The copper block bottom retainer, R1, was tightened and the resistance thermometer leads were wrapped three times around CB, about one inch from the bottom, and taped into position. RT's leads were soldered to binding posts at the bottom of copper block CB. One half of copper block top CBT was inserted into the opening at the top of CB and rotated until it fell into position over the sample cell top retaining bolt heads. The other half of CBT along with thermocouple TC9 was positioned.

Thermocouple TC8 was taped to sample cell inlet tube I1 halfway between junction TS and the top of the copper block. The tube heater J3 was wrapped around I1. All of the wires to be soldered to terminals on phenolic cap P1 were attached and the heaters were connected. CB was checked to see that it was hanging vertically; if not, adjustments were made with the turnbuckles.

Brass vacuum cannister BVC was lifted around CB and positioned to be attached to support plate SP. Water well WW was filled with water. SP and solder trough, ST, were heated until Woods' metal melted when touched to them. (The lip of SP and ST had been previously tinned.) ST was filled with Woods' metal and allowed to cool. The brass vacuum cannister BVC was pressurized (one or two psi above atmospheric was adequate) and checked for leaks with soap solution. This particular seal was bothersome because of the effort necessary to get it leak tight. When a vacuum fit was obtained the Dewar support cannister, DSC, was attached to the cryostat support plate, CSP.

Helium was leaked into brass vacuum cannister BVC until its pressure reached several centimeters and Dewar D1 was filled with liquid

nitrogen until it reached a level about six inches below the cryostat support plate. The liquid level was controlled by a Linde LL6 liquid nitrogen level control which is an all mechanical device with a valve operated by a vapor pressure thermometer. When the LL6 probe touched the liquid nitrogen surface in the Dewar, the gas in the LL6 condensed closing the valve that allowed liquid nitrogen to flow into the Dewar. When the probe was not in contact with liquid the pressure increased, opening the valve, and liquid nitrogen flowed into the system until liquid nitrogen in the Dewar touched the probe.

The liquid nitrogen bath temperature was controlled by a vapor pressure manostat. This instrument had an oxygen filled probe in the liquid nitrogen bath. Pressure in the probe was controlled by the surrounding bath temperature. The manometer had tungsten contacts along one arm. By using the lowest contact and one of the others, a circuit through mercury could be made to operate a laboratory relay which controlled a solenoid valve between the liquid nitrogen bath and a vacuum pump. When the bath was too warm, the solenoid valve was opened and the pressure above the bath was reduced. When the bath became cooler, the solenoid valve closed, isolating the pump. A second manometer was used to control another solenoid valve which vented Dewar D1 when it was being filled with liquid nitrogen. The second manometer also prevented the first from operating during liquid nitrogen filling. If a nitrogen bath temperature below the normal boiling point of nitrogen was not required, the bath temperature could be controlled by the second manometer.

While the cryostat was cooling, the manometer system was adjusted.

CM, the capacitance manometer, was zeroed with pressures less than 10^{-4} torr on both sides of the sensing head. The mercury level in manometer arm CL was adjusted until a clear meniscus was seen through microscope MC. Final adjustment was made by closing valve SV2, thus fixing the mercury level in CL. The hair lines in MC were set so that the region of dark and light appeared midway between them. MC was rotated out of the way and the meniscus position was measured with cathetometer CA about six times. Then CA was rotated so that standard meter bar MB could be seen, a reference line was chosen, and its position was measured with CA. The reference position of the mercury level in CL was:

$$\text{CL Reference} = \text{Meter Bar Reference} + \text{Meter Bar Reading with CA} - \text{CL Reading with CA}.$$

MC was rotated back into position and the meniscus checked to see that it appeared the same. If so, MC was not disturbed again until the end of the experiment.

A method for adjusting the cross hairs of the cathetometer CA on the meter bar MB had to be developed because the reference lines on MB appeared to be many cathetometer hairline widths. The cross hairs were rotated until one of the fibers made an angle of about 10°-20° with the horizontal. When reading MB, CA was adjusted so that the crossing of the hairs was very nearly equidistant from each end of the chosen reference mark. An attempt was then made to raise the cross of the hairs to the middle (vertical) of the reference mark. The distance of the ends of

the reference line from the cross hair was used to decide if the center had been found. All final telescope adjustments were in an upward direction when sighting on a reference line or meniscus so that the contact between micrometer slide and screw would always be approximately the same. This method of adjusting the telescope made setting the cross hairs on the mercury meniscus difficult because of raising the dark hairlines against a dark mercury background. To locate the position of a meniscus, the hairlines were raised until a small amount of light could be seen below the cross. Using this method, the maximum spread usually found in a series of six to eight measurements of the same meniscus setting was 0.005 millimeter. This method was also used to insure that the top of the meniscus had been found. After setting the cross hairs, the cathetometer, CA, was rotated slightly and the light below the cross observed. If the area below the cross hairs became darker, new adjustments were made because the position of the top was not measured.

A similar method was used to set the hairlines in microscope MC. The parallel hairlines were rotated so that they made a small angle with the surface. When the light to dark intersection was halfway between them, the mercury surface crossed the two lines at equal distances from the apparent edge of the microscope. These lines were not adjusted in any special way (up or down) since once they were set, the mercury was adjusted to them.

When copper block CB had cooled to about 77°K, the tube heaters H1 and J3 were activated with about 150 ma. Research grade oxygen* from

*Air Reduction Sales Company, 181 Pacific Avenue, Jersey City, New Jersey, mass spectrometer and gas chromatography analyzed. Breakseal #F-0305022, Lot #X-214610.

a one liter cylinder was allowed to leak into the system very slowly. At the same time the capacitance manometer CM was maintained near null by expanding helium into the constant level side of the manometer. This was done to prevent a pressure differential that would cause the zero balance of CM to change. When oxygen started to condense, the pressure in CL was held constant so that the capacitance manometer, CM, would remain balanced. As much oxygen as possible (about one gram) was collected at this temperature in the sample cell and the system was isolated. The brass vacuum cannister BVC was evacuated to about 10^{-5} torr and the constant current heater J1 was adjusted until the temperature of copper block CB started to increase. Then the current was decreased periodically until CB began to cool. The null meter was zeroed and the Mueller bridge was adjusted so that both positions of the commutator (R position and N position) gave nearly the same resistance reading. Current through resistance thermometer RT was regulated to .001 amp by a variable resistor built into the bridge. Then the recorder output from the null meter was switched into the photo-cell-galvanometer circuit. The photo cells were positioned so that on-off heater J2 was activated and deactivated by resistance changes in RT of .0001 ohm (0.001°K). J2's current was increased until the resistance of RT increased very slowly. If more than 30 ma was required, the current to heater J1 was increased so that smaller amperages could be used with J2. While equilibration was taking place in sample cell SC, the pressure in CL was adjusted. Mercury was pushed from mercury reservoir MR into the variable level arm of the manometer, VL, until the difference in length of the mercury columns in VL and CL was nearly equal to the gas pressure in CL. Mercury

flow valve SV3 was then closed and the constant level arm valve SV2 was opened. The gas pressure in CL was adjusted until the capacitance gauge could be zeroed on the most sensitive scale. Constant level arm illumination CI was turned on to illuminate the meniscus. The mercury level in CL was adjusted to the hairlines of MC by opening SV3 and increasing or decreasing the pressure in mercury reservoir MR. The level control, LC, was used to raise the mercury level in CL and VL for the final adjustment when valve SV3 had been closed. This method of raising the mercury was done so that the mercury levels would be zeroed in the same way for each reading. (After these measurements a small rubber headed hammer was made so that the manometer tubes could be tapped to give reproducible mercury surfaces for each reading.)

The capacitance manometer gauge, CM, was used to determine when the temperature of the oxygen had reached equilibrium. The gauge for CM could be seen to move in phase with the bridge's null meter. When RT's resistance increased, CM indicated that the pressure on the oxygen side increased, and when resistance RT decreased the pressure on the oxygen side decreased. At this time CI was switched on and the mercury level in CL was raised until it reached the reference position. The variable level arm illumination VI was turned on and raised or lowered until it was behind the meniscus in VL and the hairline in the cathetometer CA was adjusted to the meniscus level. CL and CM were checked to see that the meniscus in CL was in the reference position and that CM was very near null. Five or six readings of the meniscus position in the variable level arm VL were then made with CA. CI and VI were turned off, the switch between the recorder output of the null meter and photocell operat-

ing galvanometer was opened, and the current to RT was increased to the calibration current of two milliamps. The dc null meter used with the Mueller bridge was balanced and measurements were made in the commutator R and N positions. The manometer housing temperature was read from Beckmann thermometer BTM. Meter bar illumination MI was switched on and cathetometer CA was rotated until the calibration marks could be seen on MB. CA was then adjusted to one of the reference lines on MB as described earlier. This reference mark was recorded and several readings were made with CA to determine this position. Once these measurements were made, the temperature of the copper block CB was adjusted to another value so that another point could be taken. Eleven points were measured and then this oxygen was pumped out of the sample cell and two other series of points were taken using analyzed oxygen (Breakseal #F-0305057). Values of the temperature determined by the resistance thermometer, RT, were calculated from the National Bureau of Standards calibration booklet using the average value of the commutator readings in R and N positions. This temperature was recorded in Table 1 as T_{NBS}.

The apparent difference in height, h_a, of the mercury columns in VL and CL was determined by subtracting the CL reference setting from the final measurement in manometer arm VL, that is

$$h_a = -\text{ CL reference} + \text{MB reference} + \text{average MB cathetometer reading} - \text{average VL cathetometer reading.}$$

h_a was called the apparent difference in height of the mercury columns because it was measured on meter bar MB which was not at its calibrated

Table 1. Oxygen Vapor Pressure

P(torr)	T_{NBS}	T_{VD} *	$T_{VD}-T_{NBS}$ x 10^3	T_{Nuy} **	$T_{Nuy}-T_{NBS}$ x 10^3
March 25, 1968					
134.648	76.362	76.372	10	76.367	5
152.655	77.209	77.218	9	77.212	3
260.229	81.053	81.054	1	81.049	- 4
314.730	82.524	82.524	0	82.520	- 4
539.298	87.023	87.024	1	87.023	0
664.252	88.909	88.911	2	88.911	2
736.797	89.879	89.884	5	89.884	5
March 30, 1968					
55.335	70.876	70.914	38	70.909	33
65.047	71.797	71.842	45	71.838	41
73.441	72.516	72.557	41	72.552	36
81.487	73.513	73.544	31	73.538	25
102.060	74.551	74.575	24	74.569	18
116.553	75.420	75.424	4	75.419	- 1
152.758	77.213	77.222	9	77.218	4
169.024	77.917	77.919	2	77.914	- 3
189.025	78.706	78.706	0	78.701	- 5
216.653	79.691	79.689	- 2	79.685	- 6
273.368	81.428	81.429	1	81.425	- 3
337.719	83.087	83.084	- 3	83.081	- 6
March 31, 1968					
32.378	67.976	68.020	44	68.014	38
241.261	80.484	80.484	0	80.480	- 4
300.109	82.154	82.151	- 3	82.147	- 7
377.039	83.980	83.976	- 4	83.973	- 7
425.945	84.991	84.989	- 2	84.985	- 6

Table 1. Oxygen Vapor Pressure (Concluded)

P(torr)	T_{NBS}	T_{VD}*	$T_{VD}-T_{NBS}$ x 10^3	T_{Nuy}**	$T_{Nuy}-T_{NBS}$ x 10^3
March 31, 1968					
470.560	85.834	85.835	1	85.832	- 2
524.538	86.780	86.779	- 1	86.775	- 5
583.158	87.722	87.722	0	87.721	- 1
640.938	88.580	88.582	2	88.581	1
711.087	89.546	89.549	3	89.548	2
758.283	90.157	90.158	1	90.158	1

*$T_{VD} = T^{+}_{VD}$ (90.18/90.1777)

T^{+}_{VD} is the temperature necessary to solve Van Dijk's[47] vapor pressure equation for pressure in column P.

**$T_{Nuy} = T^{+}_{Nuy}$ (90.18/90.168)

T^{+}_{Nuy} is temperature necessary to solve Nuy's equation[47] for pressure in column P.

temperature and MB was not exactly 1000 millimeters between the zero and 100 centimeter marks at its calibrated temperature. The calibration certificate showed that MB was 1000.004 millimeters at 20°C. This error was assumed to be a linear error and h_a was corrected by multiplying by 1.000004. This value was then corrected for expansion. MB's calibration certification gave its thermal coefficient of expansion to be 9.9×10^{-6} per degree centigrade. The true height of the mercury column was given by

$$h = h_a\,(1.0000004)(1 + ((t_{mb} - 20)\ 9.9 \times 10^{-6}/°C)) \qquad (25)$$

where t_{mb} was the temperature of MB in degrees centigrade. A correction was not considered necessary in these measurements for capillarity because of the large bore tubing (25.4 mm) used.

Generally when pressures are given in cm (mm) of mercury, they refer to cm (mm) of mercury at 0°C and at a point where the acceleration of gravity is 980.665 centimeters per second per second. This means that h must be reduced to these standard conditions. The correction could be made easily if the value of acceleration of gravity, g, at the manometer were known. Acceleration of gravity measurements were made at the Georgia Institute of Technology. This value was reported to be 979.5283 cm/sec^2[44] at a station designated WU9. The elevation of this station is 979.0 feet. WU9 was about 100 yards from the manometer, so an elevation correction was all that was required to obtain the value of g at the manometer. The elevation at the manometer was estimated to be 970 ± 3 feet. This estimation was made from two separate bench marks*

*981.950 feet at the bench mark on the west steps of the Old

located near the laboratory. The gravity correction is + 0.000094 cm/sec^2 per foot elevation so that g at the manometers was 979.529 cm/sec^2.

The height of a mercury column at a place where the acceleration of gravity is 980.655 cm/sec^2 and the temperature is 0°C can be determined by using the equation for pressure P exerted by a column of fluid

$$P = hdg \tag{26}$$

where h = the height of column of fluid

d = the density of fluid

g = the acceleration of gravity.

If the pressure was the same for two columns of the same fluid under different conditions, then

$$h_1 d_1 g_1 = hdg \tag{27}$$

and

$$h_1 = h(g/g_1)(d/d_1) \tag{28}$$

where g_1 = the standard value of g (980.665 cm/sec^2)

d_1 = the density of mercury at 0°C

h_1 = the height of the mercury column at 0°C

g = 979.529 cm/sec^2.

Then

$$g/g_1 = 979.529/980.665 = 0.998842 \tag{29}$$

and

$$h_1 = h\ (.998842)(d/d_1) \tag{30}$$

Physics Building. 961.108 feet at the bench mark on the west steps of the Civil Engineering Building. (Obtained from C. W. Tooles, Civil Engineering Department.)

Equation 30 shows that a density correction must be made. This density correction was considered to be entirely a temperature correction, even though other factors could have been considered. Among the other factors were density variations because of compression, isotope effect, and dissolved impurities.

The density of mercury at 0°C and one atmosphere pressure is given to be 13.5951[46] g/cm^3 and at 0°C and zero atmosphere the density is 13.59505[46] g/cm^3. This difference is about five ppm which, for a pressure of 760 mm mercury, will cause an error of about two plus microns if the average is not used. The isotope effect could be much more serious. There are several isotopes of mercury with natural abundances greater than 10 percent. These isotopes range in atomic weights from 198 to 202. If the percentage composition of mercury varied with source, then it would certainly be necessary to determine the density of a sample before ever using it. Cook's[45] measurements on samples taken from various sources, however, show that there seems to be a maximum isotope effect of about two ppm. In order that the impurity problem need not be considered, extra effort (cleaning procedure and use of triply distilled mercury) was made to assure that the mercury was nearly pure when it entered the system. There may have been some change in density due to the time that contact was made with the glass tube walls, the stainless steel container, and helium gas used. This problem was considered to be negligible.

The correction for density would have been made using the equation[46] for the volume of mercury at a temperature t (°C) given by

$$V = V_0(1 + 10^{-8}t(18144.01 + 0.7016t + 2825t^2 \times 10^{-3} + 2.617 \times 10^{-8}t^3)) \quad (31)$$

but reference 46 showed that an error of only three parts per million was introduced near room temperature by using

$$V = V_0(1 + 1.818 \times 10^{-4}t) \quad (32)$$

where V_0 is the volume of the mercury at 0°C. For a given mass, m, the density is given by

$$d = m/V = m/(V_0(1 + 1.818 \times 10^{-4}t)) \quad (33)$$

and the density at 0°C for the same mass is

$$d_1 = m/V_0 \quad (34)$$

so that

$$d/d_1 = 1/(1 + 1.818 \times 10^{-4}t). \quad (35)$$

Substituting equations 25, 30, and 35 into equation 29 and simplifying gives:

$$h_1 = h_a \frac{(.998842)(1 + ((t_{mb} - 20) \times 9.9 \times 10^{-6}/°C))}{(1 + 1.818 \times 10^{-4}t_{mb})} \quad (36)$$

where $t_{mb} = t$ the temperature measured by the Beckmann thermometer in the manometer housing MH. If capacitance manometer CM was not exactly nulled when the pressure measurement was made, the appropriate correction,

C, was added to h_1 to give the corrected pressure h_c

$$h_c = h_1 + C. \tag{37}$$

A less obvious pressure correction that had to be considered was the hydrostatic pressure. This effect was caused by three different effects.

1. The sample cell and the mercury level in manometer arm CL were at different vertical distances from the null indicating gauge CM.

2. The temperature of the gas in the sample cell inlet tube was different from the temperature of the gas in the manometer arm CL.

3. Different gases were used in the sample cell and CL.

The first two effects occur in most manometer systems, but the third was made possible because the capacitance manometer was built into this system. Corrections for these effects were made to h_c by: (1) subtracting the pressure exerted because of the weight of the helium column in the tube CL below capacitance manometer CM and above the mercury and (2) adding the pressure exerted because of the weight of the column of gas in the inlet tube between the capacitance manometer and the bottom of the sample cell SC.

$$P = h_c - (h_{He} d_{He} g/d_1 g_1) + (h_{gas} d_g g/d_1 g_1) \tag{38}$$

where P = the pressure at a distance h_{gas} below the capacitance manometer, CM, and on the gas side of the system (in units of length of mercury)

h_{He} = the vertical length of the helium column (900 mm) from the mercury level in CL to the middle of CM

d_{He} = the density of the helium in CL

h_{gas} = the vertical length of the gas column from the sample cell to the capacitance manometer CM

$d_1 = 13.5951\ g/cm^3$.

The gases were assumed to be ideal, so that the density was given by

$$d_g = M/V = M_w p/RT \tag{39}$$

where M_w = the molecular weight of the gas

p = the pressure (atmospheres)

R = the gas constant, 82.056 cm^3-atm/mole °K

T = the gas temperature.

The gas pressure p was replaced by $h_c/760$ mm atm^{-1}. The temperature of the helium in CL was replaced by the mercury temperature (°K) in manometer arm VL. Substituting equation 39 and the various constants into equation 38 gives

$$P(mmHg) = h_c(mm)(0.999986 + (M_{wgas} h_{gas}/T_{gas})(1.18 \times 10^{-6})). \tag{40}$$

T_{gas} was approximated by the average of the temperatures measured from the sample cell to thermocouple 4 on the inlet tube I2. h_{gas} for the oxygen vapor pressure was the distance to the bottom of the sample cell (h_{O_2} = 400 mm) but for adsorption isotherms h_{gas} was measured to the middle of the sample cell (h_{gas} = 350 mm).

The final consideration was gas impurities. The manufacturer's assay reported the following impurities:

Nitrogen	159 ppm
Argon	140 ppm
Carbon Dioxide	65 ppm
No other detectable impurities	

No correction was made for the carbon dioxide. However, corrections were made for the nitrogen and argon that were present. The pressure exerted by these gases was calculated from the estimated amount of impurity that was trapped in the system when oxygen was condensed in the sample cell. An estimate of the argon and nitrogen was made from pressure, volume, and temperature values. The pressure in the 1.1 liter Pyrex flask was assumed to be 755 mm at 0°C. All impurity was assumed to remain in the gas phase. The maximum pressure correction made for these gases was -.245 mm at 90°K while .183 mm was subtracted from the pressure at 67°K. The resulting values are compared with temperatures calculated from equations in reference 47. The temperatures T_{VD}^{+} * and T_{Nuy}^{+} ** are values that will give the measured pressures. Since no equation was given in the references to convert to the NBS-55 temperature scale, the temperature values were converted for comparison by the equation

$$T = T^{+}(90.18/T_{O_2}) \qquad (41)$$

---

* T_{VD}^{+} is temperature necessary to calculate the measured pressure using van Djik's equation on page 819, reference 47.

** T_{Nuy}^{+} is temperature necessary to calculate measured pressure from the Nuy equation on page 811 of reference 47. (The coefficient of the logarithm term is in error in this paper.)

where T_{O_2} is the O_2 boiling point reported for the referenced equation. (Boiling point of oxygen for the Nuy equation is 90.168°K and van Dijk gives 90.1777°K.) Agreement with the calculated values was quite good above 75°K. Below this temperature there were large deviations from the calculated values. Since this was an experiment run to gain experience with the operation of the apparatus, no great effort was made to interpret these data. However, it was decided that copper block CB would be wrapped with an aluminum foil radiation shield for further low temperature work in case the deviation was caused by uneven heat loss from CB. Also, a rubber hammer was designed to tap the manometer arms, VL and CL, to get more reproducible mercury meniscii.

CHAPTER IV

CALIBRATION

Platinum Resistance Thermometer

This thermometer (L and N Model 8164, Ser#1593183) was calibrated by the National Bureau of Standards during January 1965 for the temperature range 11°K to 300°C. The calibration certificate indicated that the thermometer met the requirements of a standard for the International Practical Temperature Scale. Interpolation tables were furnished with the calibration for the entire temperature range. These tables were calculated using the modified Callander equation*

$$R_t/R_o = 1 + At + Bt^2 \tag{42}$$

above 0°C and

$$R_t/R_o = 1 + At + Bt^2 + C(t - 100)t^3 \tag{43}$$

from 0°C to about -183.97°C. R_o is the resistance of the resistor at 0°C, R_t is the thermometer resistance at t degrees Centigrade. A, B, and C are constants determined from measurements at fixed points. Temperature values determined from the interpolation tables were added to 273.15° and have been reported as T_{NBS-55} throughout this work. This temperature (T_{NBS-55}) was corrected as nearly as possible to the thermo-

*Notes to Supplement Resistance Thermometer Reports, National Bureau of Standards, Washington, D. C. (1963).

dynamic temperature, T, using the work of Barber[48] (see Table 25, Appendix E).

The L and N 8069-B Mueller temperature bridge (Ser#1551895) used with the resistance thermometer RT was calibrated by the manufacturer. Its calibration certificate gave corrections for each of the individual resistors when the bridge was operated at 35°C. Resistors below 0.010 ohm required no correction. The other resistors used required a maximum correction equivalent to -0.003 °C.

Thermocouples

The emf's of the copper-constantan thermocouples (TC1-TC8 and TC13-TC16) used on the inlet tubes, manometer box, and in the room were measured in various constant temperature baths. The bath temperature was determined by resistance thermometer measurements. The constantan leads of thermocouples one through eight were soldered to the constantan lead of a thermocouple that was to be used as a reference junction. Each thermocouple was pressed between two short pieces of Teflon tape. All of the leads were labeled and bound together with a rubber band. These junctions were placed in an ice bath in a one gallon Dewar. The thermocouples were positioned about three inches from the bottom of the Dewar and seven inches from the ice surface and emf measurements were made with the K-3 potentiometer. (The reference standard cell used was a 100 ohm internal resistance Epply standard cell (Ser#B7176).) These measurements indicated that there was a maximum difference between the reference junction and the others of 0.9 microvolt. Further checks showed that most of this difference was from connections made at a terminal strip and could

be reduced to 0.1-0.3 microvolt by insulating the terminal.

The reference junction was put into another ice bath in a one liter Dewar. The other junctions were fixed to the resistance thermometer and positioned about six inches below the surface of a dry ice (CO_2)-acetone bath in a one gallon Dewar. This system was covered with several towels and allowed to equilibrate about 10 hours. The reference ice bath was drained and refilled, then thermocouple emf measurements and thermometer resistance measurements were made. The bath temperature continued to change so measurements were made in the following order: resistances in commutator positions R_R, R_N followed by emf readings for thermocouples one through eight, then resistance measurements in commutator positions R_N, R_R followed by TC8 to TC1 emf measurements. This procedure was repeated several times. The emf values for the thermocouples were recorded with the resistance thermometer temperature.

A liquid nitrogen bath was prepared in the same type Dewar used for the (CO_2)-acetone bath. The thermometer and thermocouples were suspended in the liquid about six inches below the surface. Then emf and resistance measurements were made as they were in the dry ice bath, giving another set of emf versus temperature points.

The constantan leads of thermocouples 13-16 were soldered to the constantan lead of a copper constantan reference junction. These junctions were prepared with Teflon tape as TC1-TC8 were and they were checked in an ice bath. The measurements with these couples showed a difference between the reference and other thermocouples to be about 0.3 microvolt. The junctions 13-16 along with the resistance thermometer RT were immersed in an oil well in a three inch diameter by six inch long aluminum cylinder.

This cylinder was placed in a controlled temperature air bath (±0.02°). Measurements of emf and resistance were made as with nitrogen and CO_2 baths. During the time (six hours) the measurements were being made, the temperature decreased continuously. The net change for six hours was 0.03 °C. The bath temperature was changed about four Centigrade degrees and new measurements were made.

Since thermocouples 13-16 were only going to be used in the region of room temperature, a linear interpolation equation of the form

$$t^\circ\ (C) = \text{slope} \times (\text{emf}) + \text{constant} \tag{44}$$

was fit to the experimental results. The slope and constant were 24.525 °C/mv and 0.638 °C, respectively.

The original thought was to represent the interpolation equation for thermocouples 1-8 with a quadratic equation but further investigation indicated that much better fit was obtained with a cubic equation. The couples had already been attached to the inlet tubes when this was realized and since junctions 1-8 and 13-16 were made at the same time using the same procedures the points for thermocouples 13-16 were included in the interpolation equation for thermocouples TC1-TC8. This equation is

$$\text{emf (mv)} = A + Bt + Ct^2 + Dt^3 \tag{45}$$

The coefficients A, B, C, and D were determined for the average of the eight thermocouples emf's at each temperature. This difference did not amount to more than ± 0.05°C at any temperature. The coefficients for the interpolation equation used for thermocouples 1-8 were determined to

be A = 0, B = 3.8625×10^{-2}, C = 4.5161×10^{-5}, and D = -4.0975×10^{-8} when emf is in millivolts and t is in degrees Centigrade.

Beckmann Thermometer

This thermometer (ISI .01 °C thermometer; Ser#645017) was used in the thermostated manometer housing to determine the manometer mercury temperature. It was calibrated using an L and N calibrated 8163 platinum resistance thermometer (Ser#1547845). The Beckmann and resistance thermometers were immersed in a one gallon Dewar containing water. Several hours were allowed for equilibration, then Beckmann readings versus resistance were made. The data were fit to the equation

$$t\ (°C) = A \times t(\text{in Beckmann units}) + \text{constant}$$

to give

$$t(°C) = -1.0244 \times t(\text{in Beckmann units}) + 25.000. \qquad (46)$$

Capacitance Manometer

Even though the capacitance manometer (Series 212 Model B, Ser #000667) was used primarily as a null indicator, two different calibrations were necessary. The first calibration was used to determine the pressure differential that would cause full scale deflection on the most sensitive scale. The meter for this instrument was one that had 100 units on each side of zero so that full scale deflection was 200 units. The amount of gas on the pipet side of the system was increased until the meter showed maximum deflection to the right side of zero, then the pressure in the manometer arm CL was measured. Gas was expanded into CL

until the meter deflected full scale. The pressure in CL was again determined using the mercury manometer. The pressure difference was the value for 200 units deflection. The manufacturer's manual stated that the 0.1 torr range was linear so that each unit deflection could be calculated by dividing the total pressure change by the number of units deflection. The average of several sets of measurements gave a value of 0.48 micron per division.

The second calibration was necessary because the capacitance manometer zero shifted with the total pressure inside the system. This calibration was determined for the 0.1 range and maximum sensitivity.

The meter was nulled with 10^{-5} torr or less on both sides of the diaphragm. The two ports of the capacitance head were connected. Pressure was then increased inside the sensing head in steps. The pressure was measured with the mercury manometer and the deflection was read from the capacitance manometer meter. The deflection to the left increased as the pressure was increased. This deflection indicated that the distance between the capacitance probe and diaphragm increased with increased pressure. Another correction that was being made with this calibration was the increased capacitance of the system because of adding a gas with a dielectric constant greater than unity between the capacitor plates.

Meter Bar and Cathetometer

The micrometer slide (Model M-300-P; Ser#2429-P) and standard meter bar (M-1010 Type 416 stainless steel meter bar; Ser#150 AU) were purchased from Gaertner Scientific Corporation. Both were supplied with

manufacturer's calibration certificates. In each case the certificate was for the distance between the end reference marks.

The distance between the zero and 25 millimeter marks on the micrometer slide was certified to be 25.000 mm at 20°C. No verification was included for the spacing of the one mm marks on the scale. The meter bar was certified for the distance between the zero and 100 centimeter marks. This distance was 100.0004 ± 0.0003 centimeters at 20°C. The scale was marked at one millimeter intervals. The intermediate divisions were not calibrated by the manufacturer. They were assumed to be equally spaced on both instruments (meter bar and micrometer scale) and no further checks were made on them.

Volumes (Figure 31)

Pipets (Volume V_p)

The pipets were calibrated twice, using mercury, to determine the volumes between marks on their upper and lower stems (Table 2). One determination was made at room temperature and the pipet volume was calculated at the ice temperature using coefficients of expansion of glass and mercury. The coefficient of cubic expansion used for glass was $29.7 \times 10^{-6}/°C$ and $181.8 \times 10^{-6}/°C$ for mercury. The second calibration was performed after the pipets had been mounted in pipet box, BB.

For the first calibration, each pipet was filled with mercury to the upper reference line. It was then drained into a flask until the level reached the lower reference line. This mercury was weighed on a Mettler (Ser#45736) one pan balance. A mass correction was made for the air displaced from the flask by the mercury. The pipet temperature was

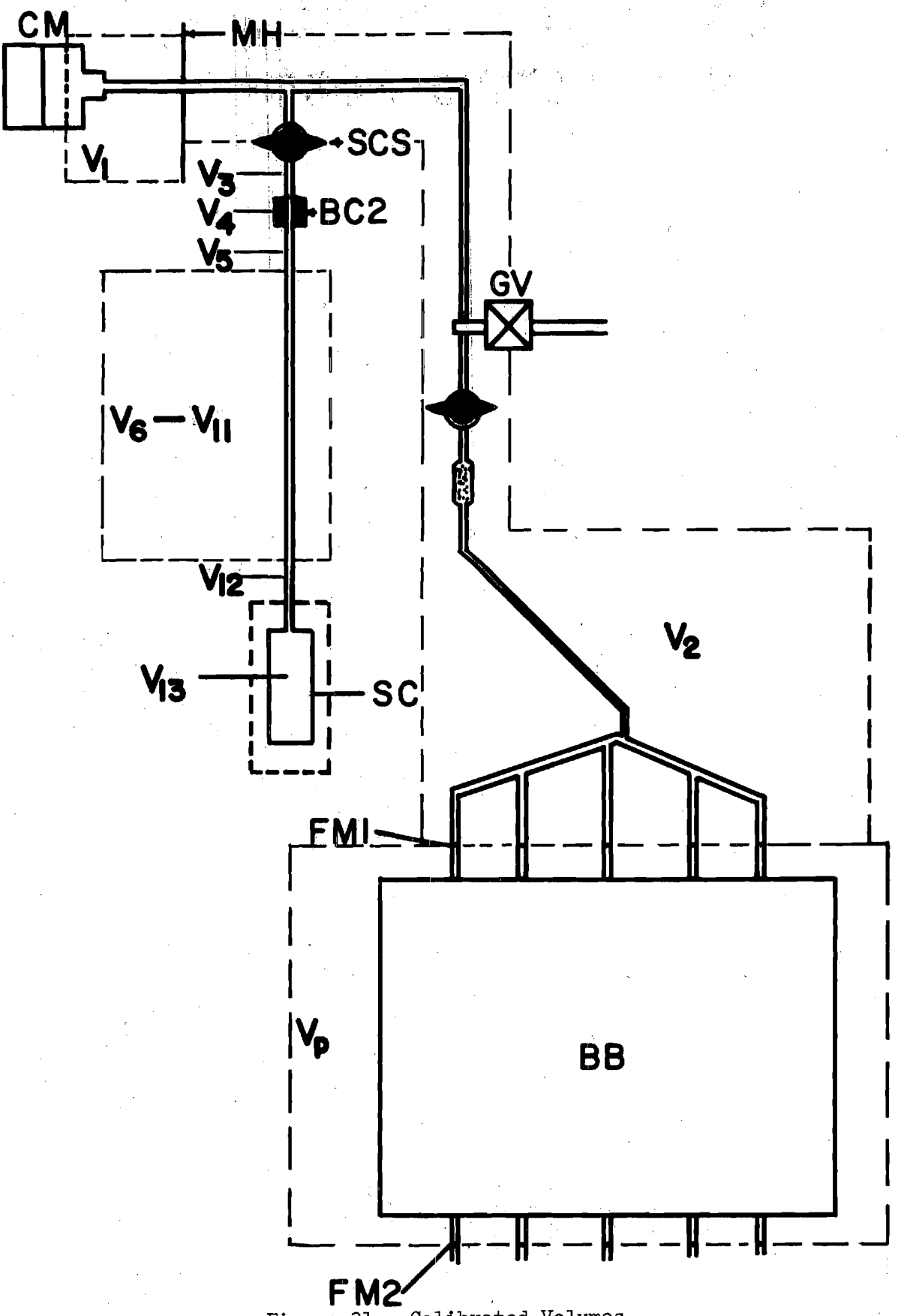

Figure 31. Calibrated Volumes

Table 2. Pipet Volumes

Pipet No./	2	3	6	8	10
First calibration (cm^3)*	11.0954	21.3694	40.5530	63.8463	150.7437
and std. dev. (cm^3)	± 0.001	± 0.002	± 0.001	± 0.001	± 0.001
In situ volume (cm^3)**	11.0971	21.3714	40.5536	63.8411	150.7375
and std. dev. (cm^3)	± 0.0004	± 0.0005	± 0.0013	± 0.0009	± 0.0007

*Corrected to new fiducial marks and 0°C.

**These volumes used for all calculations.

determined by a thermometer immersed in a container of mercury with dimensions and thermal mass similar to the pipet being calibrated. For the larger pipets, several flasks were used to catch the mercury so that their individual masses would not exceed 1000 g, the limit of the weighing instrument. The mercury volume was determined by dividing the mass by the density at the pipet temperature. After this determination was made, two more reference marks were put on the pipet stems so they could be seen when mounted in the pipet box. Corrections were made by calculating the volume increase between old and new fiducial marks. To do this the distance between the marks and the tubing radius had to be measured. Ends of the pipet capillary tubing were cut and their radii were measured with the cathetometer.

The second calibration was carried out in situ in pipet box BB using an ice bath. The ice bath was prepared in BB and maintained while calibration was in progress. Each pipet was filled slightly past the upper reference line with triply distilled mercury from a reservoir and a valve between the reservoir and pipet was closed. About one hour was allowed for the mercury temperature to equilibrate in the largest pipet and it was readjusted to the reference line. The mercury was then drained from the pipet, into a flask, through a separate valve with a small orifice at its end. After draining a pipet, the mercury in the tubing between the lower fiducial mark and the orifice was allowed to warm to room temperature. The mercury level was readjusted to the lower fiducial mark by draining the extra mercury. Flask and mercury were weighed on the Mettler balance used for the previous calibration. The flask mass was subtracted from the total mass of mercury and flask.

The mercury volume was determined by dividing the mercury mass by the density (13.5951 g/cm^3) at 0°C. Correction was made for the mass of air displaced from the flask by mercury. The second set of calibrated volumes was used in all calculations.

The balance used to weigh the mercury was checked with a set of Ainsworth and Sons, Inc., Class S weights (Set #5040; Ser#21185). Combinations of the weights were used to 100 grams, then checks were made at 100 gram intervals using bottles with lead powder in them. After the 100 gram comparison had been made, a bottle was placed on the balance and filled with lead powder until it had nearly (± 0.0005 g) the same mass as the sum of the standard weights. This bottle and the weights were used to check the balance at 200 g, etc. Agreement was very good at all points measured and did not exceed 3.6 milligrams anywhere, which would give a volume error of ± 0.0003 cm^3.

Capacitance Manometer and Connecting Tubing (V_1 and V_2)

Pressure, volume, and temperature gas measurements with neon were used to calibrate volumes V_1 and V_2. The volume of the tubing from fiducial marks FM1, just above the pipets, to stopcock SCS and the outside of the manometer housing wall (Figure 31) was designated V_2. The average value of the temperatures measured by thermocouples TC15 and TC16 was used as the temperature of volume V_2. Tubing inside the manometer housing with the capacitance manometer made up volume V_1. The temperature for volume V_1 was measured by thermocouple TC14 located on the front face of the capacitance manometer.

The pipet box was packed with crushed ice and about four standard cm^3 atmospheres of neon was expanded into the system. The pipet mercury

levels were adjusted to the reference marks FM1 or FM2 and the pressure was measured. Then emf readings were made for thermocouples TC14, TC15, and TC16. The pipet volume was changed and the measurements were repeated until data had been collected for several different pipet settings. Since two volumes, V_1 and V_2, at different temperatures were being determined simultaneously and the temperature difference was small, one volume, V_1*, was estimated and used to calculate the remaining volume V_2. This calculation was made using a virial equation of state truncated after the second term

$$PV_i/N_iRT_i = 1 + B_2P/RT_i \tag{47}$$

so that

$$N_i = PV_i/(RT_i + B_2P) \tag{48}$$

where N_i = the number of moles of gas in the i^{th} volume

V_i = the i^{th} volume (in cm^3)

T_i = the temperature (in °K) of the i^{th} volume

R = the gas constant (82.056 cm^3 atm/mole °K)

B_2 = the second virial coefficient** of the gas at T_i

P = the pressure (in atmospheres)

i = an integer which designates the section of the system being considered.

---

*Note: This calibration was done twice. For the first determination volume V_2 was estimated to be 2.722 and V_1 was calculated to be 2.931. The glass tubing above the pipets was broken and replaced with several modifications to V_2 but V_1 was not changed. So the calculated value of V_1 was used for the second calibration (the one described here).

**See Appendix A. The second gas virial coefficient will not be

The total number of moles of gas in the system, N_T, was a sum of the number in each section so that

$$N_T = N_P + \sum_{i=1}^{2} N_i \tag{49}$$

where N_P is the number of moles of gas in the pipets.

Since one volume was unknown, N_T could not be calculated directly but it could be found by calculating $N_P + N_1$ for each point and plotting this versus pressure. An extrapolation to zero pressure gave an approximate value for N_T. Equation 48 was substituted into equation 49 and through algebraic manipulation V_2 was solved for as

$$V_2 = (N_T - N_P - N_1)(RT_2 + B_2P)/P. \tag{50}$$

Using the approximate value for N_T, a V_2 was calculated for each pipet setting. Then N_T was adjusted until the smallest standard deviation for the calculated values of V_2 was found. The average of the values giving the smallest standard deviation was taken to be V_2 (see Table 3).

Inlet Tube and Stopcock, SCS (Volumes V_3 to V_{12})

The inlet tube volume was calculated from its length and the volume per unit length determined for three pieces of tubing taken from the same shipment.

Forty centimeter sections from three different tubes were cut and used for calibration. These sections were cleaned and each individual

---

labeled to indicate the associated volume but B_2 corresponds to the temperature of the volume being considered.

Table 3. Volume V_2 Determined from Gas Measurements

P (cm)	T_2 (°K)	V_2 (calculated) (cm^3)	V_1 (estimated) (cm^3)
13.5369	294.05	1.766	2.931
13.5364	293.52	1.766	
15.3582	294.37	1.778	
15.3574	293.62	1.777	
23.3253	292.94	1.769	
23.3249	293.47	1.773	
40.7382	294.58	1.773	
40.7391	294.73	1.773	
67.8583	293.52	1.769	
		1.772 average	
		± 0.004 standard deviation	

length's volume was determined with mercury. The tubes were filled by holding them vertically and forcing mercury from the bottom of the tube to the top. The metal tube was inverted after covering the top. The filling tube was carefully removed and mercury was drained into a previously weighed flask. All mercury was assumed removed if no droplets could be seen on the walls when sighting through the tube. The mercury and flask were weighed to determine the mercury mass. The mercury temperature was taken to be room temperature and the corresponding density was used to calculate the tube volume. Five such measurements were made for each tube. The average volume per centimeter for each tube was 9.707×10^{-3} cm^3/cm, 9.703×10^{-3} cm^3/cm, and 9.707×10^{-3} cm^3/cm. These values were averaged to give 9.706×10^{-3} cm^3/cm and this average was used as the volume per unit length of the inlet tube I2.

The tubing from the end of I2 under the fiducial mark FM3 to SCS and the bore of SCS were also a part of the inlet tube volume. This volume was determined before it was installed using the same methods used with the monel tubing. Mercury was forced from the bottom of the tube through the stopcock bore to reference mark FM3. The stopcock was closed and all mercury below the barrel was forced out. Mercury remaining in the bore, and between the barrel and fiducial mark FM3, was drained and weighed. The volume of the stopcock bore and tubing between the barrel and fiducial mark was $0.111\ cm^3 \pm 5 \times 10^{-4}\ cm^3$.

The length of monel tubing from reference mark FM3 to the top of brass cylinder BC2 was measured to be 14.5 centimeters (cm) which had a volume of 0.141 cubic centimeters (cm^3). This volume ($0.141\ cm^3$) added to stopcock SCS's ($0.111\ cm^3$) gave $0.252\ cm^3$ for V_3. The same temperature

was used in calculations for volumes V_2 and V_3.

V_4, the volume of monel tubing soldered inside brass cylinder BC2 (BC2's length was 3.6 cm), was 0.0349 cm^3. The temperature for volume V_4 was determined by averaging the temperature measured by TC1 and the temperature of volume V_2.

Volumes V_5 to V_{10} were defined by the positions of seven equally spaced thermocouples TC1 to TC7 on inlet tubes I2 and I3 from brass cylinder BC2 to TS where the tubes separate. The positions of the volumes are shown in Figure 31. A thermocouple was located at the top and bottom of each volume. The average temperature measured by these thermocouples was used to be the volume temperature. The distance between thermocouples TC1 and TC7 was 46.0 cm so that the distance between two consecutive thermocouples was 7.67 cm and volumes V_5 through V_{10} were 0.0744 cm^3.

Volumes V_{11} and V_{12} were between thermocouple TC7 and copper block top, CBT. TC8 was placed to divide the 12.2 cm between TC7 and CB equally so that each length of tubing was 6.1 cm and each volume was 0.0592 cm^3. The temperature for V_{11} was determined by averaging the temperatures of thermocouples TC7 and TC8. V_{12}'s temperature was an average of the copper block value measured with the resistance thermometer and the temperature at TC8.

Sample Cell (V_{13})

This volume was determined by PVT measurements after loading the cell with adsorbent. The sample was outgassed at 500°C ± 50°C for about three days (until pressures below 10^{-5} torr were indicated by Philips gauge, PG). When outgassing was completed the sample cell was allowed to cool to room temperature under vacuum of 10^{-6} torr or better. Stop-

cock SCS was closed and the sample cell was placed in a one gallon Dewar. The sample cell was positioned so that its top would be one and one half inches below the bath surface when the Dewar was filled with ice. Thermocouple eight was positioned along the inlet tube I1. Periodically water was drained from the ice bath and the Dewar was refilled with ice. The ice bath in BB was prepared and maintained throughout the experiment.

Sample cell volume, V_{13}, was calibrated with helium. This gas was expanded from a Pyrex flask on the apparatus into the gas transfer pipet system through valve GV. While helium was entering the system, the pressure differential across the capacitance manometer diaphragm was maintained near zero by increasing the gas pressure in manometer arm CL. GV was closed to a reference mark when 35-45 standard cm^3 of gas had entered the system.

The pipet mercury levels were adjusted to fiducial marks FM1 for the 10, 20, 40, and 80 cm^3 pipets and to FM2 for the 160 cm^3 pipet. About 30 minutes was allowed for the gas temperature to equilibrate. Then the capacitance meter was nulled, the pressure was measured, emf readings were made for thermocouples 14-16, and the Beckmann thermometer in the manometer housing, MH, was read. These measurements gave enough information to determine the number of moles of helium gas in the system using equation 48. Thirty minutes to an hour after the first measurements were made, they were repeated. The amount of gas in the system was calculated for each set of measurements and the two values were averaged. The average value was used as the amount of gas in the system.

When the amount of gas in the system had been determined, stopcock

SCS was opened and gas expanded into sample cell SC. For this expansion SCS was opened gradually until the pressure started to decrease on the pipet side of capacitance manometer CM, so that the pressure in manometer arm CL could be adjusted to decrease at the same rate. This was a necessary precaution when using the capacitance manometer. (Pressure differentials greater than four cm mercury across the capacitance manometer diaphragm would have caused the zero of the instrument to change.) When the system pressure equilibrated, stopcock SCS was opened fully. The pipet mercury levels were checked to see that they were on FM1 or FM2. The capacitance manometer CM was nulled by appropriate pressure adjustments in CL and the heights of the levels of mercury in the manometer arms were measured. The Beckmann thermometer was checked and thermocouples 1-8 and 14-16 were read. These measurements were repeated 20 to 30 minutes later. The volume of the pipet system was then changed by filling or emptying pipets of mercury and a new set of measurements was made using the above procedure. Measurements were made using several different pipet volumes so that the pressure changed from about 20 cm mercury to 70 cm mercury. The system was evacuated to a pressure below 10^{-5} torr. The pipets were refilled and a new series of measurements was started. Three different series of measurements were made.

The amount of gas in the system was determined from measurements made before opening SCS. These values were averaged to give the total number of moles of gas, N_T, in the system. The amount of gas in the sample cell, N13, was calculated for each measurement made after stopcock SCS was opened by subtracting the number of moles of gas in the system (except for the sample cell) from N_T.

$$N_{13} = N_T - N_P - \sum_{1}^{12} N_i \qquad (51)$$

where summation was over all volumes occupied by the calibration gas except the sample cell and pipets. The number of moles of gas in each volume was calculated using equation 48 and the volume of the sample cell, V_{13}, was calculated from the equation

$$V_{13} = N_{13}/P(RT_{13} + B_2 P). \qquad (52)$$

The calculated values of V_{13} (Table 4) were averaged to yield 40.719 cc ± 0.014 and this was assumed to be the correct volume, V_{13}, of the boron nitride filled sample cell.

Table 4. Sample Cell Volume at 273.15 °K
Helium Determination

P (torr)	Volume (cm^3)		P (torr)	Volume (cm^3)
Series 1			Series 2	
273.479	40.728		204.368	40.737
444.093	40.725		224.876	40.743
647.548	40.711		284.924	40.729
			365.236	40.722
Series 3			532.482	40.711
343.836	40.698			
440.769	40.697	average	40.719	
642.445	40.706	standard deviation	± 0.014	

Boron Nitride Sample Volume and the Total Sample Cell Volume

The total sample cell volume V_{SC} (without BN sample) was the sum of the BN sample volume at 0°C, $V_{BN}(0°C)$, and sample cell volume V_{13}. $V_{BN}(0°C)$, the BN sample volume, was determined by dividing the sample mass, 83.47 g by BN's density, 2.27 g/cm^3,[42]

$$V_{BN}(0°C) = 83.47 \text{ g}/2.27 \text{ g/cm}^3 = 36.77 \text{ cm}^3.$$

Thus the total volume of the sample cell at 0°C, $V_{SC}(0°C)$, was

$$V_{SC}(0°C) = V_{BN}(0°C) + V_{13} = 36.77 \text{ cm}^3 + 40.719 = 77.49 \text{ cm}^3.$$

The values of $V_{BN}(0°C)$ and $V_{SC}(0°C)$ were necessary to correct volume V_{13} for expansion or contraction at temperatures other than 0°C. The coefficient of cubic expansion for BN used was the same as the coefficient of linear expansion[40] since it was assumed that expansion along a plane was negligible. The volume of the BN sample, $V_{BN}(t)$, at any temperature t (in degrees Centigrade) could be calculated by

$$V_{BN}(t) = V_{BN}(0°C)(1 + 41.15 \times 10^{-6}t) = 36.77\ (1 + 41.15 \times 10^{-6}t). \quad (53)$$

The coefficient of cubic expansion, β, for polycrystalline nickel was taken to be three times the coefficient of linear expansion, α,[49-50]

$$\beta = 3\alpha.$$

Thus the volume of the sample cell, $V_{SC}(t)$, at any temperature was

$$V_{SC}(t) = V_{SC}(0°C)(1 + 3\alpha^{*}) \tag{54}$$

with $\alpha = 12.54 \times 10^{-6}t + 8.75 \times 10^{-9}t^2 - 7.5 \times 10^{-12}t^3 + 6.25 \times 10^{-15}t^4$.

V_{13} at any temperature t (in degrees Centigrade) was

$$V_{13}(t) = V_{SC}(t) - V_{BN}(t). \tag{55}$$

Substituting equations 53 and 43 into equation 55 and some algebraic manipulation yields

$$V_{13}(t) = V_{13}(0°C) + 3\alpha\, V_{SC}(0°C) - (41.15 \times 10^{-6}t) \times 36.77. \tag{56}$$

The above expression for $V_{13}(t)$ was used for V_{13} for all calculations.

---

*α has been used on this page to be the coefficient of linear expansion times the temperature.

CHAPTER V

EXPERIMENTAL PROCEDURES AND DATA TREATMENT

When calibration was completed, the system was prepared for adsorption measurements with inert gases by outgassing the sample cell at 450-550°C and the capacitance manometer at 175-225°C until the pressure was reduced to about 10^{-6} torr. When heating was discontinued, the pressure continued to decrease to about 10^{-7} torr. Other preparations for ice point (273.15°K) adsorption measurements were the same as those described earlier for determining V_{13}, the sample cell volume.

Stopcock SCS, above the sample cell, was closed and adsorbate was expanded into the gas transfer system until the desired amount of gas had been added. Several sets of pVT measurements were made and the number of moles of gas in the system, N_T, was calculated for each set of measurements from the equation

$$N_T = \frac{P}{R}\left[\frac{V_p(HC_p)}{T_p + ((B_2 P)/R)} + \sum_{i=1}^{2} \frac{V_i}{T_i + ((B_2 P)/R)}\right] \qquad (57)$$

where $HC_p = 0.999986 + (0.00000152\ M_w)$, the hydrostatic correction for pressure in the pipets (equation 40)

M_w = the atomic weight of the adsorbate

T_p = the pipet temperature

and all other symbols have been defined.

Since more than one set of measurements was made, an average value $\bar{N}_T$*

*Note: a bar above a letter will indicate an average value.

was used:

$$\bar{N}_T = \left(\sum_{i=1}^{i=m} N_{T_i}\right)/m \qquad (58)$$

where i = an integer

m = the number of determinations of the amount of gas in ths system.

When the number of moles of adsorbate in the system had been determined, stopcock SCS was opened and pressure-temperature data were collected for various pipet settings. Using values obtained from these measurements, the amount of gas adsorbed, N_a, was calculated for each point by the equation,

$$N_a = \bar{N}_T - P\left[\frac{V_p(HC_p)}{T_p + ((B_2P)/R)} + \sum_{i=1}^{12} \frac{V_i}{T_i + ((B_2P)/R)} + \frac{V_{13}(HC_{13})}{T_{13} + ((B_2P)/R)}\right] \qquad (59)$$

where $HC_{13} = \dfrac{(M_{wgas})(350)(0.00000118)}{\bar{T}} + .999986$ (see equation 40)

$\bar{T}$ = average temperature along gas inlet tube as described below equation 40

and other symbols have been defined.

Two sets of measurements were made at each pipet setting for several isotherms and an average of the two measured pressures and amounts of gas adsorbed is reported in Appendix D.

The next isotherms were measured with argon at several temperatures below the ice point. The system was outgassed as it was for the 273.15°K isotherms and the cryostat was assembled so that the temperature

could be controlled using the copper block heaters as it was during the oxygen vapor pressure measurements. An acetone-dry ice (solid CO_2) bath was used in Dewar D1 when isotherms were measured at 248, 231, 221, 210, and 198°K. For these measurements Dewar support cannister DSC was not attached to the cryostat support plate, CSP, so that dry ice could be added to the bath when required. The 221°K isotherm was measured first; afterwards the system was disassembled, outgassed, and reassembled. Then the 198, 210, 231, and 248°K isotherms were measured without changing the dose of gas. Following these measurements the cryostat was set at 273.15°K and two points were measured quickly for comparison with the previously determined values. These two points were in good agreement with the 273.15°K argon data and are given in Table 15 as 273.15°K check points.

Lower temperature isotherms, 90 and 141°K, were measured using a liquid nitrogen bath in Dewar D1. The numbers of moles of gas adsorbed for the 90-248°K isotherms were calculated using equation 59. (The correction for sample and sample cell contraction was made by substituting $V_{13}(t)$ from equation 56 into equation 59 for V_{13}.) The results are listed in Appendix D and are shown in Figures 33 and 34. The temperature in the table has been corrected to the thermodynamic scale using reference 48 (see Table 25, Appendix E).

The 90°K isotherm was used with the BET equation[33] (equation 13) to determine the sample surface area (4.98 m^2/g) reported in Chapter II for comparison with other BN samples that have been studied. (Argon's cross sectional area and vapor pressure were taken to be 14.1 $Å^2$ and 1094.2 torr, respectively.) This treatment gave RN_m to be 0.004812 cm^3-

atm/(°K gram) and the constant C was 148.4.

Isotherms shown in Figures 33 and 34 seem to have a linear region but extrapolation of a line through the points for an isotherm did not pass through the origin at zero pressure. The intercept at zero pressure was positive for every isotherm and became larger for the lower temperature isotherms. This feature was disturbing and at first was attributed to possible calibration or experimental error. However, after reviewing the procedures and considering the type calibration errors that could have caused such an effect, these sources were ruled out. Another consideration was a surface effect which could have been caused by high energy areas, such as edges on the sample surface. Due to a lack of prior knowledge that this type behavior would be displayed, the isotherms were measured at too high pressures and a Henry's law region was not observed. This complicated graphical determination of virial coefficients so that a computer fit of the data was used.

First, all isotherms (except the 90°K) were computer "fit" (Burroughs B-5500) to an equation of the form

$$N_a = \sum_{i=1}^{n} C_{i+1,s}(P/RT)^i \qquad \text{where } 1 \leqq n \leqq 4 \tag{60}$$

using a "least squares" program (Algol program A-A066) from the Georgia Tech Burroughs computer library to determine the coefficients, $C_{i+1,s}$.* This program used double precision arithmetic to fit the data, and equation

---

*$C_{i+1,s}$ will be used for the $(i+1)^{th}$ gas-solid virial coefficient when expansion is in powers of P/RT.

60 required that the isotherm pass through $N_a = 0$ at $P = 0$. The data were also fit to polynomials in P/RT of the form

$$N_a = I + \sum_{i=1}^{n} C_{i+1,s}(P/RT)^i \qquad (61)$$

where I = the intercept at P = 0

$$1 \leq n \leq 3.$$

Each point was equally weighted in the fitting technique used. This procedure was tested by fitting the experimental data of Sams, Constabaris, and Halsey[26] to equation 60 (Table 5). Good agreement was found for the B_{AS} ($C_{2S} = B_{2S} = B_{AS}$) values. The order of the polynomial to be used (see Table 6) was determined from a graph of $N_a RT/P$ versus P. If this plot was judged to give a straight line a second order equation was accepted, curvature required a third or higher order equation.

Selected values of the second gas-solid virial coefficient, C_{2S}, determined by the described technique (Tables 6 and 7) for the 198-273.15 °K argon isotherms were fit to equation 105 for the Lennard-Jones (3-9) potential function. A preliminary estimate of ϵ^*/k was made graphically (Appendix F) and the final calculation of the best fit values of ϵ^*/k and Az_o was done using a computer scanning technique at one degree intervals (see Appendix F). The resulting values of ϵ^*/k and $\overline{Az_o}$ determined using C_{2S}'s from polynomials passing through the origin and the C_{2S}'s from polynomials with an intercept are given in Table 8. The parameter z_o was estimated to be the same for the Ar-BN system as that calculated by Sams[26] for the Ar-graphite system. Using this value of z_o and $\overline{Az_o}$ from the best fit data, A was calculated and is included in Table 8.

Table 5. Halsey's Data Fit to Polynomial for Argon

T (°K)	B_{AS} (cm^3/g)	C_{AAS} ($cm^6/mol\text{-}g$)	D_{AAAS} (cm^9/mol^2g)	C_{2S} (cm^3/g)	C_{3S} ($cm^6/mol\text{-}g$)	C_{4S} (cm^9/mol^2g)
	Reference 8			Least Squares Fit		
240.019	.0812	- 91.1		.0811	- 91.8	
220.393	.1158	- 123.5		.1160	- 122.3	
207.773	.1508	- 136.5		.1507	- 123.5	
175.082	.3650	- 425.7		.3652	- 325.9	
166.135	.4933	- 442.9	- 1.3	.4927	- 165.9	- 4.7
158.077	.6720	- 248.7	- 11.1	.6724	- 173.4	- 9.20
150.140	.9421	+ 631.9	- 40.8	.9379	864.8	- 35.6
145.114	1.1850	2052.	- 68.3	1.1964	1125.0	- 58.8

Note: $B_{AS} = C_{2S}$

$C_{AAS} = C_{3S}$

$D_{AAAS} = C_{4S}$

Table 6. Polynomial Coefficients for Equations with a Zero Intercept

Order	C_{2S} (cm^3/g)	C_{3S} ($cm^6/mol\text{-}g$)	$C_{4S} \times 10^{-6}$ ($cm^9/mol^2 g$)
	neon T = 273.15		
* 1	.00076		
	krypton T = 273.15		
2	.04846	- 140.7	
* 3	.04962	- 269.3	2.67
	xenon T = 273.15		
2	.2222	- 2,317.	
* 3	.2378	- 5,349.	103.8
	argon T = 273.15		
1	.01497		
* 2	.01534	- 13.77	
	argon T = 248.467		
2	.02246	- 25.20	
* 3	.02253	- 32.27	.14
	argon T = 231.252		
2	.03045	- 52.06	
* 3	.03093	- 102.8	.99
	argon T = 221.651		
2	.03662	- 76.97	
* 3	.03749	- 167.8	1.839
	argon T = 210.172		
2	.04798	- 145.6	
* 3	.04976	- 329.1	3.600
	argon T = 198.396		
2	.06400	- 249.1	
* 3	.06600	- 457.2	4.268
	argon T = 141.345		
2	.41475	- 3,526.	
3	.47001	- 10,044.	165.6
4	.50915	- 17,280.	573.2

* These figures used for calculating virial coefficients as shown in Table 8.

Table 7. Polynomial Coefficients for Equations with a Non-zero Intercept

Order	Intercept (moles) x 10^8	C_{2S} (cm^3/g)	C_{3S} ($cm^6/mol\text{-}g$)	C_{4S} x 10^{-6} (cm^9/mol^2g)
		krypton T = 273.15		
2	1.915	.04592	- 81.5	
3	1.069	.04744	- 154.0	0.987
		xenon T = 273.15		
2	14.30	.18222	- 688.6	
3	9.09	.20097	- 2,190.	32.33
		argon T = 248.467		
1	1.149	.02120		
* 2	0.134	.02229	- 21.60	
		argon T = 231.252		
1	2.266	.02790		
* 2	0.951	.02929	- 27.24	
3	0.125	.03071	- 92.09	.850
		argon T = 221.651		
1	3.250	.03298		
* 2	1.744	.03457	- 32.19	
3	1.921	.03429	- 20.18	- 0.154
		argon T = 210.172		
1	6.337	.04090		
* 2	2.942	.04441	- 68.79	
3	2.494	.04516	- 102.8	.447
		argon T = 198.396		
1	10.899	.05221		
* 2	4.102	.05929	- 145.1	
3	1.533	.06333	- 326.0	2.396
		argon T = 141.344		
1	107.6	.28159		
2	85.66	.30744	- 656.8	
3	74.98	.32720	- 1,769.	19.24
4	65.27	.35046	- 3,725.	88.08

*These figures used for calculating virial coefficients as shown in Table 8.

Table 8. Values of ϵ^*/k and Az_o Determined from Experimental C_{2S}'s

Isotherms Used	ϵ^*/k (°K)	$\overline{Az_o} \times 10^4$ (cm^3)	z_o(est) (A)	A (m^2/g)
C_{2S}'s[a] determined with polynomial that passed through the origin at zero pressure.				
273 to 198	1212	5.27 ± .04	2.77	1.90
C_{2S}'s[b] determined with non-zero intercept at zero pressure.				
273 to 198	1111	7.31 ± .08	2.77	2.64
			BET area	4.98

[a] Table 6, 198-273.15 °K C_{2S}'s marked with an asterisk.

[b] Table 7, 198-273.15 °K C_{2S}'s marked with an asterisk.

A larger discrepancy exists between the values of the BET area and the virial area with zero intercept than was found for the argon-graphite system. This large difference was assumed to have been introduced by the presence of a high energy surface, probably the crystal edges.

Both values for the depth of the Ar-BN potential well calculated here (Table 8) were larger than the 981°K found by Pierotti using a multilayer treatment. These comparisons were taken to show that the use of a virial equation for a single uniform surface was insufficient for this system.

The next attempt to obtain information from the experimental data was to assume that two independent energy surfaces were present and that each could be represented by a virial equation. The total number of moles of gas adsorbed was then a sum of the amounts adsorbed by each surface so that

$$N_a = N_{ab} + N_{ae} \tag{62}$$

where N_{ab} = the number of moles adsorbed by the low energy surface

N_{ae} = the number of moles adsorbed by the high energy surface

b = subscript referring to the low energy surface

e = subscript referring to the high energy surface.

After substituting equation 94 (appropriately subscripted) for N_{ab} and N_{ae} in equation 62 and summing, the experimental virial coefficients from equation 60 are found to be

$$C_{2S} = C_{2Sb} + C_{2Se};\ C_{3S} = C_{3Sb} + C_{3Se};\ \text{etc.}$$

This treatment complicated the problem to the point that other workers' experimental data were used. Pierotti's experimental value of ϵ^*/k for the Ar-BN system was used with Sams'[26] value of z_o (2.77 Å) for the Ar-graphite system and the BET area of the BN to calculate a set of C_{2Sb}'s. The BET area determined here was multiplied by 8.63/12.1, the ratio of the area determined by the virial treatment of Sams to the BET area of graphite at 90°K. Since the percentage of edges was estimated to be five to ten percent, the area was multiplied by .925 to get the area of the low energy surface (assumed basal plane). This gave Az_o for the basal plane to be

$$(Az_o)_b = (.925)(4.98)(8.63/12.1)(2.77)(10^{-4}) \text{ cm}^3 = 9.10 \times 10^{-4} \text{ cm}^3.$$

The C_{2Sb}'s calculated in this manner were subtracted from those C_{2S}'s marked with asterisks in Table 7 to give a set of C_{2Se}'s. (A similar treatment was done using the C_{2S}'s marked with a dagger in Table 7.) The set of C_{2Se}'s calculated in this manner were "fit" using the technique described in Appendix F to determine ϵ^*/k and $(Az_o)_e$ (see Table 9).

This treatment gave ϵ^*/k for the high energy surface-argon system to be 1771°K and $(Az_o)_e$ to be 0.16×10^{-4} cm^3. The Az_o for each surface-gas system was then estimated by multiplying the Ar-BN Az_o's by the ratio of Sams' gas-graphite Az_o/Ar-graphite Az_o (Table 23). Levy's[57] experimental ϵ^*/k for the Kr-BN system (basal plane) was used with the Az_o's for the two surfaces to calculate ϵ^*/k for the high energy surface. The ratio of the ϵ^*/k's for the b and e surfaces, R, for the Ar-BN and Kr-BN system was averaged to give the ratio (R) used in Table 9 with the

Table 9. Values of ε^*/k and Az_o Calculated for Different Values of A Using Two Surface Treatment for the Inert Gas-BN Systems

Gas	ε^*/k (°K)	$Az_o \times 10^4$ (cm^3/g)	% surface assumed low energy[d]	ε^*/k (°K)	$Az_o \times 10^4$ (cm^3/g)	R[c]
	Low Energy Surface			High Energy Surface		
Ne	344	8.36	92.5	595	.15	1.73
Ar	981[a]	9.10	92.5	1771	.16	1.80
Kr	1321[b]	9.15	92.5	2197	.16	1.66
Xe	1647	9.98	92.5	2849	.18	1.73
Ar	981	9.35	95	1834	.12	1.87
Ar	981	8.85	90	1717	.22	1.75
Ar	981	8.60	87.5	1671	.28	1.70
Ar	981	8.35	85	1630	.35	1.66
Ar	981	8.10	82.5	1595	.42	1.63
Ne	348	7.21	80	536	.47	1.54
Ar	981	7.85	80	1563	.51	1.59
Kr	1321	7.89	80	1969	.51	1.49
Xe	1656	8.60	80	2550	.56	1.54

[a]Taken from reference 58.

[b]Taken from reference 57.

[c]Ratio of high energy surface energy to low energy surface energy.

[d]Used to estimate Az_o for the low energy surface.

[e]Calculations made using C_{2S}'s marked with an asterisk in Table 6.

neon and xenon systems. This ratio with the Az_o values estimated (as described above) was then used to determine the Xe-BN and Ne-BN energies shown in Table 9.

Since $(Az_o)_b = 9.10 \times 10^{-4}$ cm^3/g was only an estimation, calculations were made at different $(Az_o)_b$ values for the Ar-BN system as shown in Table 9. At the lower limit chosen for $(Az_o)_b$ ($(Az_o)_b = 7.85 \times 10^{-4}$ cm^3), the other inert gas data were recalculated from the Ar-BN Az_o's and R. As $(Az_o)_b$ was decreased, R decreased and within the limits chosen R could be assigned a value of 1.5-1.8.

Over the range of $(Az_o)_b$ that was assumed reasonable, the $(\epsilon^*/k)_b$'s for the Ne-BN and Xe-BN low energy surface only changed about one percent. However the $(\epsilon^*/k)_e$'s calculated over this range changed about 10-12 percent and since there was no reason for taking any individual answer, an average of the (ϵ^*/k)'s is given in Table 10. (The $(\epsilon^*/k)_e$ values have been rounded to the nearest 10°.)

Table 10. Approximated ϵ^*/k's Using Two Surfaces

Gas	$(\epsilon^*/k)_b$	$(\epsilon^*/k)_e$
Ne	346	570
Ar	981[a]	1680
Kr	1321[b]	2080
Xe	1651	2700

[a] Reference 58

[b] Reference 57

The $(\epsilon^*/k)_b$'s in Table 10 were compared with the theoretically calculated energies in Table 24 and found to be in poor agreement. This result of comparison was not surprising since experimental energies for the much better characterized and more homogeneous graphitized black (P33(2700)) with inert gases do not agree with theoretical energies (Table 23).

The energies in Table 10 were determined by assuming that:

1. Only two different types of energy surface contributed significantly to the isotherm data

2. Each of these energy surfaces could be assumed uniform

3. The BET area could be adjusted to give an area that could be used in the virial treatment

4. The argon-graphite z_o was approximately equal to z_o for the argon-BN system and the ratio Az_o(argon)/Az_o(inert gas) is the same for the graphite and BN adsorbents

5. The ratio of the interaction energies on the two surfaces depends only on the adsorbent

6. The one gas molecule-solid interaction energy can be represented by an L-J (3-9) potential.

Since the multisurface problem was encountered and was only qualitatively resolved, further treatment of the data to consider the interaction between two admolecules was abandoned.

CHAPTER VI

CONCLUSIONS AND RECOMMENDATIONS

Conclusions

The apparatus described here and used for this work was sufficiently sensitive for Henry's law adsorption studies in the pressure range from 10 torr to about 800 torr and over the temperature range 77-298°K. The sensitivity of the apparatus was demonstrated by measuring an adsorption isotherm for the neon-boron nitride system at 273.15°K.

The hexagonal modification of boron nitride presents at least two different energy surfaces for adsorption. (These energy surfaces were assumed to be the basal plane and crystal edges.) The two surface effect complicated a virial treatment and made necessary lower pressure points and isotherms measured over larger ranges of ϵ^*/kT than are presented here. The high energy surface present had an inert gas-BN potential well about 1.5-1.8 times as deep as the low energy surface-inert gas potential well. It is concluded that the values for ϵ^*/k determined here should prove valuable until further experimental data are made available.

Recommendations

Apparatus

The apparatus should be altered to reduce the system's internal volume between the pipets and sample cell. Cryostat modifications should be made so that sample temperatures to about 400°K can be attained.

Experimental

The systems studied here should be investigated in greater detail with particular effort directed toward the Ne-BN system. Isotherms should be measured over as wide a range of ϵ^*/kT as possible for each system. Care should be taken to make measurements for each isotherm in the Henry's law region. The treatment should be extended to consider the pair interactions of admolecules.

APPENDICES

APPENDIX A

VIRIAL TREATMENT OF IMPERFECT GAS

Consider an ensemble of systems, each of which is representative of a typical imperfect gas system. Each system contains an unspecified number of moles of gas in volume V at temperature T. The walls of the systems are permeable to the gas so that the chemical potential is uniform throughout the ensemble at equilibrium. The partition function for the ensemble is[51]

$$\Xi(\mu,V,T) = \sum_{N\geq 0} Q(N,V,T)\ \lambda^N \tag{63}$$

where $\Xi(\mu,V,T)$ = the grand partition function

μ = chemical potential of the gas

V = volume of a system

T = temperature of the ensemble

$Q_N = Q(N,V,T)$ = canonical partition function for N molecules in volume V at temperature T

λ = absolute activity = $e^{\mu/kT}$

The notation can be simplified by defining two new variables, Z_N and z. z is the activity,

$$z = Q_1 \lambda/V \tag{64}$$
$$= f/kT$$

f = fugacity of the gas

and

$$Z_N/N! = Q_N V^N/Q_1^N$$

where Z_N = the configuration integral from classical statistical mechanics

$$Z_N = \int\int_{\text{volume}} e^{-E/kT}\, dq_1 \ldots\ldots\ldots dq_{3N} \tag{65}$$

E = sum of the pair wise interaction energies for N molecules

$$E = \sum_{1\leq i<j\leq N} \epsilon_{ij}\,(q_{ij}) \tag{66}$$

ϵ_{ij} = interaction energy between molecules i and j with position coordinates q_{ij}.

Substituting Z_N and z into equation 63 gives

$$\Xi = (\mu,V,T) = 1 + \sum_{N\geq 1} \frac{Z_N(V,T)z^N}{N!} \tag{67}$$

Taking the logarithm of both sides of equation 67 and expanding the right side gives

$$\ln \Xi\,(\mu,V,T) = V \sum_{j\geq 1} b_j Z^j \tag{68}$$

where $Vb_1 = Z_1 = V$

$Vb_2 = (Z_2 - Z_1^2)/2!$

$Vb_3 = (Z_3 - 3Z_1Z_2 + Z_1^3)/3!$

Vb_j = (see page 135, reference 19).

The thermodynamic characteristic function for $\ln\Xi(\mu,V,T)$ is PV/kT so that[59]

$$P/kT = \sum_{j\geq 1} b_j z^j \tag{69}$$

and

$$\bar{N}/V = \frac{z}{V}\left(\frac{\partial \ln\Xi}{\partial z}\right)_{V,T} = \sum_{j\geq 1} j\, b_j z^j. \tag{70}$$

Taking the reciprocal of both sides of equation 70 gives

$$V/\bar{N} = 1/z - C_1 + C_2 z^1 - C_3 z^2 + C_4 z^3 - \cdots + C_j z^j \tag{71}$$

where

$$C_j = \sum_{i=1}^{j-1} (i+1) C_{j-i}\, b_{i+1}\, (-1)^{i+1} \tag{72}$$

$C_1 = 2b_2$

$C_2 = (2b_2)^2 - 3b_3$

$C_3 = (2b_2)^3 - 12b_3 b_2 + 4b_4$.

Equation 69 can be inverted to give z as a series in P/kT by substituting

$$z = a_1(P/kT) + a_2(P/kT)^2 + a_3(P/kT)^3 + \cdots\cdots\cdots \tag{73}$$

and equating like powers of P/kT gives a's in terms of b's as follows

$a_1 = b_1 = 1$

$$a_2 = - b_2$$

$$a_3 = 2b_2^2 - b_3$$

$$a_4 = - 5b_2^3 + 5b_3 b_2 - b_4 .$$

After substituting equation 73 into equation 71, multiplying both sides by P/kT, dividing the polynomial in the first term on the right side into one and collecting like terms of P/kT yields

$$PV/\bar{N}kT = 1 + B_2(P/kT) + B_3(P/kT)^2 + B_4(P/kT)^3 + \cdots\cdots \qquad (74)$$

where $B_2 = - b_2$

$$B_3 = 3b_2^2 - 2b_3$$

$$B_4 = 2b_2^3 - 3b_2 b_3 - 3b_4 .$$

(B's are the virial coefficients for expansion in P/kT and are related to the more commonly used coefficients for the density expansion.)

(Substitution of B's into equation 73 yields

$$z = P/kT + B_2(P/kT)^2 + \tfrac{1}{2}(B_3 - B_2^2)(P/kT)^3 + \cdots \qquad (75)$$

The virial coefficients are related to configuration integrals, and to calculate B_2

$$B_2 = - b_2 = (1/2V)(Z_2 - Z_1^2)$$

$$= (- 1/2V)\left(\iint_{VV} e^{-\epsilon_{12}/kT}\, dq_1\, dq_2 - \int_V dq_1 \int_V dq_2\right)$$

Since ϵ_{12} is a function of the distance between molecule one and molecule two, a change of variables from q_1 and q_2 to q_1 and q_{12}

($q_{12} = q_2 - q_1$ = the position of molecule two relative to molecule one) leads to two independent integrations

$$B_2 = (-1/2V) \int_V dq_1 \int_V (\exp(-\epsilon_{12}/kT) - 1)\, dq_{12} . \qquad (76)$$

Integrating over q_1 yields

$$B_2 = -\tfrac{1}{2} \int (\exp(-\epsilon_{12}/kT) - 1)\, dq_{12} . \qquad (77)$$

If molecular interaction is assumed to obey a Lennard-Jones (6-12) model, equation 77 can be solved analytically to give[60]

$$B_2 = b_o \sum_{j=o}^{\infty} \frac{(-2^{j+\frac{1}{2}})}{4(j!)} \left[\frac{kT}{\epsilon_{3D}}\right]^{((-2j+1)/4)} \Gamma\left(\frac{2j-1}{4}\right). \qquad (78)$$

where B_2 = the second gas virial coefficient at temperature T

ϵ_{3D} = the depth of the potential well for two interacting gas molecules

T = the absolute temperature

k = Boltzmann's constant

j = an integer

$b_o = \frac{2\pi\tilde{N}\sigma^3}{3}$

σ = the collision diameter

$\tilde{N}$ = Avogadro's number

$\Gamma[\,]$ = the gamma function.

The second virial coefficients for all inert gases used were cal-

culated on a Burroughs B-5500 computer using equation 78. Summation was terminated when the absolute value of the j^{th} term of the series divided by the absolute value of the sum of the terms through the j^{th} was less than 0.001.

Values for σ, ϵ_{3D}/k, and $\tilde{N}$ used were:

	$\epsilon_{3D}/k(^\circ K)$	$\sigma(Å)$
He	6.03	2.63
Ne	35.6	2.749
Ar	119.8	3.405
Kr	171.0	3.600
Xe	221.0	4.100

$\tilde{N} = 6.023 \times 10^{23}$

APPENDIX B

DERIVATION OF THE GAS-SOLID VIRIAL EQUATION

The preceding virial treatment (Appendix A) can be extended to the problem of an imperfect gas interacting with a surface. First consider the ensemble from Appendix A where

$$\Xi(\mu,V,T) = \sum_{N\geq 0} \frac{Z_N z^N}{N!} \tag{79}$$

$$Z_N = (V/Q_1)^N \, N! \, Q_N \tag{80}$$

$$z = (Q_1/V) \, e^{\mu/kT}. \tag{81}$$

If the same imperfect gas is allowed to interact with one wall of the container (adsorbent) without changing the chemical potential of the adsorbent, then the grand partition function and configuration integrals can be written

$$a\Xi(\mu,V,T) = \sum_{N\geq 0} \frac{aZ_N z^N}{N!} \tag{82}$$

$$aZ_N = (V/Q_1)^N \, N! \, aQ_N \tag{83}$$

---

*See T. L. Hill, "Statistical Mechanics," page 425 for derivation and other references.

$$ {}_aZ_N = \int_{\text{volume}} \cdots \int \left[\exp\left(- {}_aE_N / kT \right) \right] dq_1 \cdots\cdots dq_N \tag{84} $$

$$ {}_aE_N = E_N + \sum_{i=1}^{N} \epsilon(q_i) \tag{85} $$

where

E_N = total intermolecular energy for N gas molecules (equation 66)

$\epsilon(q_i)$ = potential energy of interaction of molecule i at q_i

${}_aE_N$ = total potential energy of interaction for the adsorbate-adsorbent system. (The presubscript a will be used to indicate that the gas system interacts with the adsorbent.)

Following the procedures from Appendix A:

$$ \ln \Xi = \sum_{j \geq 1} V b_j z^j \tag{86} $$

$$ \ln ({}_a\Xi) = \sum_{j \geq 1} V {}_a b_j z^j \tag{87} $$

$$ 1! V({}_a b_1) = {}_aZ_1 $$

$$ 2! V({}_a b_2) = {}_aZ_2 - {}_aZ_1^2 $$

and

$$ {}_a\bar{N} = z \left(\frac{\partial \ln({}_a\Xi)}{\partial z} \right) \tag{88} $$

$$ \bar{N} = z \left(\frac{\partial \ln \Xi}{\partial z} \right) \tag{89} $$

where

$_a\bar{N}$ = the average number of molecules of an imperfect gas in volume V, at temperature T, and at chemical potential μ, if the molecules can interact with one wall of the container

$\bar{N}$ = the average number of molecules of an imperfect gas in a system with a volume V, temperature T, and chemical potential μ.

The excess number of molecules in the system (number of molecules adsorbed) due to interaction with the wall is

$$\bar{N}_a = {}_a\bar{N} - \bar{N}.$$

When equations 88 and 89 are substituted for $_a\bar{N}$ and $\bar{N}$ and equations 86 and 87 for ln Ξ and ln ($_a\Xi$), the average number of molecules is

$$N_a = \sum_{j\geq 1} V\,({}_ab_j - b_j)\,z^j = \sum_{j\geq 1} B_{j+1,S}(f/kT)^j \qquad (90)$$

where

$$B_{2S} = V({}_ab_1 - b_1) = {}_aZ_1 - Z_1$$

$$B_{3S} = V({}_ab_2 - b_2) = \tfrac{1}{2}({}_aZ_2 - {}_aZ_1^2 - Z_2 + Z_1^2)$$

$$B_{2S} = \int_V [\exp -(\epsilon_1/kT) - 1]\, dq_1 \qquad (91)$$

$$B_{3S} = \int_{\text{volume}} \int [\exp -(\epsilon_{12} + \epsilon_1 + \epsilon_2)/kT]\, dq_1\, dq_2 \qquad (92)$$

$$- \int_{\text{volume}} \int \exp -(\epsilon_{12}/kT)\, dq_1\, dq_2 - \int_{\text{volume}} \int dq_1\, dq_2$$

$$- \int_{\text{volume}} \int \exp -(\epsilon_1 + \epsilon_2)/kT)\, dq_1\, dq_2 .$$

Substituting equation 75 into equation 90 and simplifying yields:

$$N_a = B_{2S}(P/kT) + (B_{3S} + B_{2S}B_2)(P/kT)^2 + (B_{4S} + 2B_{3S}B_2 + \tfrac{1}{2}B_{2S}(B_3 + B_2^2))(P/kT)^3 + \cdots\cdots \quad (93)$$

$$N_a = \sum_{i\geq 1}^{\infty} C_{i+1,s}(P/kT)^i \quad (94)$$

where

$C_{i+1,s}$ = $i+1^{th}$ gas-solid virial coefficient for an expansion in pressure

$$C_{2S} = B_{2S} \quad (95)$$

$$C_{3S} = B_{3S} + B_{2S}B_2 \quad (96)$$

$$C_{4S} = B_{4S} + 2B_{3S}B_2 + \tfrac{1}{2}B_{2S}(B_3 + B_2^2). \quad (97)$$

APPENDIX C

ANALYTIC SOLUTION FOR THE SECOND GAS-SOLID VIRIAL COEFFICIENT USING A LENNARD-JONES (3-9) POTENTIAL FUNCTION

Equation 91 can be solved analytically in terms of the parameters ϵ^* and z_o (Figure 2) if Lennard-Jones (m-n) potential functions of the form

$$\epsilon = K\epsilon^* [(z_o/z)^m - (z_o/z)^n] \qquad m > n \tag{98}$$

where

$K\epsilon^* (z_o/z)^n$ = the attractive term

$K\epsilon^* (z_o/z)^m$ = the repulsive term

ϵ = energy of interaction between an adsorbate molecule at z and the adsorbent

ϵ^* = depth of the potential well

$K = \left(\frac{n}{n-m}\right)\left(\frac{n}{m}\right)^{\frac{m}{n-m}}$

z_o = vertical distance of an adsorbate molecule from the adsorbent surface when the interaction energy is zero

z = vertical distance of an adsorbate molecule from the adsorbent surface

are assumed for the energy of interaction between an adsorbate molecule and the surface. (The notation will be simplified by substituting $K\epsilon^*/kT = E$.) When equation 98 is substituted into equation 91

$$B_{2S} = \int_V (\exp \{- E((r_o/r)^m - (r_o/r)^n)\} - 1)\, dxdydz. \tag{99}$$

The surface will be considered to be defined by a plane (x,y,0) passing through the centers of the surface atoms. Further, it will be assumed that the potential energy of interaction is independent of the x,y position of an adsorbate molecule, i.e. the potential energy is only a function of the vertical distances from the surface. Since adsorptive forces are short range, the integration over V/A can be replaced by integration from zero to infinity and integration can be carried out over x and y to yield

$$B_{2S} = A \int_0^\infty (\exp \{- E((z_o/z)^m - (z_o/z)^n)\} - 1)\, dz. \qquad (100)$$

The above equation can be integrated by parts to give

$$B_{2S}/A = [(\exp \{- E((z_o/z)^m - (z_o/z)^n)\} - 1)z]_o^\infty - \int_o^\infty z \exp \qquad (101)$$

$$[- E((z_o/z)^m - (z_o/z)^n)]\, d\, \frac{-E((z_o/z)^m - (z_o/z)^n)}{dz}\, dz$$

The first term on the right side of equation 101 can be evaluated by l'hospitals' rule to give zero and the second term can be rewritten

$$B_{2S}/Az_o = \int_o^\infty [(n/m)(z_o/z)^{n-m-1} - (z_o/z)^{-1}] \exp \{- E((z_o/z)^m \qquad (102)$$

$$- (z_o/z)^n)\}\, dE\, (z_o/z)^m$$

and after expanding $\exp (E(z_o/z)^n)$ in powers of $E(z_o/z)^n$ and rearranging, equation 102 yields

$$B_{2S}/Az_o = \sum_{i=o}^{\infty} (1/i!) \left[\left(- E^i/E^{\frac{ni-1}{m}} \right) \int_o^{\infty} \exp\ (- E(z_o/z)^m) \right.$$

$$\left(E(z_o/z)^m \right)^{\frac{ni-1}{m}} dE(z_o/z)^m + \left(nE^i/mE^{\frac{ni+n-m-1}{m}} \right)$$

$$\left. \int_o^{\infty} \exp \left(- E(z_o/z)^m \right) \left(E(z_o/z)^m \right)^{\frac{ni+n-m-1}{m}} dE(z_o/z)^m \right].$$

This equation has two terms that are of the form of the gamma function

$$\Gamma(s) = \int_o^{\infty} e^{-t}\ t^{s-1}\ dt$$

which can be substituted to yield

$$B_{2S}/Az_o = \sum_{i \geq 0}^{\infty} (1/i!) \left[(n/m) E^{\frac{(m-n)(i+1)+1}{m}} \Gamma\ ((n(i+1) - 1)/m) \right. \quad (103)$$

$$\left. - E^{\frac{(m-n)i+1}{m}} \Gamma\ ((ni-1)/m + 1) \right].$$

Since $\Gamma(s+1) = s\Gamma(s)$, the last gamma term can be replaced by $((ni-1)/m)\ \Gamma\ ((ni-1)/m)$ and if $i+1$ in the first term on the right side of equation 103 is replaced by j and the numerator and denominator are multiplied by j, then equation 103 yields

$$B_{2S}/Az_o = \sum_{j \geq 1}^{\infty} (j/j!) \left[(n/m) E^{\frac{(m-n)j+1}{m}} \Gamma\ ((nj-1)/m) \right] \quad (104)$$

$$+ \sum_{i \geq 0}^{\infty} (1/i!)((1-ni)/m) E^{\frac{(m-n)i+1}{m}} \Gamma\ ((ni-1)/m)$$

The first term on the right side of equation 104 has j in the numerator so that summation can be changed from $j \geq 1$ to $j \geq 0$, then after replacing j by i and simplifying, equation 103 yields the desired result

$$B_{2S}/Az_o = \sum_{i \geq 0}^{\infty} (1/i!)(1/m)E^{\frac{(m-n)i+1}{m}} \Gamma((ni-1)/m) = I \qquad (105)$$

where

$$E = K\epsilon^*/kT$$

$$m > n.$$

Table 11 gives B_{2S}/Az_o for a Lennard-Jones (3-9) function ($m = 9$, $n = 3$). This table was calculated from equation 105 using a Burroughs B-5500 computer. The series summation was terminated when the absolute value of the i^{th} term divided by the absolute value of the sum of terms through the i^{th} term was less than 0.0001. Figure 32 shows a plot of $\ln (B_{2S}/Az_o)$ as a function of ϵ^*/kT.

Table 11. Calculated B_{2S}/Az_o from Selected Values of ϵ^*/kT for Lennard-Jones (3-9) Functions

ϵ^*/kT	B_{2S}/Az_o	ln (B_{2S}/Az_o)	ϵ^*/kT	B_{2S}/Az_o	ln (B_{2S}/Az_o)
1.0	.35623	- 1.03	5.6	80.438	4.39
1.2	.72667	- .32	5.8	95.941	4.56
1.4	1.1517	.14	6.0	114.51	4.74
1.6	1.6403	.50	6.2	136.75	4.92
1.8	2.2036	.79	6.4	163.44	5.10
2.0	2.8549	1.05	6.6	195.45	5.28
2.2	3.6104	1.28	6.8	233.89	5.45
2.4	4.4889	1.50	7.0	280.07	5.64
2.6	5.5133	1.70	7.2	335.58	5.82
2.8	6.7111	1.90	7.4	402.33	6.00
3.0	8.1147	2.09	7.6	482.65	6.18
3.2	9.7639	2.28	7.8	579.32	6.36
3.4	11.705	2.46	8.0	695.76	6.55
3.6	13.995	2.64	8.2	836.00	6.73
3.8	16.701	2.82	8.4	1005.0	6.91
4.0	19.904	2.99	8.6	1208.8	7.10
4.2	23.702	3.17	8.8	1454.5	7.28
4.4	28.210	3.34	9.0	1751.0	7.47
4.6	33.572	3.51	9.2	2108.7	7.65
4.8	39.954	3.69	9.4	2540.7	7.84
5.0	47.561	3.86	9.6	3062.0	8.03
5.2	56.636	4.04	9.8	3691.8	8.21
5.4	67.478	4.21	10.0	4452.5	8.40

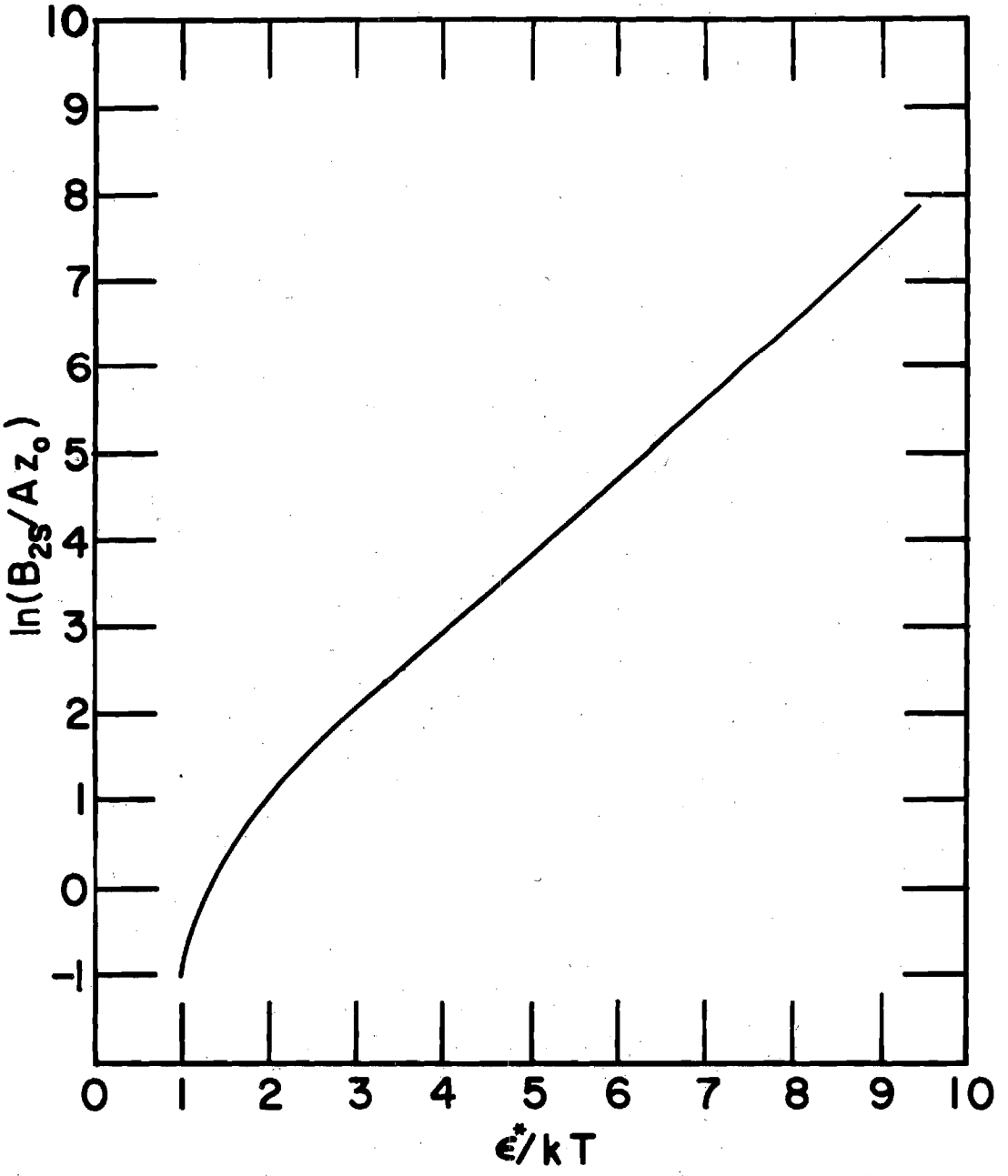

Figure 32. $\ln (B_{2S}/Az_o)$ as a Function of ϵ^*/k for a L-J (3-9) Potential

APPENDIX D

ISOTHERM DATA AND FIGURES

All pressures are reported in standard centimeters of mercury and temperatures have been corrected to the thermodynamic temperature scale as described earlier.

Table 12. Ne-BN Isotherm at 273.15°K

P (cm Hg)	T (°K)	$N_a \times 10^8$ (mol/g)
26.7784	273.150	1.19
29.5353	273.150	1.26
32.6475	273.150	1.30
36.8345	273.150	1.71
40.6380	273.150	1.70
47.3381	273.150	2.20
55.8725	273.150	2.53
69.3687	273.150	3.53

Table 13. Kr-BN Isotherm at 273.15°K

P (cm Hg)	T (°K)	$N_a \times 10^7$ (mol/g)
10.8345	273.150	3.051
13.3602	273.150	3.781
19.5898	273.150	5.328
23.7152	273.150	6.435
29.7814	273.150	7.992
36.0708	273.150	9.567
40.5203	273.150	10.669
51.4977	273.150	13.320
60.2596	273.150	15.389
73.8178	273.150	18.582

Table 14. Xe-BN Isotherm at 273.15°K

P (cm Hg)	T (°K)	$N_a \times 10^7$ (mol/g)
4.2956†	273.150	5.760
5.2533†	273.150	6.879
6.1184†	273.150	7.921
7.5501†	273.150	9.450
15.2462*	273.150	17.473
18.2413*	273.150	20.402
22.5365*	273.150	24.419
24.2235*	273.150	25.826
24.5837*	273.150	26.323
24.7872†	273.150	26.446
26.8459*	273.150	28.409
32.4267*	273.150	33.469
36.8585*	273.150	37.482
42.2191*	273.150	42.264
50.0959*	273.150	49.250

†Series 1
*Series 2

Table 15. Ar-BN Isotherm at 273.15°K

P (cm Hg)	T (°K)	$N_a \times 10^7$ (mol/g)
29.3239*	273.150	2.569
36.3953*	273.150	3.214
46.4687*	273.150	4.067
67.1690*	273.150	5.842
22.2852†	273.150	2.010
38.3569†	273.150	3.388
48.9704†	273.150	4.294
57.4902†	273.150	5.009
70.7890†	273.150	6.170
	Check Points	
10.5948	273.150	0.919
20.4996	273.150	1.894

*Series 1
†Series 2

Table 16. Ar-BN Isotherm at 248°K

P (cm Hg)	T (°K)	$N_a \times 10^7$ (mol/g)
10.4439	248.467	1.506
18.7803	248.467	2.677
28.3700	248.468	4.038
42.0040	248.467	5.890
56.2469	248.469	7.819
68.2778	248.468	9.420

Table 17. Ar-BN Isotherm at 231°K

P (cm Hg)	T (°K)	$N_a \times 10^8$ (mol/g)
10.3149	231.252	2.164
18.3696	231.251	3.792
27.4506	231.252	5.587
40.0283	231.254	7.998
52.7746	231.252	10.440
63.2209	231.252	12.427

Table 18. Ar-BN Isotherm at 221°K

P (cm Hg)	T (°K)	$N_a \times 10^7$ (mol/g)
11.5250	221.651	3.033
13.4914	221.650	3.522
15.9736	221.652	4.149
18.0164	221.648	4.581
22.7194	221.650	5.796
31.9102	221.649	7.973
38.6173	221.653	9.583
43.9653	221.649	10.838
50.4299	221.652	12.372
59.9657	221.651	14.561

Table 19. Ar-BN Isotherm at 210°K

P (cm Hg)	T (°K)	$N_a \times 10^7$ (mol/g)
10.1098	210.172	3.676
17.7441	210.171	6.176
26.0887	210.167	8.878
37.2227	210.172	12.340
48.0318	210.173	15.640
56.5713	210.170	18.185

Table 20. Ar-BN Isotherm at 198°K

P (cm Hg)	T (°K)	$N_a \times 10^7$ (mol/g)
9.9628	198.396	5.079
12.1463	198.398	6.056
14.1077	198.395	6.979
16.2025	198.395	7.969
17.3082	198.396	8.376
20.5685	198.396	9.929
25.1669	198.396	11.898
29.6898	198.396	13.814
35.4128	198.396	16.146
39.8527	198.396	17.979
45.1002	198.397	20.066
52.5769	198.396	23.019

Table 21. Ar-BN Isotherm at 141°K

P (cm Hg)	T (°K)	$N_a \times 10^6$ (mol/g)
8.2386	141.345	3.6667
9.3918	141.345	4.0618
12.8683	141.344	5.2080
13.9892	141.344	5.5734
16.7624	141.344	6.4642
22.7444	141.343	8.3453
26.5411	141.343	9.5224

Table 22. Ar-BN Isotherm at 90°K

P (cm Hg)	T (°K)	$N_a \times 10^5$ (mol/g)	$\frac{P}{RN_a(P_o-P)}$
0.6140*	90.003	2.0948	---
0.8789*	90.004	3.0545	---
1.4654	90.003	4.0580	4.076
2.3769	90.007	4.6927	5.767
3.4354	90.000	5.0777	7.779
6.1342	89.999	5.5894	12.959
8.2196	89.999	5.8498	16.920
12.4352	89.999	6.2575	24.971
16.1861	89.995	6.5852	32.128
22.4176	89.997	7.1313	44.033
33.0025	89.995	8.3154	63.293

Note: P_o = 1094.2 torr

*Not used in BET fit.

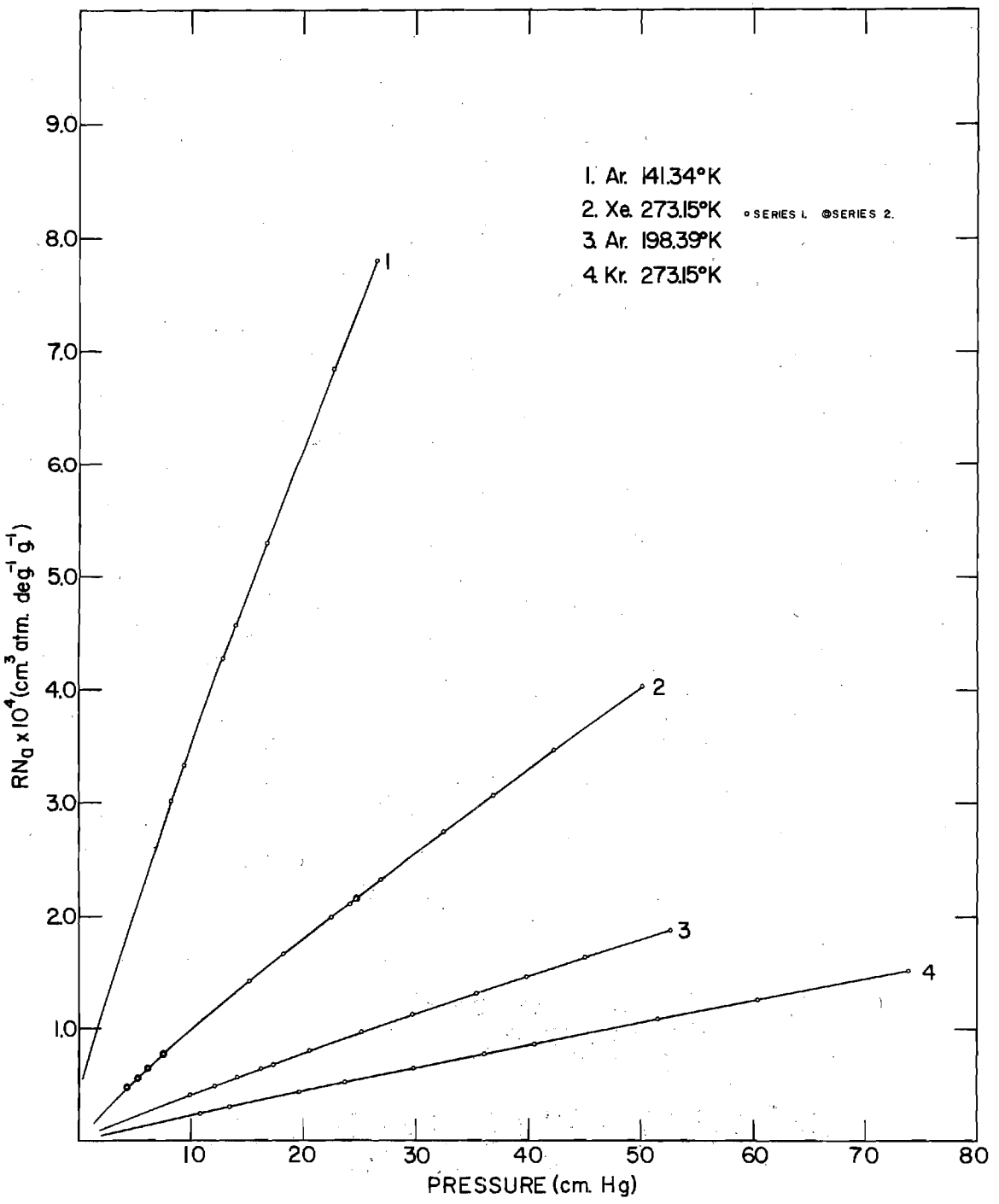

Figure 33. Isotherms

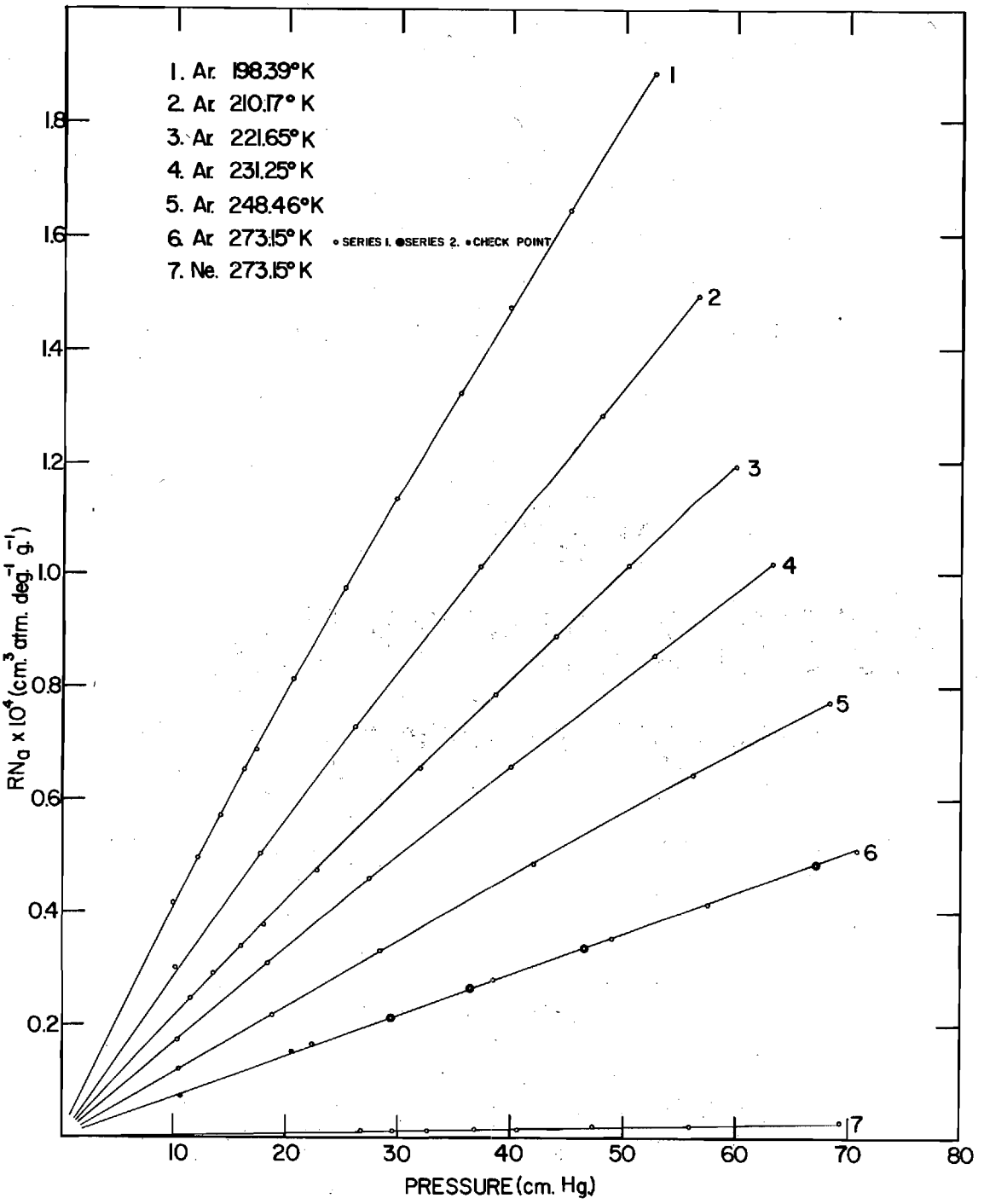

Figure 34. Isotherms

APPENDIX E

MISCELLANEOUS

Table 23. Inert Gas-Graphite Data

	Ne	Ar	Kr	Xe	Ref.
ϵ^*/k(expt'l)°K	382	1107	1460	1919	26
Az_o(expt'l)$cm^3 \times 10^3$	2.199	2.393	2.406	2.625	26
ϵ^*/k(calc)°K	486	1130	1355	1790	53
ϵ^*/k(calc)°K	375	906	1369	1696	54
ϵ^*/k(calc)°K	474	1123	1370	1797	55
ϵ^*/k(calc)°K	369	1067	1432	1890	56
ϵ^*/k(calc)°K edges	493	1535	2068	2742	56

Table 24. Some Inert Gas-BN Data

	Ne	Ar	Kr	Xe	Ref.
ϵ^*/k(expt'l)°K		981			58
ϵ^*/k(expt'l)°K			1321		57
ϵ^*/k(calc)°K	387	986			34
ϵ^*/k(calc)°K	433	1047	1409	1855	35
ϵ^*/k(calc)°K	509	1123	1312	1783	52

Table 25. Approximate Difference Between the Thermodynamic Temperature Scale and the International Practical Temperature Scale of 1948

T	$T - T_{NBS}$	T	$T - T_{NBS}$
90	0.002	190	0.035
100	- 0.008	200	0.036
110	- 0.018	210	0.034
120	- 0.023	220	0.027
130	- 0.021	230	0.020
140	- 0.012	240	0.015
150	- 0.002	250	0.010
160	0.010	260	0.006
170	0.019	270	0.001
180	0.029		

Note: This table was estimated from Figure 2, reference 48.

The following formula was used to convert the NBS temperatures to thermodynamic temperatures.

$$T = T_{NBS} + (T - T_{NBS})$$

where T_{NBS} was taken from the calibrated resistance thermometer interpolation tables and $(T - T_{NBS})$ was estimated from the above table.

APPENDIX F

DETERMINATION OF Az_o AND ϵ^*/k

A preliminary estimate of ϵ^*/k was made from a graph of Az_o versus ϵ^*/k. Using the equation

$$Az_o = B_{2S}/I \tag{106}$$

where B_{2S} = experimental B_{2S} at temperature T

T = isotherm temperature

Az_o = the surface area times z_o

I = function in equation 105

a value of Az_o was calculated for each ϵ^*/k from a trial set. (This set of trial ϵ^*/k values was started at 900°K and ran to 1200°K at 50 degree intervals for the argon data.) The points (Az_o, ϵ^*/k) were plotted on one graph and those calculated from a given experimental B_{2S} were connected by a smooth curve. The intersection of the lines gave an estimate of the "best fit" values of Az_o and ϵ^*/k. (Figure 35 demonstrates the type plot that was used.) Since experimental data were used to determine the points, all of the lines do not intersect at one point. A starting point was then chosen 25° below the graphically estimated value of ϵ^*/k to determine the "best fit" Az_o and ϵ^*/k using a Burroughs B-5500 computer. Values of Az_o were calculated for each isotherm temperature for the trial ϵ^*/k from equation 106. The calculated Az_o's were averaged to give $\overline{Az_o}$ and the standard deviation of $((Az_o/\overline{Az_o}) - 1)$ was

calculated for each trial ϵ^*/k. The value of ϵ^*/k which gave the smallest standard deviation of $((Az_o/\overline{Az_o}) - 1)$ was chosen to be ϵ^*/k and the corresponding $\overline{Az_o}$ was accepted as the best value of Az_o.

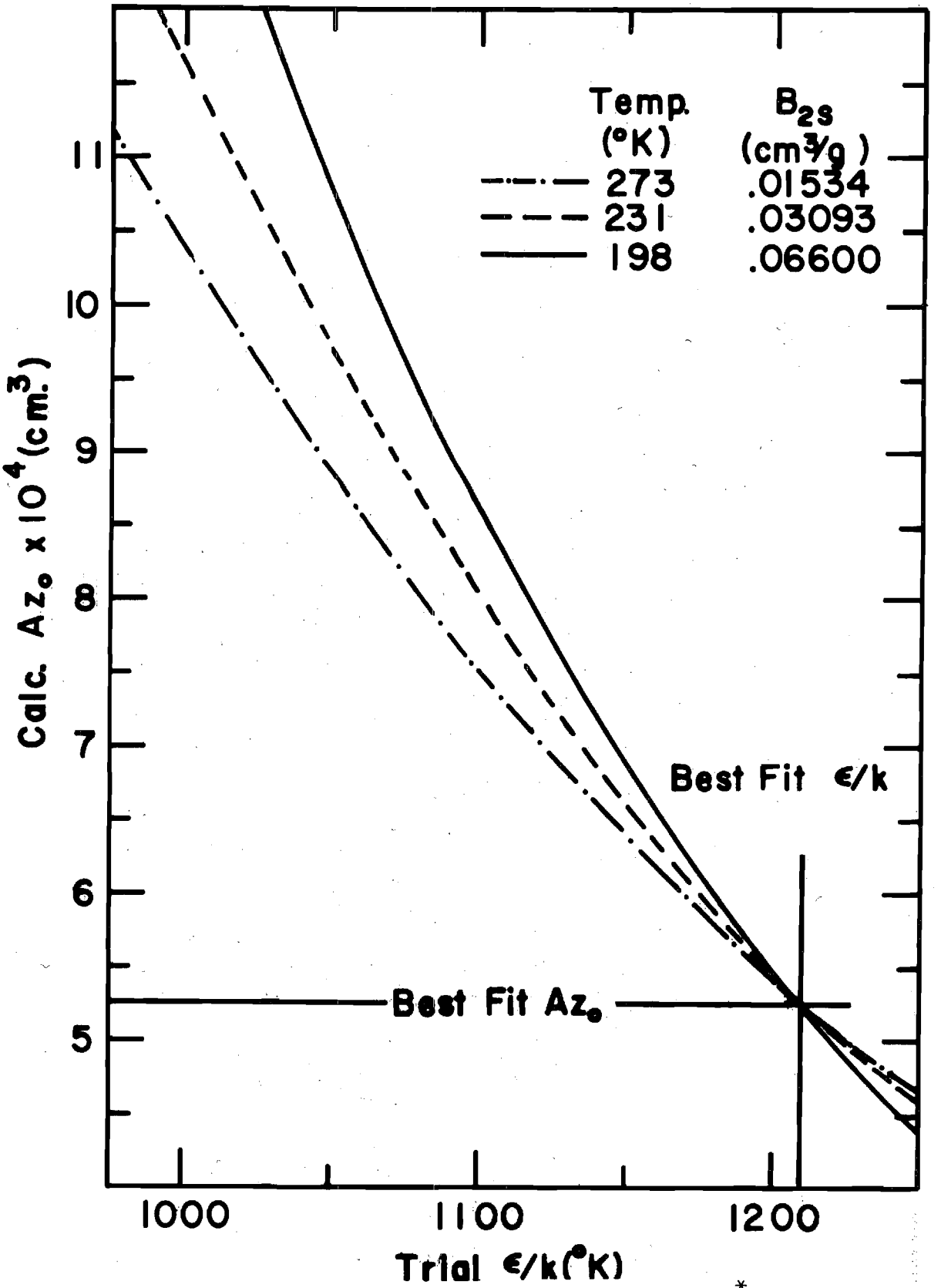

Figure 35. Determination of "Best Fit" Az_o and ϵ^*/k Graphically

BIBLIOGRAPHY

1. Leo A. Aroian, et al., eds., "Van Nostrand's Scientific Encyclopedia," 3rd ed., D. Van Nostrand Company, Inc., Princeton, New Jersey, 1958, p. 607.

2. R. H. Fowler and E. A. Guggenheim, "Statistical Thermodynamics," Cambridge University Press, Cambridge, 1965, p. 274.

3. Fowler and Guggenheim, p. 275.

4. J. A. Beattie and O. C. Bridgeman, Journal of the American Chemical Society, 49, 1665 (1927).

5. H. Kamerlingh Onnes, Communications from the Physical Laboratory at the University of Leiden, 71, 5 (1901).

6. W. A. Steele, Advances in Colloid and Interface Science, 2, 385 (1968).

7. R. H. Fowler, Proceedings of the Cambridge Philosophical Society, 31, 260 (1935).

8. A. L. McClellan and H. F. Harnsberger, Journal of Colloid and Interface Science, 23, 577 (1967).

9. D. M. Young and A. D. Crowell, "Physical Adsorption of Gases," Butterworths, London, 1962, pp. 226-230.

10. T. L. Hill, Journal of Chemical Physics, 14, 263 (1946).

11. A. B. D. Cassie, Transactions of the Faraday Society, 41, 450 (1946).

12. J. H. Singleton and G. D. Halsey, Jr., Canadian Journal of Chemistry, 33, 184 (1954).

13. M. Volmer, Zeitschrift für Physikalische Chemie, 115, 253 (1925).

14. J. H. deBoer, "The Dynamical Character of Adsorption," Clarendon Press, Oxford, 1953, p. 170.

15. A. F. Devonshire, Proceedings of the Royal Society of London, A163, 53 (1937).

BIBLIOGRAPHY (Continued)

16. W. A. Steele, Journal of Physical Chemistry, 69, 3446 (1965).

17. J. J. McAlpin and R. A. Pierotti, Journal of Chemical Physics, 41, 68 (1964); Journal of Chemical Physics, 42, 1842 (1965).

18. H. Erying, T. Ree, and N. Hirai, Proceedings of the National Academy of Sciences, U.S., 44, 683 (1958).

19. T. L. Hill, "Statistical Mechanics," McGraw-Hill Book Company, Inc., New York, 1956, p. 424.

20. R. A. Pierotti, Chemical Physics Letters, 2, 385 (1968).

21. W. A. Steele and G. D. Halsey, Jr., Journal of Chemical Physics, 22, 979 (1954).

22. J. R. Sams, Jr., G. Constabaris, and G. D. Halsey, Jr., Journal of Physical Chemistry, 64, 1689 (1960).

23. M. P. Freeman and G. D. Halsey, Jr., Journal of Physical Chemistry, 59, 181 (1955).

24. G. Constabaris, J. H. Singleton, and G. D. Halsey, Jr., Journal of Physical Chemistry, 63, 1350 (1959); also, G. Constabaris, Ph.D. Thesis, University of Washington (1957).

25. G. Constabaris, J. R. Sams, Jr., and G. D. Halsey, Jr., Journal of Physical Chemistry, 65, 367 (1961).

26. J. R. Sams, Jr., G. Constabaris, and G. D. Halsey, Jr., Journal of Chemical Physics, 36, 1334 (1962); also, J. R. Sams, Jr., Ph.D. Thesis, University of Washington (1962).

27. W. A. Steele and G. D. Halsey, Jr., Journal of Physical Chemistry, 59, 57 (1955).

28. J. O. Hirschfelder, C. F. Curtiss, and R. B. Bird, "Molecular Theory of Gases and Liquids," John Wiley and Sons, Inc., New York, 1967, p. 32.

29. R. A. Pierotti, Vacuum Microbalance Techniques, 6, 1 (1967).

30. O. Sinanoglu and K. S. Pitzer, Journal of Chemical Physics, 32, 1279 (1960).

31. J. A. Barker and D. H. Everett, Transactions of the Faraday Society, 58, 1608 (1962).

BIBLIOGRAPHY (Continued)

32. D. H. Everett, Discussions of the Faraday Society, 40, 177 (1965).

33. Sidney Ross and James P. Oliver, "On Physical Adsorption," Interscience Publishers, New York, 1964, p. 221.

34. R. A. Pierotti and J. C. Petricciani, Journal of Physical Chemistry, 64, 1596 (1960); and, J. C. Petricciani, Master's Thesis, University of Nevada (1960).

35. G. Curthoys and P. A. Elkington, Journal of Physical Chemistry, 71, 1477 (1967).

36. A. D. Crowell and D. M. Young, Transactions of the Faraday Society, 49, 1080 (1953).

37. J. A. Morrison and D. M. Young, Review of Scientific Instruments, 25, 518 (1954).

38. R. Brymner and W. Steckelmacher, Journal of Scientific Instruments, 36, 278 (1959).

39. S. C. Collins and B. E. Blaisdell, Review of Scientific Instruments, 7, 213 (1936).

40. A. A. Gairdini, "Boron Nitride," Bureau of Mines Information Circular 7664, U. S. Department of Interior (1953).

41. Earl L. Muetterties, "The Chemistry of Boron and Its Compounds," John Wiley and Sons, Inc., New York, 1967, pp. 141-148.

42. R. S. Pease, Acta Crystallographica, 5, 356 (1952).

43. Norbert A. Lange, ed., "Handbook of Chemistry," McGraw-Hill Book Company, Tenth edition, 1961, p. 1425.

44. H. W. Straley, III, and John E. Husted, "Georgia Gravity Project," (Final Report Project A-943), Georgia Institute of Technology, Engineering Experiment Station, Atlanta, Georgia, 1967.

45. A. H. Cook and N. W. B. Stone, Philosophical Transactions of the Royal Society, A250, 279 (1957).

46. W. G. Bronbacher, D. P. Johnson, and J. L. Cross, "Mercury Barometers and Manometers," N B S Monograph 8, 1960.

47. R. Muijlwijk, M. R. Moussa, and H. Van Dijk, Physica, 32, 805 (1966).

BIBLIOGRAPHY (Concluded)

48. C. R. Barber and Anne Horsford, Metrologia, 1, 75 (1965).

49. Francis Weston Sears, "Mechanics, Wave Motion, and Heat," Addison-Wesley Publishing Company, Reading, Massachusetts, 1958, p. 509.

50. Clarence J. West, Ed., "International Critical Tables of Numerical Data," McGraw-Hill Book Company, Inc., New York, Vol. 2, 1927, p. 9459.

51. T. L. Hill, "Introduction to Statistical Thermodynamics," Addison-Wesley Publishing Company, Reading, Massachusetts, 1962, pp. 262-268.

52. A. D. Crowell and Chai Ok Chang, Journal of Chemical Physics, 43, 4364 (1965).

53. A. D. Crowell and R. B. Steele, Journal of Chemical Physics, 34, 1347 (1961).

54. A. D. Crowell, Journal of Chemical Physics, 26, 1407 (1957).

55. A. D. Crowell and Chai Ok Chang, Journal of Chemical Physics, 38, 2584 (1963).

56. Edwin F. Mayer and Victor R. Deitz, Journal of Physical Chemistry, 71, 1512 (1967).

57. Alvin C. Levy, Master's Thesis, Georgia Institute of Technology, 1966, p. 41.

58. R. A. Pierotti, Journal of Physical Chemistry, 66, 1810 (1962).

59. Hill, "Thermodynamics," p. 25.

60. Hirschfelder, Curtiss, and Bird, p. 163.

61. Howard E. Thomas, Ph.D. Thesis, University of Bristol, England (1969).

VITA

Reginald Norris Ramsey was born August 13, 1938, in Chester, South Carolina to Mary Fields and John Lafayette Ramsey. He was reared in Chester and graduated from Chester High School in June, 1956. He served in the United States Army from June 1956 - June 1959. He entered Erskine College, Due West, South Carolina in September, 1959, and received the degree Bachelor of Arts in August, 1962. He served as a physics instructor at Erskine College from September, 1962 - June, 1964. He entered the graduate division of the Georgia Institute of Technology in June, 1964, to study for the Doctor of Philosophy in the School of Chemistry. During his graduate work, he held a National Aeronautics and Space Administration Fellowship and a Rayonier Fellowship.